Transparent boundary conditions for wave propagation in fractal trees: convolution quadrature approach (extended report)

Patrick Joly, Maryna Kachanovska

Noname manuscript No.
(will be inserted by the editor)

Transparent boundary conditions for wave propagation in fractal trees: convolution quadrature approach

Patrick Joly · Maryna Kachanovska

Received: date / Accepted: date

Abstract In this work we propose high-order transparent boundary conditions for the weighted wave equation on a fractal tree, with an application to the modeling of sound propagation in a human lung. This article follows the recent work [29], dedicated to the mathematical analysis of the corresponding problem and the construction of low-order absorbing boundary conditions. The method proposed in this article consists in constructing the exact (transparent) boundary conditions for the semi-discretized problem, in the spirit of the convolution quadrature method developed by Ch. Lubich. We analyze the stability and convergence of the method, and propose an efficient algorithm for its implementation. The exposition is concluded with numerical experiments.

Keywords Convolution quadrature · transparent boundary conditions · fractal trees · DtN operator · quantum graph

1 Introduction

Sound propagation in a human lung can be used for non-invasive diagnosis of the respiratory diseases, see e.g. [40] for some experimental studies, a PhD thesis [24], and, in particular, the Audible Human Project [1] and references therein. A human lung can be viewed as a network of small tubes (bronchioles), immersed into the lung tissue (parenchyma) and coupled with their ends to microscopic cavities in the parenchyma (alveoli). The physical phenomenon of the wave propagation in a lung is highly complex, due to the fractal geometry of lung airways, heterogeneity of parenchyma, interactions/couplings between various types of tissues, and, eventually, multiscale nature of the problem, and thus in practice one uses simplified models. For instance, in the mathematical literature, in [13,12], the sound propagation in a highly heterogeneous

POEMS (INRIA-CNRS-ENSTA), ENSTA ParisTech, 828 Boulevard des Maréchaux, 91120 Palaiseau France
E-mail: patrick.joly@inria.fr, maryna.kachanovska@inria.fr

parenchyma is modelled using the homogenization techniques. In [36] Sobolev spaces associated to the Laplace equation on a fractal tree that models the network of bronchioli are studied, and in [20] the wave equation with a viscous non-local term on a dyadic infinite tree is analyzed, see as well the monograph [35]. This point of view at the bronchioli as a self-similar network (with possibly multiple levels of self-similar structure) seems to be rather classical (though indeed simplified) in the medical and medical engineering literature, see in particular [43,15,38,25] for the related discussion. In this article we adapt this, simplified, approach of studying wave propagation in lungs.

In the limit when the thickness of the bronchiolar tubes tends to zero, the problem becomes essentially one-dimensional inside each of the tubes. A rigorous asymptotic analysis [30,42] allows to take into account the differences between the thicknesses of the tubes at different levels of the bronchiolar tree via incorporating weights into the originally homogeneous wave equation. Constructing an efficient numerical method for the resolution of such a 1D weighted wave equation defined on a fractal tree is the subject of the present work. In the literature [8] the type of problems we consider is sometimes referred to as problems posed on a quantum graph, to underline the distinction between this kind of models and discrete, finite-difference-like models on graphs.

This problem gives rise to numerous interesting questions from the analytical (relations between associated weighted Sobolev spaces on fractal trees, in particular, embeddings and existence of a trace), and from the numerical point of views (since the fractal tree has an infinite number of edges). The analysis related questions have been answered in [29], while the construction of efficient numerical methods for such problems is mainly the subject of the present work. Our principal idea is to construct transparent boundary conditions for the wave propagation in a fractal tree that would allow to perform all the computations on a truncated tree. Most of such boundary conditions are based on an approximation of the Dirichlet-to-Neumann (DtN) operator.

In this work we construct an exact DtN operator for a semi-discretized in time system, in the spirit of the convolution quadrature (CQ) methods [33,34], see in particular numerous recent works dedicated to the coupling of boundary integral equations and volumic wave equations (FEM-BEM coupling) [6,32, 23,37]. Let us mention a related approach, based on constructing transparent boundary conditions for problems discretized in space and time, see e.g. [3,10, 11,9,31] and references therein. Our transparent boundary conditions can be viewed as Johnson-Nédélec style coupling [26], which was, in the context of the acoustic wave equation, studied in the PhD thesis [21], or, for the Schrödinger equation, in [41]. In this work we perform the convergence and stability analysis for such a coupling. The principal difference between our work and many other works on CQ is that we perform the analysis purely in the time domain (unlike e.g. [6,32]), and use an explicit time discretization for the volumic terms and an implicit discretization for the boundary terms (unlike [23,37]).

Another important difficulty for the CQ treatment is that neither the convolution kernel, nor its Fourier-Laplace transform are known in a closed form

(unlike many other applications of the CQ); we thus propose a procedure for its approximation, suitable for the use in the convolution quadrature.

This article is organized as follows. In Section 2 we recall the notation and formulate the problem. Section 3 is dedicated to the construction of transparent boundary conditions, as well as their analysis (stability and convergence). In Section 4 we provide algorithmic aspects of the method and perform its complexity analysis. Finally, Section 5 is dedicated to the numerical experiments. We conclude with a discussion of the obtained results in Section 6.

2 Problem setting

2.1 Notation

We will adhere to the notation and terminology used in [29]. Let us recall some of the geometric assumptions:

1. By $\mathcal{T}$ we will denote a p-adic tree [29, Definiton 2.1] with an infinite number of edges. These edges are ordered in generations (collections of edges) $\mathcal{G}^i$ in the following manner: $\mathcal{G}^0$ consists of a root edge; $\mathcal{G}^{n+1}$ is a union of children edges of all the edges from the generation $\mathcal{G}^n$. Each generation $\mathcal{G}^n$, $n \in \mathbb{N}$, contains p^n edges $\Sigma_{n,k}$, $k = 0, \dots, p^n - 1$.

The children of the edge $\Sigma_{n,k}$ (of the generation $n+1$) are indexed as

$$\Sigma_{n+1,pk+j}, \qquad j = 0, \dots, p-1. \tag{1}$$

The root vertex of the tree is denoted by M^*. Every edge $\Sigma_{n,k}$ can be as-

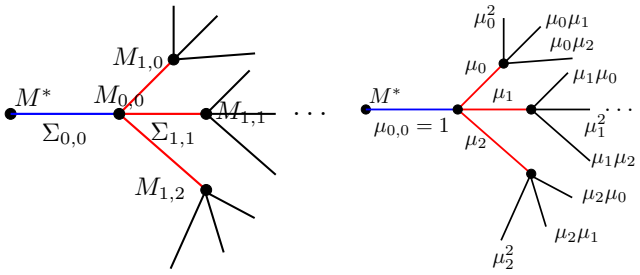

Fig. 1 A self-similar 3-adic infinite tree. Left: In blue we mark the edges that belong to $\mathcal{G}^0$, in red the edges of $\mathcal{G}^1$, in black the edges of $\mathcal{G}^2$. Right: Distribution of weights on the edges of a 3-adic infinite self-similar tree.

sociated with two vertices $[A_{n,k}, B_{n,k}]$. Given a vertex M, let $d(M)$ be the length of the path (sum of the respective edge lengths) between the root edge M^* and M; then we denote by $M_{n,k} = \operatorname{argmax}(d(A_{n,k}), d(B_{n,k}))$. This vertex uniquely identifies the edge $\Sigma_{n,k}$, see Figure 1.

2. Each edge $\Sigma_{n,k}$ is assigned two numbers: its length $\ell_{n,k}$ and a weight $\mu_{n,k} > 0$.

3. We will assume that the tree is self-similar (fractal), in the sense of [29, Definition 2.3]. Let us explain this in more details. Let $\boldsymbol{\alpha} = (\alpha_0, \dots, \alpha_{p-1})$ and $\boldsymbol{\mu} = (\mu_0, \dots, \mu_{p-1})$ be two vectors with positive elements. Then the length and the weight of the edge $\Sigma_{n+1,pk+j}$ are related to the length and the weight of the parent edge $\Sigma_{n,k}$, cf. (1), as follows:

$$\ell_{n+1,pk+j} = \alpha_j \ell_{n,k}, \qquad \mu_{n+1,pk+j} = \mu_j \mu_{n,k}, \qquad j = 0, \dots, p-1.$$

Without loss of generality, we will assume that $\mu_{0,0} = 1$. An illustration to the above is given in Figure 1.

Finally, we will denote by $\mathcal{T}^m$ the subtree of $\mathcal{T}$ truncated to m generations, whose edges are given by a collection

$$\mathcal{T}^m := \{\Sigma_{n,k},\, 0 \le k \le p^n - 1,\, 0 \le n \le m\} \equiv \bigcup_{\ell=0}^{m} \mathcal{G}^\ell. \tag{2}$$

By $\mathcal{T}_{m,j}$ we will denote a p-adic subtree of the tree $\mathcal{T}$, whose root edge is $\Sigma_{m,j}$.

All over the article we will assume that $|\boldsymbol{\alpha}|_\infty < 1$ (i.e. the tree can be compactly embedded into $\mathbb{R}^d$, $d \ge 2$). We will refer to a weighted tree $\mathcal{T}$ as to a reference tree if the length of its root edge satisfies $\ell_{0,0} = 1$.

2.2 Wave propagation in self-similar weighted trees

We consider the problem of wave propagation on a self-similar weighted reference tree $\mathcal{T}$. For this we introduce a parametrization of each edge $\Sigma_{n,j}$ of the tree, associated with the segment $[M^*_{n,j}, M_{n,j}]$, by an abscissa $s_{n,j} \in [a_{n,j}, b_{n,j}]$, $a_{n,j}$, $b_{n,j} \in \mathbb{R}$. This parametrization is chosen so that

$$[M^*_{n,j},\, M_{n,j}] \equiv \{M \in \mathbb{R}^d :\, M = M^*_{n,j} + (M_{n,j} - M^*_{n,j})(s_{n,j} - a_{n,j})(b_{n,j} - a_{n,j})^{-1}\}.$$

With s being an abscissa on the tree $\mathcal{T}$, defined on each edge $\Sigma_{n,j}$ as above, we define the weight function $\mu(s)$ on $\mathcal{T}$:

$$\mu(s) = \mu_{n,j}, \qquad s \in \Sigma_{n,j}.$$

An acoustic pressure $u(s,t)$ satisfies the weighted wave equation, which can be written in a compact manner as

$$\mu \partial_t^2 u - \partial_s(\mu \partial_s u) = f(s,t), \qquad u(.,0) = \partial_t u(.,0) = 0, \tag{3}$$

with f being a source term. We equip this problem with a boundary condition $u(M^*, t) = 0$. It remains to pose the boundary conditions at the 'infinite' boundary of the tree, the meaning of which will become clear in Section 2.3.

For the moment, let us explain in more detail the meaning behind (3). With the notation $u_{n,j} = u|_{\Sigma_{n,j}}$, the above problem reads:

$$\partial_t^2 u_{n,j} - \partial_s^2 u_{n,j} = f_{n,j} \quad \text{on } \Sigma_{n,j}, \qquad j = 0, \dots p^n - 1, \quad n \geq 0, \tag{4}$$

$$u(.,0) = \partial_t u(.,0) = 0, \quad u(M^*, t) = 0, \tag{5}$$

which we additionally equip with the continuity ($\mathcal{C}$) and Kirchoff ($\mathcal{K}$) conditions at each of the vertices, cf. (1),

$$u_{n,j}(M_{n,j}, t) = u_{n+1,pj+k}(M_{n,j}, t), \quad k = 0, \dots, p-1, \tag{$\mathcal{C}$}$$

$$\partial_s u_{n,j}(M_{n,j}, t) = \sum_{k=0}^{p-1} \mu_k \, \partial_s u_{n+1,pj+k}(M_{n,j}, t), \quad j = 0, \dots p^n - 1, \; n \geq 0, \tag{$\mathcal{K}$}$$

with an abuse of notation $u(M_{n,j}, t) \equiv u(b_{n,j}, t)$, see the start of this section.

Remark 1 In this work we chose to study the problem with vanishing initial conditions and the source term; however, all the stability/convergence results easily extend to the case when the problem with initial conditions and vanishing source is examined. Then the results for the problem with non-vanishing i.c. and non-vanishing source can be obtained by linearity.

2.3 Dirichlet and Neumann problems for the wave equation

The problem (4, 5, $\mathcal{C}$, $\mathcal{K}$) needs to be equipped with some conditions at the 'infinite' boundary of the tree. This becomes more clear when studying the family of problems (3) posed on subtrees $\mathcal{T}^m$, $m \to \infty$: for their well-posedness, it is necessary to define boundary conditions on the 'outer' boundary of the tree $\mathcal{T}^m$, consisting of the points $\{M_{m,j},\, j = 0, \dots, p^m - 1\}$. This will be done variationally, via the Sobolev spaces.

2.3.1 Sobolev Spaces on $\mathcal{T}$

Provided an abscissa s on $\mathcal{T}$, we can define a function $v = v(s)$, $v : \mathcal{T} \to \mathbb{C}$. For brevity, let us denote

$$\int_{\mathcal{T}} \mu v := \sum_{n=0}^{\infty} \sum_{k=0}^{p^n - 1} \int_{\Sigma_{n,k}} \mu_{n,k} v(s) ds. \tag{6}$$

We will need the following three spaces:

– square-integrable functions

$$\mathrm{L}^2_\mu(\mathcal{T}) = \{v : \; v|_{\Sigma_{n,j}} \in \mathrm{L}^2(\Sigma_{n,j}),\, \|v\|_{\mathrm{L}^2_\mu(\mathcal{T})} < \infty\},$$

$$\|v\|^2_{\mathrm{L}^2_\mu(\mathcal{T})} = \|v\|^2 = \int_{\mathcal{T}} \mu |v|^2, \qquad (v, g) := \int_{\mathcal{T}} \mu \, v \, g.$$

– square-integrable continuous functions with square-integrable derivatives: denoting by $C(\mathcal{T})$ continuous functions on $\mathcal{T}$,

$$\mathrm{H}^1_\mu(\mathcal{T}) := \{v \in C(\mathcal{T}) \cap \mathrm{L}^2_\mu(\mathcal{T}) : |v|_{\mathrm{H}^1_\mu(\mathcal{T})} < \infty\},$$
$$|v|_{\mathrm{H}^1_\mu(\mathcal{T})} \equiv \|\partial_s v\|_{\mathrm{L}^2_\mu(\mathcal{T})}, \quad \|v\|^2_{\mathrm{H}^1_\mu(\mathcal{T})} = \|v\|^2_{\mathrm{L}^2_\mu(\mathcal{T})} + |v|^2_{\mathrm{H}^1_\mu(\mathcal{T})}.$$

– closure of compactly supported H^1_μ-functions. For this let us define

$$C_0(\mathcal{T}) := \{v \in C(\mathcal{T}) : \quad v = 0 \text{ on } \mathcal{T} \setminus \mathcal{T}^m, \quad \text{for some } m \in \mathbb{N}\},$$

i.e. functions which are supported inside $\mathcal{T}^m$, for some $m \in \mathbb{N}$. Then

$$\mathrm{H}^1_{\mu,0}(\mathcal{T}) := \overline{C_0(\mathcal{T}) \cap \mathrm{H}^1_\mu(\mathcal{T})}^{\|.\|_{\mathrm{H}^1_\mu(\mathcal{T})}}.$$

The above definitions can be naturally extended to the spaces defined on a truncated tree $\mathcal{T}^m$, with an associated L^2_μ-scalar product denoted by $(.,.)_{\mathcal{T}^m}$.

2.3.2 The boundary value problems

To derive the variational formulation, we test (4) with a compactly supported $v \in C_0(\mathcal{T})$, $v(M^*) = 0$; then any $\mathrm{H}^1_\mu(\mathcal{T})$-solution of (4, 5, $\mathcal{C}$, $\mathcal{K}$) satisfies

$$\int_{\mathcal{T}} \mu \frac{d^2}{dt^2} u\, v + \int_{\mathcal{T}} \mu \partial_s u\, \partial_s v = \int_{\mathcal{T}} \mu f v, \quad \text{for all } v \in C_0(\mathcal{T}), \text{ s.t. } v(M^*) = 0.$$

Reciprocally, any $\mathrm{H}^1_\mu(\mathcal{T})$-solution to the above problem solves (4, $\mathcal{C}$, $\mathcal{K}$).
To formulate Dirichlet/Neumann problems for (3), let us introduce

$$V_{\mathfrak{n}}(\mathcal{T}) = \{v \in \mathrm{H}^1_\mu(\mathcal{T}) : v(M^*) = 0\}, \qquad V_{\mathfrak{d}}(\mathcal{T}) = \{v \in \mathrm{H}^1_{\mu,0}(\mathcal{T}) : v(M^*) = 0\}.$$

Let the final time $T > 0$ be fixed.

Definition 1 (Neumann problem) Find

$$u_{\mathfrak{n}} \in C([0,T]; V_{\mathfrak{n}}(\mathcal{T})) \cap C^1([0,T]; \mathrm{L}^2_\mu(\mathcal{T})),$$

s.t. $u_{\mathfrak{n}}(.,0) = \partial_t u_{\mathfrak{n}}(.,0) = 0$, and

$$\int_{\mathcal{T}} \mu \frac{d^2}{dt^2} u_{\mathfrak{n}}\, v + \int_{\mathcal{T}} \mu \partial_s u_{\mathfrak{n}} \partial_s v = \int_{\mathcal{T}} \mu f v, \qquad \text{for all } v \in V_{\mathfrak{n}}(\mathcal{T}). \tag{N}$$

Definition 2 (Dirichlet problem) Find

$$u_{\mathfrak{d}} \in C([0,T]; V_{\mathfrak{d}}(\mathcal{T})) \cap C^1([0,T]; \mathrm{L}^2_\mu(\mathcal{T})),$$

s.t. $u_{\mathfrak{d}}(.,0) = \partial_t u_{\mathfrak{d}}(.,0) = 0$, and

$$\int_{\mathcal{T}} \mu \frac{d^2}{dt^2} u_{\mathfrak{d}}\, v + \int_{\mathcal{T}} \mu \partial_s u_{\mathfrak{d}} \partial_s v = \int_{\mathcal{T}} \mu f v, \qquad \text{for all } v \in V_{\mathfrak{d}}(\mathcal{T}). \tag{D}$$

Remark 2 Although, strictly speaking, the problem (N) is a mixed problem (because of the Dirichlet condition at the root of $\mathcal{T}$), we call it 'Neumann', since we are interested in the behaviour at the 'infinite' boundary of $\mathcal{T}$.

These problems are well-posed, as summarized below.

Theorem 1 *Let $f \in L^1(0,\, T; \mathrm{L}^2_\mu(\mathcal{T}))$. Then the problem (N) (resp. (D)) has a unique solution $u_\mathfrak{a} \in C([0,T]; V_\mathfrak{a}(\mathcal{T})) \cap C^1([0,T]; \mathrm{L}^2_\mu(\mathcal{T}))$, $\mathfrak{a} = \mathfrak{n}$ (resp. $\mathfrak{a} = \mathfrak{d}$). This solution $u_\mathfrak{a}$, $\mathfrak{a} \in \{\mathfrak{n}, \mathfrak{d}\}$, satisfies the following bound*

$$\|\partial_t u_\mathfrak{a}(T)\|_{\mathrm{L}^2_\mu(\mathcal{T})} + \|\partial_s u_\mathfrak{a}(T)\|_{\mathrm{L}^2_\mu(\mathcal{T})} \le \sqrt{2} \int_0^T \|f(t)\|_{\mathrm{L}^2_\mu(\mathcal{T})} dt. \tag{7}$$

Proof The proof is classical. The existence and uniqueness result follows from the semigroup theory (in particular, the arguments of [39, Section 7.4] (semigroup framework for the wave equation) and [39, Section 4.2] (existence and uniqueness of mild solutions) extend almost verbatim to our case).

To show (7), one first tests e.g. (N) with $\partial_t u_\mathfrak{n}$, which gives

$$\frac{d}{dt}\mathcal{E}_\mathfrak{n}(t) = (f, \partial_t u_\mathfrak{n}), \qquad \mathcal{E}_\mathfrak{n} = \frac{1}{2}\left(\|\partial_t u_\mathfrak{n}\|^2 + \|\partial_s u_\mathfrak{n}\|^2\right).$$

The application of the Gronwall inequality yields the desired result. □

Later on we will make use of the following corollary about the dependence of the time regularity of the solution on the regularity of the source f.

Corollary 1 *Let $f \in W^{k,1}(0,\, T; \mathrm{L}^2_\mu(\mathcal{T}))$, $k \ge 1$, and*

$$f(.,0) = \ldots = \partial_t^{k-1} f(.,0) = 0.$$

Then the problem (N) (resp. (D)) has a unique solution $u_\mathfrak{a}$, $\mathfrak{a} = \mathfrak{n}$ (resp. $\mathfrak{a} = \mathfrak{d}$). Moreover, this solution satisfies:

$$u_\mathfrak{a} \in C^k([0,T]; V_\mathfrak{a}(\mathcal{T})) \cap C^{k+1}([0,T]; \mathrm{L}^2_\mu(\mathcal{T})),$$

$$\|\partial_t^{\ell+1} u_\mathfrak{a}(T)\|_{\mathrm{L}^2_\mu(\mathcal{T})} + \|\partial_s \partial_t^\ell u_\mathfrak{a}(T)\|_{\mathrm{L}^2_\mu(\mathcal{T})} \le \sqrt{2} \int_0^T \|\partial_t^\ell f(t)\|_{\mathrm{L}^2_\mu(\mathcal{T})} dt, \qquad 0 \le \ell \le k.$$

Proof It suffices to notice that $\varphi = \partial_t^\ell u_\mathfrak{a}$, $\ell \le k$, solves the problem (N) (resp. (D)) with f replaced by $f^{(\ell)} \in L^1(0,T; \mathrm{L}^2_\mu(\mathcal{T}))$, hence Theorem 1 applies. □

It is natural to ask whether the solutions to (N) and (D) coincide (as in the case $p = 1$, $\mu = 1$ and $\alpha = 1$, when $\mathcal{T}$ can be identified with $\mathbb{R}^+$). The answer depends on the following two quantities:

$$\langle \boldsymbol{\mu}\boldsymbol{\alpha} \rangle := \sum_{i=0}^{p-1} \mu_i \alpha_i, \qquad \left\langle \frac{\boldsymbol{\mu}}{\boldsymbol{\alpha}} \right\rangle := \sum_{i=0}^{p-1} \frac{\mu_i}{\alpha_i}.$$

Because of the assumption $|\boldsymbol{\alpha}|_\infty < 1$, $\langle \boldsymbol{\mu}\boldsymbol{\alpha} \rangle < \left\langle \frac{\boldsymbol{\mu}}{\boldsymbol{\alpha}} \right\rangle$.

Theorem 2 ([29]) *If $\langle \boldsymbol{\mu}\boldsymbol{\alpha} \rangle \ge 1$ or $\left\langle \frac{\boldsymbol{\mu}}{\boldsymbol{\alpha}} \right\rangle \le 1$, the spaces $\mathrm{H}^1_{\mu,0}(\mathcal{T})$ and $\mathrm{H}^1_\mu(\mathcal{T})$ coincide, and thus $u_\mathfrak{n} = u_\mathfrak{d}$. Otherwise, $\mathrm{H}^1_{\mu,0}(\mathcal{T}) \subsetneq \mathrm{H}^1_\mu(\mathcal{T})$, and $u_\mathfrak{n} \ne u_\mathfrak{d}$.*

2.4 Transparent boundary conditions

In [29] it was shown how to construct exact (transparent) boundary conditions for the problems (N) and (D). To recall the main ideas, we fix $m \geq 1$, and assume the following.

Assumption 1 *The source $f(s,t)$ is s.t. for all $t \geq 0$, $\operatorname{supp} f(s,t) \subseteq \mathcal{T}^{m-1}$.*

We will use this assumption without reference in the remainder of the article. When f satisfies Assumption 1, for all $\ell \geq 0$, $\partial_t^\ell u(M_{m,j},0) = 0$, $j = 0,\dots,p^m-1$, because of finiteness of the speed of wave propagation.

2.4.1 Auxiliary notation

We will denote by $\boldsymbol{V}(\mathcal{T}^m)$ the following subspace of $\mathrm{H}^1_\mu(\mathcal{T}^m)$:

$$\boldsymbol{V}(\mathcal{T}^m) := \{v \in \mathrm{H}^1_\mu(\mathcal{T}^m) : v(M^*) = 0\}.$$

Let us introduce additionally the following partial trace operator

$$\boldsymbol{\gamma}_m : \quad \boldsymbol{V}(\mathcal{T}^m) \to \mathbb{R}^{p^m},$$

defined for $v \in \boldsymbol{V}(\mathcal{T}^m)$ (recall that v is continuous) by

$$\boldsymbol{\gamma}_m v = \Big(v(M_{m,0}),\dots,v(M_{m,p^m-1})\Big).$$

It is not difficult to verify that $\boldsymbol{\gamma_m}$ is continuous:

$$\|\boldsymbol{\gamma}_m v\|_{\mathbb{R}^{p^m}} \leq C_{\gamma_m}\|\partial_s v\|_{\mathrm{H}^1_\mu(\mathcal{T}^m)}, \qquad v \in \boldsymbol{V}(\mathcal{T}^m).$$

Remark 3 Let us remark that $\boldsymbol{\gamma}_m$ differs from the partial trace operator τ_m introduced in [29], which maps $\boldsymbol{V}(\mathcal{T}^m)$ into $L^2(0,1)$. The reason for this discrepancy is that in [29] we were interested in a trace of a function v defined on $\mathcal{T}$, considered as a limit of its traces on $\mathcal{T}^m$, as $m \to \infty$, and thus needed to introduce a common 'boundary' for all the trees $\mathcal{T}^m$, $m \geq 0$. In the present work, we fix m and consider functions defined on truncated trees $\mathcal{T}^m$, which enables us to work with the more classical definition of the trace.

In the sequel, by $\langle .,. \rangle$ we will denote the Eucledian scalar product in $\mathbb{R}^{p^m}$.

2.4.2 Transparent boundary conditions

We truncate the computational domain to the tree $\mathcal{T}^m$, and impose transparent boundary conditions at the ('right') boundary of this tree in the form:

$$-\mu_{m,j}\partial_s u_{m,j}(M_{m,j},t) = \mathcal{B}^{\mathfrak{a}}_{m,j}(\partial_t)u_{m,j}(M_{m,j},t), \quad j = 0,\dots,p^m-1, \tag{8}$$

where $\mathfrak{a} \in \{\mathfrak{d},\mathfrak{n}\}$ and $\mathcal{B}^{\mathfrak{a}}_{m,j}(\partial_t)$ is an exact DtN map for the Dirichlet (corresp. Neumann problem), associated to the point $M_{m,j}$, that we describe below. Let

$$H^1_c([0,\,T];X) = \{v \in H^1([0,\,T];X),\, v(0) = 0\}.$$

Then this operator is a continuous mapping

$$\mathcal{B}^{\mathfrak{a}}_{m,j}(\partial_t) \in \mathcal{L}\left(H^1_c([0,\,T];\mathbb{R}), L^2([0,\,T];\mathbb{R})\right).$$

This is a corollary of (15) and Theorem 6. To define its action, recall that the point $M_{m,j}$ is a root vertex of p subtrees of the tree $\mathcal{T}$, which we denote for simplicity by $\mathcal{T}_k^{(m,j)}$, $k = 0, \dots, p-1$. The weights assigned to their roots edges are respectively $\mu_{m,j}\mu_k$ (because of the self-similarity property, see Section 2.1). Then the DtN map $\mathcal{B}^{\mathfrak{a}}_{m,j}(\partial_t)$ associates to a function $g \in H^1_c([0,\,T];\mathbb{R})$ the sum of conormal derivatives (weighted normal derivatives):

$$\mathcal{B}^{\mathfrak{a}}_{m,j}(\partial_t)g = -\sum_{k=0}^{p-1} \mu_{m,j}\mu_k \partial_s u^{\mathfrak{a}}_{g,k}, \tag{9}$$

where, depending on the considered problem,

1. if $\mathfrak{a} = \mathfrak{n}$ (Neumann), $u^{\mathfrak{n}}_{g,k} \in C^1([0,T];\mathrm{L}^2_\mu(\mathcal{T}_k^{(m,j)})) \cap C([0,T];\mathrm{H}^1_\mu(\mathcal{T}_k^{(m,j)}))$ solves the following Neumann initial boundary-value problem:

$$\begin{aligned} &\int_{\mathcal{T}_k} \mu v\, \partial_t^2 u^{\mathfrak{n}}_{g,k} + \int_{\mathcal{T}_k} \mu \partial_s v\, \partial_s u^{\mathfrak{n}}_{g,k} = 0, \qquad \text{for all } v \in \boldsymbol{V}_{\mathfrak{n}}(\mathcal{T}_k^{(m,j)}), \\ &u^{\mathfrak{n}}_{g,k}(M_{m,j},t) = g(t), \quad u^{\mathfrak{n}}_{g,k}(.,0) = \partial_t u^{\mathfrak{n}}_{g,k}(.,0) = 0,\ k = 0,\dots,p-1. \end{aligned} \tag{10}$$

2. if $\mathfrak{a} = \mathfrak{d}$ (Dirichlet), $u^{\mathfrak{d}}_{g,k} \in C^1([0,T];\mathrm{L}^2_\mu(\mathcal{T}_k)) \cap C([0,T];\mathrm{H}^1_{\mu,0}(\mathcal{T}_k^{(m,j)}))$ solves (10), where $u^{\mathfrak{n}}_{g,k}$ is substituted by $u^{\mathfrak{d}}_{g,k}$ and $\boldsymbol{V}_{\mathfrak{n}}(\mathcal{T}_k^{(m,j)})$ by $\boldsymbol{V}_{\mathfrak{d}}(\mathcal{T}_k^{(m,j)})$.

This definition of the DtN map is obviously consistent with the Kirchoff conditions, cf. (8) and $(\mathcal{K})$. In a short form, we will write

$$\mathcal{B}^{\mathfrak{a}}_m(\partial_t) = \mathrm{diag}\left(\mathcal{B}^{\mathfrak{a}}_{m,0}(\partial_t), \dots, \mathcal{B}^{\mathfrak{a}}_{m,p^m-1}(\partial_t)\right). \tag{11}$$

Since the coefficients of the problem do not depend on time, $\mathcal{B}^{\mathfrak{a}}_m(\partial_t)$ is a convolution operator; the corresponding convolution kernel is not known in closed form. The goal of this work is to provide an accurate discrete approximation to $\mathcal{B}^{\mathfrak{a}}_m(\partial_t)$, which relies on a tractable characterization of its convolution kernel that was obtained in [29]. In order to show how to obtain an expression for $\mathcal{B}^{\mathfrak{a}}_m$, let us first introduce the notion of the **reference** DtN operator.

Remark 4 The above boundary conditions are called transparent, because any $u_{\mathfrak{a}}$ solving the Dirichlet (corresp. the Neumann problem) satisfies (9) exactly.

2.4.3 Reference DtN operator

A reference DtN operator associated to the Dirichlet/Neumann problems on the **reference** tree $\mathcal{T}$ is a continuous operator, see Theorem 6,

$$\Lambda_{\mathfrak{a}}(\partial_t):\ H^1_c([0,\,T];\mathbb{R}) \to L^2([0,\,T];\mathbb{R}), \qquad \mathfrak{a} \in \{\mathfrak{d},\mathfrak{n}\},$$

defined as

$$\Lambda_{\mathfrak{a}}(\partial_t)g(t) = -\partial_s u_g^{\mathfrak{a}}(M^*,t), \tag{12}$$

where, depending on the problem considered,

1. for $\mathfrak{a} = \mathfrak{n}$ (Neumann), $u_g^{\mathfrak{n}} \in C([0,T];\mathrm{H}^1_\mu(\mathcal{T})) \cap C^1([0,T];\mathrm{L}^2_\mu(\mathcal{T}))$ solves

$$\begin{aligned} &\int_{\mathcal{T}} \mu\, \partial_t^2 u_g^{\mathfrak{n}}\, v + \int_{\mathcal{T}} \mu \partial_s u_g^{\mathfrak{n}}\, \partial_s v = 0, \qquad \text{for all } v \in V_{\mathfrak{n}}, \\ &v_g^{\mathfrak{n}}(M^*,t) = g(t), \quad u_g^{\mathfrak{n}}(.,0) = \partial_t u_g^{\mathfrak{n}}(.,0) = 0. \end{aligned} \tag{13}$$

2. for $\mathfrak{a} = \mathfrak{d}$ (Dirichlet), $u_g^{\mathfrak{d}} \in C([0,T];\mathrm{H}^1_{\mu,0}(\mathcal{T})) \cap C^1([0,T];\mathrm{L}^2_\mu(\mathcal{T}))$ solves (13) where $u_g^{\mathfrak{n}}$ is substituted by $u_g^{\mathfrak{d}}$ and $V_{\mathfrak{n}}$ by $V_{\mathfrak{d}}$.

This operator is a convolution operator, formally defined as follows:

$$\Lambda_{\mathfrak{a}}(\partial_t)g(t) = \int_0^t \lambda_{\mathfrak{a}}(t-\tau)g(\tau)d\tau.$$

Defining the Fourier-Laplace transform of a causal tempered distribution λ as

$$(\mathcal{F}\lambda)(\omega) = \int_0^\infty \mathrm{e}^{i\omega t}\lambda(t)dt, \qquad \omega \in \mathbb{C},$$

we denote the symbol $(\mathcal{F}\lambda_{\mathfrak{a}})(\omega)$ of the convolution operator $\Lambda_{\mathfrak{a}}(\partial_t)$ by $\mathbf{\Lambda}_{\mathfrak{a}}(\omega)$.

Characterization and properties of $\mathbf{\Lambda}_{\mathfrak{a}}(\omega)$. Positivity of $\Lambda_{\mathfrak{a}}(\partial_t)$. To use the convolution quadrature, it is necessary to be able to compute the symbol of the DtN map, cf. (9), for various complex frequencies ω. In Section 2.4.4 we will show that this symbol can be easily expressed with the help of $\mathbf{\Lambda}_{\mathfrak{a}}(\omega)$. The latter function, in turn, satisfies the following non-linear equation, which will serve the computational purposes.

Lemma 1 (Lemma 5.3 in [29]) *The symbol of the reference DtN operator $\mathbf{\Lambda}(\omega) = \mathbf{\Lambda}_{\mathfrak{a}}(\omega)$, $\mathfrak{a} \in \{\mathfrak{n},\mathfrak{d}\}$, $\mathbf{\Lambda} : \mathbb{C}\setminus\mathbb{R}$, satisfies*

$$\mathbf{\Lambda}(\omega) = -\omega\frac{\omega\tan\omega - \mathbf{F}_{\alpha,\mu}(\omega)}{\tan\omega\mathbf{F}_{\alpha,\mu}(\omega) + \omega}, \qquad \mathbf{F}_{\alpha,\mu}(\omega) = \sum_{i=0}^{p-1}\frac{\mu_i}{\alpha_i}\mathbf{\Lambda}(\alpha_i\omega) \tag{14}$$

Since the solutions of (14) are, in general, non-unique, to single out the solutions that correspond to the symbols of the DtN operators, we restrict the solution space to meromorphic even functions analytic in the origin, cf. Theorem 4. It remains to distinguish between the solutions corresponding to the DtNs for the Dirichlet and Neumann problems (where applicable, cf. Theorem 2). For this we fix the value $\mathbf{\Lambda}(0)$; this leads to the uniqueness of the solution to (14). This is similar to initial-value problems, where fixing the value in zero leads to the uniqueness as well.

Theorem 3 (Lemma 5.5, Corollary 5.6 in [29])

- *if* $\left\langle \frac{\boldsymbol{\mu}}{\boldsymbol{\alpha}} \right\rangle \leq 1$, *the symbol of the reference DtN operator* $\boldsymbol{\Lambda}_{\mathfrak{d}}(\omega) = \boldsymbol{\Lambda}_{\mathfrak{n}}(\omega)$ *is a unique even meromorphic solution of (14) that satisfies* $\boldsymbol{\Lambda}(0) = 0$.
- *let* $\left\langle \frac{\boldsymbol{\mu}}{\boldsymbol{\alpha}} \right\rangle > 1$ *and* $\langle \boldsymbol{\mu}\boldsymbol{\alpha} \rangle < 1$. *Then the function* $\boldsymbol{\Lambda}_{\mathfrak{d}}(\omega)$ *is a unique even meromorphic solution of (14) that satisfies* $\boldsymbol{\Lambda}(0) = 1 - \left\langle \frac{\boldsymbol{\mu}}{\boldsymbol{\alpha}} \right\rangle^{-1}$.
  Similarly, the function $\boldsymbol{\Lambda}_{\mathfrak{n}}(\omega)$ *is a unique even meromorphic solution of the equation* (14) *that satisfies* $\boldsymbol{\Lambda}(0) = 0$.
- *if* $\langle \boldsymbol{\mu}\boldsymbol{\alpha} \rangle \geq 1$, $\boldsymbol{\Lambda}_{\mathfrak{d}}(\omega) = \boldsymbol{\Lambda}_{\mathfrak{n}}(\omega)$ *is a unique even meromorphic solution of (14) that satisfies* $\boldsymbol{\Lambda}(0) = 1 - \left\langle \frac{\boldsymbol{\mu}}{\boldsymbol{\alpha}} \right\rangle^{-1}$.

Additionally, the symbol $\boldsymbol{\Lambda}_{\mathfrak{a}}(\omega)$ satisfies the following property, useful in the sequel, which is an extension of the well-known identities for the DtN map for the classical wave equation [16].

Theorem 4 $\boldsymbol{\Lambda}_{\mathfrak{a}}(\omega) : \mathbb{C} \to \mathbb{C}$ *is an even meromorphic function, whose poles are all real. Moreover,*

(a) $\operatorname{Im}\left(\omega^{-1}\boldsymbol{\Lambda}_{\mathfrak{a}}(\omega)\right) < 0$ *for* $\omega \in \mathbb{C}^+ = \{z \in \mathbb{C} : \operatorname{Im} z > 0\}$.
(b) there exists $C > 0$, *s.t. for all* $\omega \in \mathbb{C}^+$, $|\boldsymbol{\Lambda}_{\mathfrak{a}}(\omega)| < C|\omega| \max\left(1, (\operatorname{Im}\omega)^{-1}\right)$.

Proof See Appendix A.

These properties can be translated as positivity/regularity mapping properties of $\Lambda_{\mathfrak{a}}(\partial_t)$, cf. e.g. Lemma 2.2 in [6]. In particular, the time-domain analogue of Theorem 4 (a), important for the stability of the coupled problem, reads.

Theorem 5 *Let* $g \in H^1_c([0,T])$. *The reference DtN operator satisfies*

$$\int_0^T \left(\Lambda_{\mathfrak{a}}(\partial_t) g\right)(t)\, \partial_t g \, dt \geq 0, \qquad \mathfrak{a} \in \{\mathfrak{d}, \mathfrak{n}\}.$$

Proof The proof is classical. Without loss of generality, let us take $\mathfrak{a} = \mathfrak{d}$. Then testing the strong form of (13) with $\partial_t u_g^{\mathfrak{d}}$ and integrating by parts gives

$$\begin{aligned}\Lambda_{\mathfrak{a}}(\partial_t) g\, \partial_t g \equiv -\partial_s u_g^{\mathfrak{d}}(t, M^*)\, \partial_t u_g^{\mathfrak{d}}(t, M^*) &= \int_{\mathcal{T}} \mu \partial_t^2 u_g^{\mathfrak{d}}\, \partial_t u_g^{\mathfrak{d}} + \int_{\mathcal{T}} \mu \partial_s u_g^{\mathfrak{d}}\, \partial_t \partial_s u_g^{\mathfrak{d}} \\ &= \frac{d}{dt}\mathcal{E}_g^{\mathfrak{d}}, \qquad \mathcal{E}_g^{\mathfrak{d}}(t) = \frac{1}{2}\left(\|\partial_t u_g^{\mathfrak{d}}\|^2 + \|\partial_s u_g^{\mathfrak{d}}\|^2\right).\end{aligned}$$

The result follows by integrating the above from 0 to T and using $\mathcal{E}_g^{\mathfrak{d}}(0) = 0$.

On the other hand, Theorem 4 (b) translates into the time domain as.

Theorem 6 *The operator* $\Lambda_{\mathfrak{a}}(\partial_t) : H^1_c([0,T]; \mathbb{R} \to L^2([0,T]; \mathbb{R}$ *is continuous.*

Proof The proof mimics the proof of Theorem 4, see Appendix F.

2.4.4 Transparent boundary conditions via the reference DtN

Using the reference DtN, we can express the operator $\mathcal{B}^{\mathfrak{a}}_{m,j}(\partial_t)$ as follows [29]:

$$\mathcal{B}^{\mathfrak{a}}_{m,j}(\partial_t) = \mu_{m,j}\alpha^{-1}_{m,j}\sum_{k=0}^{p-1}\frac{\mu_k}{\alpha_k}\mathbf{\Lambda}_{\mathfrak{a}}(\alpha_k\alpha_{m,j}\partial_t). \tag{15}$$

Recall that $\alpha_{m,j}$ is the length of the branch $\Sigma_{m,j}$. The above representation was derived using the Kirchoff conditions and a scaling argument. We have thus reduced the problem of the construction of transparent boundary conditions to the problem of approximating a convolution operator with the symbol $\mathbf{\Lambda}_{\mathfrak{a}}(\omega)$.

Remark 5 Everything that follows, unless stated otherwise, holds true for the Dirichlet and for the Neumann problems, and the distinction between these two problems is encoded in the proper choice of the symbol $\mathbf{\Lambda}_{\mathfrak{a}}$. Hence, where possible, we will omit the index $\mathfrak{a} = \{\mathfrak{d}, \mathfrak{n}\}$. We will study the Neumann problem, keeping in mind that the Dirichlet problem can be handled similarly.

Remark 6 The construction of the transparent boundary conditions in the present article can be extended to the case when the tree $\mathcal{T}$ is not fractal (self-similar, as defined in [29]), however, some of its subtrees are.

2.4.5 Coupled formulation

With the notation from Section 2.4.1 and (11), the coupled problem with the transparent BCs reads:

$$\text{Find } u_m \in C([0,\,T];\boldsymbol{V}(\mathcal{T}^m))\cap C^1([0,\,T];\mathrm{L}^2_\mu(\mathcal{T}^m)), \tag{16a}$$

$$\text{s.t. } u_m(.,0) = \partial_t u_m(.,0) = 0, \text{ and} \tag{16b}$$

$$\begin{aligned}(\partial_t^2 u_m, v)_{\mathcal{T}^m} + (\partial_s u_m, \partial_s v)_{\mathcal{T}^m} + \langle \mathcal{B}_m(\partial_t)\boldsymbol{\gamma}_m u_m,\, \boldsymbol{\gamma}_m v\rangle \\ = (f, v)_{\mathcal{T}^m}, \qquad \text{for all } v \in \boldsymbol{V}(\mathcal{T}^m).\end{aligned} \tag{16c}$$

We have the following easy-to-prove result.

Theorem 7 *For all $f \in L^1(0,T;\mathrm{L}^2_\mu(\mathcal{T}))$, satisfying Assumption 1, the problem (16) has a unique solution u_m, which satisfies the stability bound (7) with u replaced by u_m.*

The restriction of the solution $u = u_{\mathfrak{n}}$ to (N) to $\mathcal{T}^m$ satisfies $u|_{\mathcal{T}^m} = u_m$.

Proof It is not difficult to verify that $u|_{\mathcal{T}^m} = u_m$ (by definition of the transparent boundary conditions, cf. (10)). This implies the existence for (16). If we show the uniqueness for (16), then the bound (7) is a corollary of (7) for $u = u_{\mathfrak{n}}$. However, the uniqueness follows easily by energy techniques: set $f = 0$ in (16c), test it with $\partial_t u_m$, and next integrate from 0 to T. This gives (where we use as well vanishing initial conditions (16b))

$$\frac{1}{2}\left(\|\partial_t u_m(T)\|^2_{\mathcal{T}^m} + \|\partial_s u_m(T)\|^2_{\mathcal{T}^m}\right) + \int_0^T \langle \mathcal{B}_m(\partial_t)\boldsymbol{\gamma}_m u_m,\, \boldsymbol{\gamma}_m \partial_t u_m\rangle\, dt = 0.$$

Using (15) and the positivity property of Theorem 5, we deduce from the above identity that $\|\partial_t u_m(t)\|^2_{\mathcal{T}^m} = 0$. With (16b), we conclude that $u_m = 0$. □

3 Discrete transparent boundary conditions (Convolution Quadrature (CQ))

The main idea behind the CQ is to construct the exact transparent boundary conditions for the problem (3) semi-discretized in time [41,4]. Provided that the time discretization scheme is chosen so that the resulting problem is stable, the corresponding exact transparent boundary conditions inherit its stability.

Remark 7 For the implementation of the convolution quadrature, it is important that $\mathcal{B}^{\mathfrak{a}}_{m,j}(\omega)$ (consequently, $\mathbf{\Lambda}_{\mathfrak{a}}(\omega)$) can be evaluated for any frequency $\omega \in \mathbb{C}^+ = \{z \in \mathbb{C} : \operatorname{Im} z > 0\}$. The description of the respective method is postponed to Section 4, while here we address the questions of stability and convergence of the method.

This section is organized as follows:

- in Section 3.1 we derive discrete transparent boundary conditions based on the (implicit) trapezoid rule (also called θ-scheme with $\theta = \frac{1}{4}$);
- Section 3.2 is dedicated to the semi-discretization in space, its stability and convergence;
- in Section 3.3 we show the time discretization, demonstrate its stability and prove the convergence estimates;
- finally, Section 3.4 is dedicated to the solution of the discretized system.

3.1 Derivation of a CQ approximation for the transparent BCs

First, we will derive a discrete approximation for the reference DtN operator, see Section 2.4.3, and next employ the obtained results to derive an approximation for the transparent boundary conditions. Let Δt be a time step, $t^n = n\Delta t$. We denote by u^n an approximation to $u(., t^n)$. Let $N_t = \lceil T(\Delta t)^{-1} \rceil$. Also,

$$
\begin{aligned}
&D_{\Delta t} v^n = \frac{v^{n+1} - v^{n-1}}{2\Delta t}, \qquad D^2_{\Delta t} v^n = \frac{v^{n+1} - 2v^n + v^{n-1}}{(\Delta t)^2}, \\
&\{v^n\}_{1/4} = \frac{v^{n+1} + 2v^n + v^{n-1}}{4}, \qquad v^{n+1/2} = \frac{v^n + v^{n+1}}{2}, \\
&D_{\Delta t} v^{n+1/2} = \frac{v^{n+1} - v^n}{\Delta t}.
\end{aligned} \tag{17}
$$

3.1.1 Discrete approximation of $\mathbf{\Lambda}$

To derive the CQ approximation of $\Lambda(\partial_t)$, we will proceed like in the continuous case, see Section 2.4.3. The reference DtN is then defined analogously to the continuous case (12), $\Lambda(\partial_t^{\Delta t}) : \mathbb{R}^{N_t+1} \to \mathbb{R}^{N_t+1}$. To define its action, we start

with the problem (13), which we semi-discretize in time using the trapezoid rule (θ-scheme with $\theta = \frac{1}{4}$). As well-known [14], this scheme is unconditionally stable, and thus the discretization results in the following well-posed and stable problem (where without loss of generality we assume that $g(0) = g'(0) = g''(0) = 0$ to ensure that taking $u_g^1 = 0$ does not alter the order of the scheme):

$$\begin{aligned} &\text{Given } u_g^0 = 0,\ u_g^1 = 0,\ u_g^n(M^*) = g^n, \text{ find } (u_g^n)_{n=0}^{N_t} \subset \mathrm{H}^1_\mu(\mathcal{T}),\ \text{s.t.} \\ &\big(D^2_{\Delta t} u_g^n, v\big) + \big(\partial_s\{u_g^n\}_{1/4}, \partial_s v\big) = 0, \qquad \text{for all } v \in V_{\mathfrak{n}}, \quad n < N_t. \end{aligned} \tag{18}$$

The reference DtN associates to the vector $(g^n)_{n=0}^{N_t} \in \mathbb{R}^{N_t+1}$ the following quantity:

$$\big(\Lambda(\partial_t^{\Delta t})g\big)^n = -\partial_s u_g^n(M^*), \qquad n = 0, \dots, N_t. \tag{19}$$

Where convenient, we will write instead of the above $\Lambda(\partial_t^{\Delta t})g^n$, with the obvious abuse of notation. In the above form, the reference DtN operator is not suitable for the computations; thus, let us find a tractable expression for its discrete symbol. For this we will use the Z-transform.

The symbol of the discrete DtN operator. Let us apply Z-transform to the above problem, assuming that $N_t = \infty$. Recall that for a sequence (v^n), s.t. $|v^n| < C(1+n)^q$, $q \geq 0$, its Z-transform is defined as follows:

$$Z:\ v = (v^n) \to V(z) = \sum_{n=0}^{\infty} v^n z^n, \qquad z \in B_1 = \{z \in \mathbb{C} : |z| < 1\}. \tag{20}$$

The function $V(z)$ is obviously analytic in B_1. Applying the Z-transform to (18), and using the standard property of the Z-transform of the shift operator

$$\tau : v = (v^n)_{n\geq 0} \to (v^{n-1})_{n\geq 1}, \qquad Z\tau v = zV(z), \tag{21}$$

we deduce that $U_g(z) \in \mathrm{H}^1_\mu(\mathcal{T})$ satisfies $U_g(z)|_{M^*} = G(z)$ and

$$-\left(i\frac{\delta(z)}{\Delta t}\right)^2 (U_g, v) + (\partial_s U_g, \partial_s v) = 0, \quad \forall\, v \in V_{\mathfrak{n}}, \quad \delta(z) = 2\,\frac{1-z}{1+z}. \tag{22}$$

Since $i\delta :\ B_1 \to \mathbb{C}^+ = \{\omega \in \mathbb{C} :\ \mathrm{Im}\,\omega > 0\}$, the problem (22) is coercive for any $z \in B_1$. With the help of (22), we can then define the discrete symbol of the reference DtN as the mapping

$$\mathbf{\Lambda}_{\Delta t} :\ \mathbb{C} \to \mathbb{C}, \qquad \mathbf{\Lambda}_{\Delta t}(z) :\ G(M^*, z) \to -\partial_s U_g(M^*, z). \tag{23}$$

Comparing (22) and the definition of the symbol $\mathbf{\Lambda}_{\mathfrak{d}}(\omega)$, we obtain

$$\mathbf{\Lambda}_{\Delta t}(z) \equiv \mathbf{\Lambda}\left(i\frac{\delta(z)}{\Delta t}\right). \tag{24}$$

Because $\mathbf{\Lambda}(\omega)$ is analytic in $\mathbb{C}^+ := \{\omega \in \mathbb{C} : \mathrm{Im}\,\omega > 0\}$, cf. Theorem 4, and because $z \to i\delta(z)$ is an analytic function from B_1 into $\mathbb{C}^+$, we conclude that $\mathbf{\Lambda}_{\Delta t}(z)$ is analytic inside B_1. Thus, $\mathbf{\Lambda}_{\Delta t}$ can be expressed via its Laurent series

$$\mathbf{\Lambda}_{\Delta t}(z) = \sum_{\ell=0}^{\infty} \lambda_\ell^{\Delta t} z^\ell, \qquad |z| < 1. \tag{25}$$

The coefficients $\lambda_\ell^{\Delta t}$ are called convolution weights. Alternatively, they can be represented via the Cauchy integrals (with γ being a contour inside B_1):

$$\lambda_\ell^{\Delta t} = \frac{1}{2\pi i} \int_\gamma z^{-\ell-1} \mathbf{\Lambda}\left(i\frac{\delta(z)}{\Delta t}\right) dz. \tag{26}$$

$\Lambda(\partial_t^{\Delta t})$ as a convolution operator. Inverting the Z-transform in (23), using (25) and the property (21), we obtain the discretization of the reference DtN:

$$-\partial_s u_g^n(M^*) = \sum_{\ell=0}^{n} \lambda_\ell^{\Delta t} g^{n-\ell} =: \Lambda(\partial_t^{\Delta t}) g^n. \tag{27}$$

To compute the above convolution it is sufficient to know the convolution weights $\lambda_\ell^{\Delta t}$; classically [34], their evaluation is done based on the fast numerical computation of the Cauchy integrals (26), see Section 4.1.

Positivity properties of $\Lambda(\partial_t^{\Delta t})$. The following property, which we state here for consistency reasons, is a discrete version of Theorem 5.

Theorem 8 *Let $(g^n)_{n=0}^N \in \mathbb{R}^{N+1}$, with $g^0 = 0$. Then*

$$\sum_{n=1}^{N-1} \left\{\Lambda(\partial_t^{\Delta t}) g^n\right\}_{1/4} D_{\Delta t} g^n \geq 0.$$

Proof The proof mimics the proof of Theorem 5, namely, the result is obtained by testing (18) with $D_{\Delta t} u_g^n$. The details are left to the reader.

3.1.2 Discrete transparent BCs

To derive the discrete transparent boundary condition at the vertex $M_{m,j}$, corresponding to (8), we use the same arguments as in continuous case, cf. Sections 2.4.2 and 2.4.4. This yields the following discrete counterpart of (15):

$$\mathcal{B}_{m,j}\left(\partial_t^{\Delta t}\right) = \mu_{m,j}\alpha_{m,j}^{-1} \sum_{k=0}^{p-1} \frac{\mu_k}{\alpha_k} \Lambda\left(\alpha_{m,j}\alpha_k \partial_t^{\Delta t}\right), \tag{28}$$

where $\Lambda(\partial_t^{\Delta t})$ is defined in (19). The discrete symbol of the above operator is

$$\boldsymbol{\mathcal{B}}_{m,j}^{\Delta t}(z) = \mu_{m,j}\alpha_{m,j}^{-1} \sum_{k=0}^{p-1} \frac{\mu_k}{\alpha_k} \mathbf{\Lambda}\left(i\alpha_{m,j}\alpha_k \frac{\delta(z)}{\Delta t}\right), \tag{29}$$

cf. (24). As a consequence, the convolution weights $\left(b^{\Delta t}_{m,j;n}\right)$ of $\boldsymbol{\mathcal{B}}^{\Delta t}_{m,j}(z)$ are related to the convolution weights $\left(\lambda^{\Delta t}_{n}\right)$ via the simple identity

$$b^{\Delta t}_{m,j;n} = \mu_{m,j}\alpha^{-1}_{m,j}\sum_{k=0}^{p-1}\frac{\mu_k}{\alpha_k}\lambda_n^{\Delta t_{m,j;k}}, \qquad \Delta t_{m,j;k} = \frac{\Delta t}{\alpha_{m,j}\alpha_k}. \tag{30}$$

Finally, let us introduce the notation for the discrete version of the aggregate operator $\mathcal{B}_m(\partial_t)$, cf. (11): its discretization will be denoted by $\mathcal{B}_m(\partial_t^{\Delta t})$, the corresponding symbol by $\boldsymbol{\mathcal{B}}^{\Delta t}_m(z)$, and the respective convolution weights by $\boldsymbol{b}^{\Delta t}_{m,n}$ (remark that they are $m\times m$ diagonal matrices).

3.1.3 Motivation for the analysis that follows

One could first discretize (16) with the θ-scheme in time, next in space and proceed to its resolution, but in this case one would end up with an implicit scheme. Thus, we will proceed as follows (see [27] for a general framework):

- first semi-discretize the system (16) in space and perform the respective convergence analysis;
- next discretize the resulting system in time, using the explicit leapfrog scheme for the volume terms and trapezoid rule for the boundary terms.

3.2 Semi-discretization in space

3.2.1 Semi-discretization in space: basics

To semi-discretize the system (16) in space, we use the Lagrange $\mathbb{P}_1$-elements. Let us parametrize each edge $\Sigma_{n,j}$, identified with a segment $[M^*_{n,j},\, M_{n,j}]\subset\mathcal{T}^m$, with an abscissa $s_{n,j}\in(0,\alpha_{n,j})$, and define a quasi-uniform mesh

$$T_{n,j} = \{s^k_{n,j},\quad k=0,\dots,K_{n,j}\},\ \text{s.t. } s^k_{n,j} < s^{k+1}_{n,j}, \tag{31}$$

where $s^0_{n,j}$ is identified with $M^*_{n,j}$, and $s^{K_{n,j}}_{n,j}$ with $M_{n,j}$. The mesh on the truncated tree $\mathcal{T}^m$ is then defined as $\bigcup_{n=0}^{m}\bigcup_{j=0}^{p^n-1} T_{n,j}$. Let

$$h_{n,j} := \max_{1\le k\le K_{n,j}} |s^k_{n,j} - s^{k-1}_{n,j}|, \qquad h := \max_n \max_j h_{n,j}. \tag{32}$$

Let the finite element space be defined as $U_h\subset \boldsymbol{V}(\mathcal{T}^m)$, $U_h = \operatorname{span}\{\varphi_k,\ k=0,\dots,N_s-1\}$. The construction of this basis is classical on the nodes interior to $\Sigma_{n,j}$, but a special treatment is needed in the vertices of the graph $M_{n,j}$, see [2]: we define the respective shape function as a piecewise-linear function that equals to 1 in $M_{n,j}$ and vanishes in the rest of the nodes, see Figure 2. We denote by $u_h = \sum_{k=0}^{N_s-1} u_{(k)}\varphi_k$ an approximation to the exact solution u_m, with $u_{(k)}$ being a nodal value of u_h. Remark that for convenience we omit the index m in the definition of u_h.

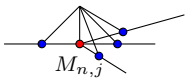

Fig. 2 A shape function φ s.t. $\varphi(M_{n,j}) = 1$.

3.2.2 Semi-discrete system: formulation and stability

The semi-discrete formulation of (16) with the exact transparent boundary conditions thus reads:
Find $u_h \in C^1([0,T];U_h)$, s.t. $u_h(.,0) = \partial_t u_h(.,0) = 0$, and, for all $v_h \in U_h$,

$$\left(\partial_t^2 u_h, v_h\right)_{\mathcal{T}^m} + (\partial_s u_h, \partial_s v_h)_{\mathcal{T}^m} + \langle \mathcal{B}_m(\partial_t)\boldsymbol{\gamma}_m u_h,\, \boldsymbol{\gamma}_m v_h\rangle = (f, v_h). \tag{33}$$

The stability of the above problem follows trivially using the argument of Theorem 1; however, the existence of the solution is somewhat more difficult. For analysis purposes, we will rewrite the above problem in a different form.

Rewriting of (33). Let us introduce the following two Hilbert spaces:

$$\begin{aligned} L_h &:= \{v \in \mathrm{L}^2_\mu(\mathcal{T}) :\ v|_{\mathcal{T}^m} \in U_h\}, \quad \|.\|_{L_h} := \|.\|_{\mathrm{L}^2_\mu}, \\ X_h &:= \{v \in V_{\mathfrak{n}}(\mathcal{T}) :\ v|_{\mathcal{T}^m} \in U_h\}, \qquad \|.\|_{X_h} := \|.\|_{\mathrm{H}^1_\mu}. \end{aligned} \tag{34}$$

Contrary to the space U_h, these spaces are infinite-dimensional. In particular, the restriction of functions from X_h to each $\mathcal{T}_{m,j}$ (see the end of Section 2.1 for the notation) coincides with the space $\mathrm{H}^1_\mu(\mathcal{T}_{m,j})$ (had we considered the Dirichlet problem, it would have coincided with $\mathrm{H}^1_{\mu,0}(\mathcal{T}_{m,j})$).
Let us now study the following counterpart of (33):

$$\begin{aligned} &\text{find } \bar{u}_h \in C([0,\,T];X_h) \cap C^1([0,T];L_h),\ \text{s.t. } \bar{u}_h(0) = \partial_t \bar{u}_h(0) = 0,\ \text{and} \\ &(\partial_t^2 \bar{u}_h, v_h) + (\partial_s \bar{u}_h, \partial_s v_h) = (f, v_h), \qquad \text{for all } v_h \in X_h. \end{aligned} \tag{35}$$

Using the above auxiliary problem, it is easy to show the well-posedness and stability of (33). Let us remark that this approach to the analysis of the coupled problem bears some similarities with [23,37], see also references therein.

Well-posedness and stability of (33). We proceed as follows: first, in Lemma 2 we show the well-posedness/stability of (35), next, in Lemma 3 argue that $\bar{u}_h|_{\mathcal{T}^m}$ solves (33). Finally, a complete well-posedness/stability result for (33) is summarized in Theorem 9.

Lemma 2 (Well-posedness, stability of (35)) *For all $f \in L^1(0,T;\mathrm{L}^2_\mu(\mathcal{T}))$, the problem (35) has a unique solution. Moreover, it satisfies the stability bound (7) with u replaced by $\bar{u}_h$.*

Proof The existence and uniqueness to (35) follows from the semigroup theory. In particular, let us introduce the operator $A_h : D(A_h) \to L_h$ defined for $v_h, w_h \in X_h$ by $(A_h v_h, w_h) = (\nabla v_h, \nabla w_h)$. Here

$$D(A_h) = \{v_h \in X_h : \exists C_{v_h} > 0,\ |a(v_h, w_h)| \le C_{v_h} \|w_h\|_{L_h},\ \forall w_h \in L_h\}.$$

Then the problem (35) can be reformulated as an abstract wave equation

$$\frac{d^2}{dt^2}\bar{u}_h + A_h \bar{u}_h = P_h f,$$

where P_h is an L^2_μ-orthogonal projector on L_h. We conclude using the same arguments as in the proof of Theorem 1. The stability bound also follows like in the proof of Theorem 1.

In the following we state that the solution of (35) solves (33).

Lemma 3 *Let $f \in L^1(0,T;\mathrm{L}^2_\mu(\mathcal{T}))$, and $\bar{u}_h$ solve (35). Then $u_h = \bar{u}_h|_{\mathcal{T}^m}$ satisfies (33).*

Proof We can split the variational formulation in (35) into two parts:

$$\begin{aligned}&(\partial_t^2 \bar{u}_h, v_h)_{\mathcal{T}^m} + (\partial_s \bar{u}_h, \partial_s v_h)_{\mathcal{T}^m} \\ &+ (\partial_t^2 \bar{u}_h, v_h)_{\mathcal{T}\setminus\mathcal{T}^m} + (\partial_s \bar{u}_h, \partial_s v_h)_{\mathcal{T}\setminus\mathcal{T}^m} = (f, v_h)_{\mathcal{T}^m}, \quad \forall v_h \in X_h.\end{aligned} \tag{36}$$

By definition (34) of X_h, the function $\bar{u}_h|_{\mathcal{T}\setminus\mathcal{T}^m} \in C([0,T];\mathrm{H}^1_\mu(\mathcal{T}\setminus\mathcal{T}^m))$. Moreover, taking the test functions v_h vanishing in $\mathcal{T}^m$, we deduce that

$$\begin{aligned}&(\partial_t^2 \bar{u}_h, v_h)_{\mathcal{T}\setminus\mathcal{T}^m} + (\partial_s \bar{u}_h, \partial_s v_h)_{\mathcal{T}\setminus\mathcal{T}^m} = 0,\\ &\text{for all } v_h \in \mathrm{H}^1_\mu(\mathcal{T}\setminus\mathcal{T}^m),\ \text{s.t. } v_h(M_{m,j}) = 0,\ j = 0,\dots,p^m - 1,\end{aligned}$$

i.e. (10), with appropriate boundary conditions in $M_{m,j}$. Integrating by parts the two last terms in rhs of (36) and using the definition of the transparent BCs (9) (and continuity of $\bar{u}_h$ in $M_{m,j}$, $j = 0,\dots,p^m - 1$), we conclude that $\bar{u}_h \in X_h$ satisfies

$$\begin{aligned}&(\partial_t^2 \bar{u}_h, v_h)_{\mathcal{T}^m} + (\partial_s \bar{u}_h, \partial_s v_h)_{\mathcal{T}^m} \\ &+ \langle \mathcal{B}_m(\partial_t)\boldsymbol{\gamma}_m \bar{u}_h, \boldsymbol{\gamma}_m v_h\rangle = (f, v_h)_{\mathcal{T}^m}, \qquad \forall v_h \in X_h.\end{aligned} \tag{37}$$

Because $X_h|_{\mathcal{T}^m} \equiv U_h$, we deduce that $\bar{u}_h|_{\mathcal{T}^m}$ solves (33).

The following theorem is a simple corollary of the two above results.

Theorem 9 (Well-posedness, stability of (33)) *For all $f \in L^1(0,T;\mathrm{L}^2_\mu(\mathcal{T}))$, the problem (33) has a unique solution. It satisfies*

$$\|\partial_t u_h(T)\|_{\mathcal{T}^m} + \|\partial_s u_h(T)\|_{\mathcal{T}^m} \le \sqrt{2}\|f\|_{L^1(0,T;\mathrm{L}^2_\mu(\mathcal{T}^m))}. \tag{38}$$

Proof Existence: by Lemma 2, there exists a unique $\bar{u}_h$ solving (33); by Lemma 3, $\bar{u}_h|_{\mathcal{T}^m} \in U_h$ satisfies (35). The uniqueness is a corollary of (38), which, in turn, follows from the same argument as in the proof of Theorem 7.

3.2.3 Convergence estimates for the spatial semi-discretization

In this section we will compare u_m solving (16) to u_h solving (33). The proofs presented below use classical techniques of convergence of FEM for time-dependent problems, see e.g. [27] and references therein, or the monograph [17, Chapter 6]. The difference between our case and these works lies in the fact that we analyze the problem (35), posed on an infinite-dimensional, rather than FEM, space. The principal result of this section is summarized below.

Theorem 10 (Convergence of the spatial discretization) *Let u_h solve (33), and u_m solve (16). Then, with $C(T) = C\max(1, T)$, $C > 0$,*

$$\|\partial_t(u_m - u_h)\|_{\mathrm{L}^2_\mu(\mathcal{T}^m)} + \|\partial_s(u_m - u_h)\|_{\mathrm{L}^2_\mu(\mathcal{T}^m)} \le C(T)h\|f\|_{W^{3,1}(0,T;\mathrm{L}^2_\mu(\mathcal{T}^m))}.$$

We will prove this result by comparing the solution u of (N) to the solution $\bar{u}_h$ of (35), which is justified by Theorem 7 and Lemma 3. Obviously,

$$\begin{aligned}\|\partial_t(u_m - u_h)\|_{\mathrm{L}^2_\mu(\mathcal{T}^m)} + \|\partial_s(u_m - u_h)\|_{\mathrm{L}^2_\mu(\mathcal{T}^m)} \le \\ \|\partial_t(u - \bar{u}_h)\|_{\mathrm{L}^2_\mu(\mathcal{T}^m)} + \|\partial_s(u - \bar{u}_h)\|_{\mathrm{L}^2_\mu(\mathcal{T})}.\end{aligned} \tag{39}$$

The proof itself is quite classical. Let us introduce an elliptic projection operator $P_h : V_{\mathtt{n}}(\mathcal{T}) \to X_h$ defined for $v \in V_{\mathtt{n}}(\mathcal{T})$ via

$$(v - P_h v, v_h)_{\mathcal{T}} + (\partial_s(v - P_h v), \partial_s v_h)_{\mathcal{T}} = 0, \qquad \text{for all } v_h \in X_h. \tag{40}$$

To analyze the convergence, we split the error into two parts:

$$u - \overline{u}_h = \eta_h + \varepsilon_h, \qquad \eta_h = u - P_h u, \qquad \varepsilon_h = P_h u - \overline{u}_h, \tag{41}$$

and estimate ε_h in terms of η_h (which, in turn, will be shown to be small), via the energy techniques. Let us first provide lemmas that quantify η_h.

Estimates on the projection error Let us introduce the space

$$\begin{aligned}&\widetilde{H}^2_\mu(\mathcal{T}^m) := \{u \in \mathrm{H}^1_\mu(\mathcal{T}^m) : \partial_s^2 u \in \mathrm{L}^2_\mu(\mathcal{T}^m)\},\\ &\|u\|^2_{\widetilde{H}^2_\mu(\mathcal{T}^m)} = \|u\|^2_{\mathcal{T}^m} + \|\partial_s u\|^2_{\mathcal{T}^m} + \int\limits_{\mathcal{T}^m} \mu \left|\partial_s^2 u\right|^2.\end{aligned}$$

The following is a usual approximation result extended to X_h.

Lemma 4 *For $v \in V_{\mathtt{n}}(\mathcal{T})$, s.t. $v|_{\mathcal{T}^m} \in \widetilde{H}^2_\mu(\mathcal{T}^m)$, it holds*

$$\|v - P_h v\|_{\mathrm{L}^2_\mu(\mathcal{T})} + \|\partial_s(v - P_h v)\|_{\mathrm{L}^2_\mu(\mathcal{T})} \le Ch\|\partial_s^2 v\|_{\mathrm{L}^2_\mu(\mathcal{T}^m)},$$

where C depends on p, m only.

Proof Thanks to Céa's Lemma,

$$\|v - P_h v\|_{\mathcal{T}} + \|\partial_s(v - P_h v)\|_{\mathcal{T}} \leq \inf_{v_h \in X_h} \|v - v_h\|_{\mathrm{H}^1_\mu(\mathcal{T})} \leq \inf_{v_h \in X_h:\ v_h|_{\mathcal{T}\setminus\mathcal{T}^m} = v|_{\mathcal{T}\setminus\mathcal{T}^m}} \|v - v_h\|_{\mathrm{H}^1_\mu(\mathcal{T}^m)}.$$

It suffices to bound the above quantity using as v_h a piecewise-linear interpolant of v on the mesh $\bigcup_{n=0}^{m} \bigcup_{j=0}^{p^n-1} T_{n,j}$. □

As a corollary of this result, we obtain the following.

Lemma 5 (Estimate for $\|\partial_t^k \eta_h\|$) *Let $f \in W^{3,1}([0,T], \mathrm{L}^2_\mu(\mathcal{T}))$, with $f(.,0) = \partial_t f(.,0) = \partial_t^2 f(.,0) = 0$. Let u solve (N) and η_h be defined in (41). Then,*

$$\|\partial_t^\ell \eta_h\|_{\mathrm{H}^1_\mu(\mathcal{T})} \leq Ch \|\partial_t^{\ell+1} f\|_{L^1(0,t;\mathrm{L}^2_\mu(\mathcal{T}))}, \qquad 0 \leq \ell \leq 2. \tag{42}$$

Proof By Lemma 4,

$$\|\partial_t^\ell \eta_h\|_{\mathrm{H}^1_\mu(\mathcal{T})} \leq Ch \|\partial_t^\ell \partial_s^2 u\|_{\mathrm{L}^2_\mu(\mathcal{T}^m)}. \tag{43}$$

Our goal is to provide an explicit bound for the right-hand side. By Corollary 1, $u \in C^4([0,T]; \mathrm{L}^2_\mu(\mathcal{T}))$. Moreover,

$$\partial_t^2 u - \partial_s^2 u = f, \quad \text{on } \Sigma_{n,j}, \qquad 0 \leq n \leq m, \qquad j = 0, \dots, p^n - 1. \tag{44}$$

Therefore,

$$\|\partial_t^\ell \partial_s^2 u\|_{\mathrm{L}^2_\mu(\mathcal{T}^m)} \leq \|\partial_t^{2+\ell} u\|_{\mathrm{L}^2_\mu(\mathcal{T}^m)} + \|\partial_t^\ell f\|_{\mathrm{L}^2_\mu(\mathcal{T}^m)}, \quad \ell = 0, \dots, 2. \tag{45}$$

To bound the first term we use the bound of Corollary 1; for the second term,

$$\|\partial_t^\ell f\|_{\mathrm{L}^2_\mu(\mathcal{T}^m)} = \left\| \int_0^t \partial_t^{\ell+1} f \, dt \right\|_{\mathrm{L}^2_\mu(\mathcal{T}^m)} \leq \int_0^t \left\| \partial_t^{\ell+1} f \right\|_{\mathrm{L}^2_\mu(\mathcal{T}^m)} d\tau.$$

Finally, (42) follows by combining all the above bounds with (43). □

Proof (Proof of Theorem 10) As discussed, see (39), we will compare the solution u of (N) to $\bar{u}_h$ from (35). With (41), we can see that $\varepsilon_h \in X_h$ satisfies

$$\left(\partial_t^2 \varepsilon_h, v_h\right) + (\partial_s \varepsilon_h, \partial_s v_h) = -(\partial_t^2 \eta_h, v_h) - (\partial_s \eta_h, \partial_s v_h), \qquad v_h \in X_h.$$

By (40) and the definition of η_h,

$$\left(\partial_t^2 \varepsilon_h, v_h\right) + (\partial_s \varepsilon_h, \partial_s v_h) = -(\partial_t^2 \eta_h, v_h) + (\eta_h, v_h), \qquad v_h \in X_h.$$

By Lemma 2, the bound (7) applies to ε_h defined as above; thus,

$$\|\partial_t \varepsilon_h(T)\| + \|\partial_s \varepsilon_h(T)\| \le C \int_0^T \left(\|\partial_t^2 \eta_h\|_{\mathrm{L}^2_\mu(\mathcal{T})} + \|\eta_h\|_{\mathrm{L}^2_\mu(\mathcal{T})} \right) dt$$
$$\le \tilde{C} h^2 T \int_0^T \left(\|\partial_t^3 f\|_{\mathrm{L}^2_\mu(\mathcal{T}^m)} + \|\partial_t f\|_{\mathrm{L}^2_\mu(\mathcal{T}^m)} \right) dt,$$

where the last inequality follows from (42). Combining the above bound with the triangle inequality

$$\|\partial_t(u - \overline{u}_h)\| + \|\partial_s(u - \overline{u}_h)\| \le \|\partial_t \eta_h\| + \|\partial_s \eta_h\| + \|\partial_t \varepsilon_h\| + \|\partial_s \varepsilon_h\|,$$

and using (42) to bound the first two terms in the right hand side, we obtain the desired result in the statement of the theorem. □

Remark 8 Obviously, the convergence is only $O(h)$ because we measure the error in the energy norm; using the Aubin-Nitsche techniques, we can deduce the convergence $O(h^2)$ when measuring $\|u - u_h\|$.

3.3 Fully discrete problem

3.3.1 Formulation

In what follows we denote by u_h^n ($\bar{u}_h^n$) a discrete approximation to $u_h(t^n)$ ($\bar{u}_h(t^n)$). To discretize (33) in time, as discussed in Section 3.1.3, we use the trapezoid rule, however, replace the implicit term $(\partial_s\{u^n\}_{1/4}, \partial_s v)_{\mathcal{T}^m}$ by an explicit discretization $(\partial_s u_h^n, \partial_s v_h)_{\mathcal{T}^m}$. To explain the intuition behind the stable discretization of the transparent boundary condition term, let us first start with the implicit discretization of the equivalent problem (35).

Derivation. The trapezoid rule discretization in time of (35) reads:

$$\left(D^2_{\Delta t} \bar{u}_h^n, v_h\right) + \left(\partial_s\{\bar{u}_h^n\}_{1/4}, \partial_s v_h\right) = (f^n, v_h), \qquad \forall v_h \in X_h. \tag{46}$$

The above can be equivalently rewritten as

$$\begin{aligned} &\left(D^2_{\Delta t} \bar{u}_h^n, v_h\right)_{\mathcal{T}^m} + \left(\partial_s\{\bar{u}_h^n\}_{1/4}, \partial_s v_h\right)_{\mathcal{T}^m} \\ &+ \left(D^2_{\Delta t} \bar{u}_h^n, v_h\right)_{\mathcal{T}\setminus\mathcal{T}^m} + \left(\partial_s\{\bar{u}_h^n\}_{1/4}, \partial_s v_h\right)_{\mathcal{T}\setminus\mathcal{T}^m} = (f^n, v_h)_{\mathcal{T}^m}, \quad \forall v_h \in X_h. \end{aligned} \tag{47}$$

It remains to integrate by parts the last two terms in the left hand side, similarly to the proof of Lemma 3. Because $\bar{u}_h^n|_{\mathcal{T}\setminus\mathcal{T}^m}, v_h|_{\mathcal{T}\setminus\mathcal{T}^m} \in \mathrm{H}^1_\mu(\mathcal{T}\setminus\mathcal{T}^m)$, we can use the definition of the discrete DtN, cf. (19) and Section 3.1.2:

$$\begin{aligned} &\left(D^2_{\Delta t} \bar{u}_h^n, v_h\right)_{\mathcal{T}^m} + \left(\partial_s\{\bar{u}_h^n\}_{1/4}, \partial_s v_h\right)_{\mathcal{T}^m} \\ &+ \langle\{\mathcal{B}_m(\partial_t^{\Delta t})\boldsymbol{\gamma}_m \bar{u}_h^n\}_{1/4}, \boldsymbol{\gamma}_m v_h\rangle = (f^n, v_h)_{\mathcal{T}^m}, \qquad \forall v_h \in X_h. \end{aligned} \tag{48}$$

The above formulation inherits its unconditional stability from (46): the corresponding energy identity can be obtained by testing the above with $D_{\Delta t}\bar{u}_h^n$. However, now the above problem is posed on a fully discrete space $X_h|_{\mathcal{T}^m} \equiv U_h$, and thus we can make it explicit, by attempting to preserve the property that the respective energy is obtained by testing the above with $D_{\Delta t}\bar{u}_h^n$. This is easily achieved by replacing the term $\{\bar{u}_h^n\}_{1/4}$ by $\bar{u}_h^n$, which results in the leap-frog discretization of the volume terms.

Fully discrete (16). Without loss of generality we will assume that the source term is sufficiently regular, and that $f(.,0) = \partial_t f(.,0) = 0$ (this will ensure that taking $u_h^1 = 0$ in the discretization does not alter the scheme order). In this case we end up with the following problem:

$$\begin{aligned}\text{find } (u_h^n)_{n=0}^{N_t} \subset U_h, \text{ s.t. } u_h^0 = 0, u_h^1 = 0, \text{ and for all } v_h \in U_h,\ 1 \le n \le N_t - 1,\\ \big(D_{\Delta t}^2 u_h^n, v_h\big)_{\mathcal{T}^m} + (\partial_s u_h^n, \partial_s v_h)_{\mathcal{T}^m} \\ + \langle \{\mathcal{B}_m(\partial_t^{\Delta t})\boldsymbol{\gamma}_m u_h^n\}_{1/4}, \boldsymbol{\gamma}_m v_h\rangle = (f^n, v_h)_{\mathcal{T}^m}.\end{aligned} \tag{49}$$

3.3.2 Well-posedness and stability of the fully discrete problem (49)

This section is dedicated to the stability analysis of (49). We will demonstrate that, provided that the CFL condition holds true, i.e.

$$C_{CFL}^2 = \left(\frac{\Delta t}{2}\right)^2 \sup_{v_h \in U_h : \|v_h\|_{\mathrm{L}^2_\mu(\mathcal{T}^m)}=1} \|\partial_s v_h\|^2_{\mathrm{L}^2_\mu(\mathcal{T}^m)} < 1, \tag{50}$$

the problem (49) is well-posed and stable.

Remark 9 It is easy to see that C_{CFL} can be reduced to the CFL number for the classical wave equation on the interval, and can be bounded independently of $\boldsymbol{\mu}$. For this let us introduce a broken space $\widetilde{U}_h = \bigoplus_{\Sigma \in \mathcal{T}^m} V_h(\Sigma)$. Here $V_h(\Sigma) \subset H^1(\Sigma)$ is a $\mathbb{P}_1$-finite element space constructed on the quasi-uniform mesh $T_{n,j}$ (see (31)) associated to the edge $\Sigma = \Sigma_{n,j}$. The space $\tilde{U}_h$ is larger than U_h, since the functions that lie in this space are not necessarily continuous in the vertices $M_{m,j}$ of the tree $\mathcal{T}^m$. Thus, by definition of the space $\tilde{U}_h$,

$$\begin{aligned} C_{CFL}^2 &\le \left(\frac{\Delta t}{2}\right)^2 \sup_{v_h \in \tilde{U}_h : \|v_h\|_{\mathrm{L}^2_\mu(\mathcal{T}^m)}=1} \|\partial_s v_h\|^2_{\mathrm{L}^2_\mu(\mathcal{T}^m)} \\ &= \left(\frac{\Delta t}{2}\right)^2 \sup_{v_h^{n,j} \in V_h(\Sigma_{n,j}) :\, \|v_h\|_{\mathrm{L}^2_\mu(\mathcal{T}^m)} \neq 0} \frac{\sum_{n=0}^{m} \sum_{j=0}^{p^n-1} \int_{\Sigma_{n,j}} \mu_{n,j} |\partial_s v_h|^2 ds}{\sum_{n=0}^{m} \sum_{j=0}^{p^n-1} \int_{\Sigma_{n,j}} \mu_{n,j} |v_h|^2 ds} \\ &\le \left(\frac{\Delta t}{2}\right)^2 \max_{\substack{0 \le n \le m,\\ 0 \le j \le p^n - 1}} \sup_{v_h \in V_h(\Sigma_{n,j}) \setminus \{0\}} \frac{\int_{\Sigma_{n,j}} \mu_{n,j} |\partial_s v_h|^2 ds}{\int_{\Sigma_{n,j}} \mu_{n,j} |v_h|^2 ds}, \end{aligned} \tag{51}$$

where the last inequality follows from $\left(\sum_{i=1}^{n}\lambda_i\right)\left(\sum_{i=1}^{n}\eta_i\right)^{-1} \le \max_{i=1,\dots,n}\lambda_i\eta_i^{-1}$. In other words,

$$C_{CFL}^2 \le \max_{\Sigma\in\mathcal{T}^m}\left(\frac{\Delta t}{2}\right)^2 \sup_{\substack{v_h\in V_h(\Sigma):\\ \|v_h\|_{L^2(\Sigma)}=1}} \int_{\Sigma} |\partial_s v_h|^2 ds$$

where in the last expression we recognize the CFL number (squared) for the trapezoid-rule/$\mathbb{P}_1$-discretization (on the mesh $T_{n,j}$ associated to the edge $\Sigma = \Sigma_{n,j}$) for the non-weighted wave equation with Neumann BCs on Σ.

Theorem 11 *Let (50) hold true. For all $(f^n)_{n=0}^{N_t-1} \subset \mathrm{L}^2_\mu(\mathcal{T}^m)$, the problem (49) has a unique solution $(u_h^n)_{n=0}^{N_t}$. Moreover, the discrete energy*

$$\begin{aligned} E_h^{n+\frac12} = \frac12\left(\left\|D_{\Delta t}u_h^{n+\frac12}\right\|_{\mathcal{T}^m}^2 - \left(\frac{\Delta t}{2}\right)^2\left\|\partial_s D_{\Delta t}u_h^{n+\frac12}\right\|_{\mathcal{T}^m}^2\right) \\ + \frac12\|\partial_s u_h^{n+\frac12}\|_{\mathcal{T}^m}^2 \end{aligned} \tag{52}$$

satisfies $\sqrt{E_h^{n+\frac12}} \le C\Delta t\sum_{k=1}^{n}\|f^k\|_{\mathcal{T}^m}$, where C depends on the CFL (50) only.

Remark 10 It is not difficult to verify that when (50) holds true, $E_h^{n+1/2}$ defines an energy: with $v_h^{n+\frac12} := D_{\Delta t}u_h^{n+\frac12}$,

$$\left\|v_h^{n+\frac12}\right\|_{\mathcal{T}^m}^2 - \left(\frac{\Delta t}{2}\right)^2\left\|\partial_s v_h^{n+\frac12}\right\|_{\mathcal{T}^m}^2 \ge (1-C_{CFL}^2)\left\|v_h^{n+\frac12}\right\|_{\mathcal{T}^m}^2. \tag{53}$$

Proof It suffices to show the stability bound (52), which implies uniqueness. Then the existence is obvious, since the problem is finite-dimensional.
Derivation of (52) is simple: testing (49) written for $n=k$ with $D_{\Delta t}u_h^k$ yields

$$\frac{1}{\Delta t}\left(E_h^{k+\frac12} - E_h^{k-\frac12}\right) + \langle\{\mathcal{B}_m(\partial_t^{\Delta t})\boldsymbol{\gamma}_m u_h^k\}_{1/4},\, D_{\Delta t}\boldsymbol{\gamma}_m u_h^k\rangle = (f^k, D_{\Delta t}u_h^k)_{\mathcal{T}^m}.$$

Summing the above in $k=1,\dots,n$, and using $E_h^{\frac12}=0$ results in

$$\begin{aligned} E_h^{n+\frac12} + \Delta t\sum_{k=1}^{n}\langle\{\mathcal{B}_m(\partial_t^{\Delta t})\boldsymbol{\gamma}_m u_h^k\}_{1/4},\, D_{\Delta t}\boldsymbol{\gamma}_m u_h^k\rangle \\ = \Delta t\sum_{k=1}^{n}(f^k, D_{\Delta t}u_h^k)_{\mathcal{T}^m}. \end{aligned} \tag{54}$$

Let us bound the right-hand side via $E_h^{j+\frac12}$, $j\le n$. First of all,

$$\left\|D_{\Delta t}u_h^k\right\|_{\mathcal{T}^m} \le \frac12\left(\|D_{\Delta t}u_h^{k+\frac12}\|_{\mathcal{T}^m} + \|D_{\Delta t}u_h^{k-\frac12}\|_{\mathcal{T}^m}\right) \overset{(53)}{\le} C\left(\sqrt{E_h^{k+\frac12}} + \sqrt{E_h^{k-\frac12}}\right).$$

The above yields (where we again use $E_h^{\frac{1}{2}} = 0$)

$$\left| \Delta t \sum_{k=1}^{n} (f^k, D_{\Delta t} u_h^k)_{\mathcal{T}^m} \right| \leq C\Delta t \left(\|f^n\|_{\mathcal{T}^m} \sqrt{E_h^{n+\frac{1}{2}}} + \sum_{k=1}^{n-1} \left(\left\|f^k\right\|_{\mathcal{T}^m} + \left\|f^{k+1}\right\|_{\mathcal{T}^m} \right) \sqrt{E_h^{k+\frac{1}{2}}} \right). \tag{55}$$

Since the last term in the left-hand side of (54) is non-negative (see (28) and Theorem 8), we deduce that

$$E_h^{n+\frac{1}{2}} \leq C\Delta t \left(\|f^n\|_{\mathcal{T}^m} \sqrt{E_h^{k+\frac{1}{2}}} + \sum_{k=0}^{n-1} \left(\left\|f^k\right\|_{\mathcal{T}^m} + \left\|f^{k+1}\right\|_{\mathcal{T}^m} \right) \sqrt{E_h^{k+\frac{1}{2}}} \right).$$

The discrete Gronwall inequality yields the desired stability bound. □

3.3.3 Convergence of the time discretization

The principal result of this section reads.

Theorem 12 *Given $f \in W^{3,1}(0, T; \mathrm{L}^2_\mu(\mathcal{T}^m))$ with $f(.,0) = \partial_t f(.,0) = \partial_t^2 f(.,0) = 0$, let u_h solve (33), and u_h^n be the solution to (49), with the CFL condition (50) holding true. Then*

$$\|u_h(t^n) - u_h^n\|_{\mathcal{T}^m} + \left\| \partial_s (u_h(t^{n-\frac{1}{2}}) - u_h^{n-\frac{1}{2}}) \right\|_{\mathcal{T}^m} \leq C(t^n)(\Delta t)^2 \int_0^{t_n} \|\partial_t^3 f\|_{\mathcal{T}^m} dt,$$

where $C(t^n) = C \max(1, t^n)^2$, and $C > 0$.

To prove the convergence of the time discretization, we will use an idea already employed in Section 3.2, where we reformulated the problem (33), posed on the truncated tree $\mathcal{T}^m$, in the form (35), posed on the tree $\mathcal{T}$.

Let us remark that such a result can be alternatively obtained by using the existing convergence estimates for the trapezoid rule discretization of the operator $\mathcal{B}_m(\partial_t)$, see [4, Appendix A] or a recent work [18], which requires frequency dependent coercivity/continuity bounds on the symbol $\boldsymbol{\mathcal{B}}_m(\omega)$. However this may lead to non-optimal estimates (at least in terms of the powers of the final time).

An auxiliary problem used for the analysis of (49). The auxiliary problem which will serve the analysis purposes resembles an explicit version of (47):

$$\begin{aligned} &\text{Given } \bar{u}_h^0 = \bar{u}_h^1 = 0, \text{ find } (\bar{u}_h^n)_{n=0}^{N_t} \subset X_h, \text{ s.t. for all } v \in X_h,\ 1 \leq n \leq N_t - 1, \\ &\left(D_{\Delta t}^2 \bar{u}_h^n, v\right)_{\mathcal{T}} + (\partial_s \bar{u}_h^n, \partial_s v)_{\mathcal{T}^m} + \left(\partial_s \{\bar{u}_h^n\}_{1/4}, \partial_s v\right)_{\mathcal{T}\setminus\mathcal{T}^m} = (f^n, v)_{\mathcal{T}^m}. \end{aligned} \tag{56}$$

We start with the well-posedness and stability result.

Lemma 6 (Well-posedness and stability of (56)) *For any* $(f^n) \subset \mathrm{L}^2_\mu(\mathcal{T})$, *the problem (56) has a unique solution.*

If, additionally, the CFL condition (50) holds true, then the energy

$$\overline{E}_h^{n+1/2} = \frac{1}{2}\left(\left\|D_{\Delta t}\bar{u}_h^{n+\frac{1}{2}}\right\|^2_{\mathcal{T}^m} - \left(\frac{\Delta t}{2}\right)^2 \left\|\partial_s D_{\Delta t}\bar{u}_h^{n+\frac{1}{2}}\right\|^2_{\mathcal{T}^m}\right) + \frac{1}{2}\|\partial_s \bar{u}_h^{n+1/2}\|^2_{\mathcal{T}^m} + \frac{1}{2}\left(\left\|D_{\Delta t}\bar{u}_h^{n+\frac{1}{2}}\right\|^2_{\mathcal{T}\setminus\mathcal{T}^m} + \|\partial_s \bar{u}_h^{n+1/2}\|^2_{\mathcal{T}\setminus\mathcal{T}^m}\right)$$

satisfies $\sqrt{\overline{E}_h^{n+\frac{1}{2}}} \leq C\Delta t \sum_{k=1}^{n} \|f^n\|$, *where* C *depends on the CFL (50) only.*

Proof Well-posedness. This part of the proof is slightly non-classical, because X_h is infinite-dimensional. On X_h we can define an equivalent scalar product:

$$(v,g)_{X_h} = \int_{\mathcal{T}} \mu(s)v(s)g(s) + \int_{\mathcal{T}\setminus\mathcal{T}^m} \mu(s)\partial_s v \partial_s g. \tag{57}$$

Equipped with above scalar product, X_h is a Hilbert space, because $X_h|_{\mathcal{T}^m} = U_h$, where U_h is a finite-dimensional space, and thus the respective norm is equivalent to the H^1_μ-norm on X_h.

Let us next rewrite (56), by singling out terms with $\bar{u}_h^{n+1}$, cf. (57):

$$\begin{aligned}\left(\bar{u}_h^{n+1}, v_h\right)_{\mathcal{T}} + \left(\frac{\Delta t}{2}\right)^2 (\partial_s \bar{u}_h^{n+1}, \partial_s v_h)_{\mathcal{T}\setminus\mathcal{T}^m} &= (\Delta t)^2 (f^n, v_h)_{\mathcal{T}^m} \\ &+ \left(2\bar{u}_h^n - \bar{u}_h^{n-1}, v_h\right)_{\mathcal{T}} - \left(\frac{\Delta t}{2}\right)^2 (\partial_s(2\bar{u}_h^n + \bar{u}_h^{n-1}), \partial_s v_h)_{\mathcal{T}\setminus\mathcal{T}^m} \\ &- (\Delta t)^2 (\partial_s \bar{u}_h^n, \partial_s v_h)_{\mathcal{T}^m}.\end{aligned}$$

The right-hand defines a bounded linear functional on X_h; in particular,

$$|(\partial_s \bar{u}_h^n, \partial_s v_h)_{\mathcal{T}^m}| \leq C(h)\|\bar{u}_h\|_{\mathcal{T}^m}\|v_h\|_{\mathcal{T}^m},$$

because $\bar{u}_h|_{\mathcal{T}^m}$, $v_h|_{\mathcal{T}^m} \in U_h$. The existence and uniqueness of the solution to the above are thus a direct consequence of the Lax-Milgram lemma (cf. (57)).

Stability. The stability proof mimics the proof of Theorem 11. □

The next lemma relates the problem (56) posed on X_h to (49) posed on U_h.

Lemma 7 *The solutions of (49) and (56) satisfy* $\bar{u}_h^n|_{\mathcal{T}^m} = u_h^n$, $0 \leq n \leq N_t - 1$.

Proof The proof is a trivial consequence of the definition of the discrete transparent boundary conditions, cf. Section 3.1.1, as well as the proof of Lemma 3 in the semi-discrete case.

We now have all the auxiliary results needed to prove Theorem 12.

Proof (Proof of Theorem 12) By Lemmas 3 and 7, instead of comparing $u_h(t^n)$ with u_h^n, we will compare the solution to (56) $\bar{u}_h(t^n)$ with $\bar{u}_h$ solving (35). The proof is not fully standard, because in one part of the domain in (56) an explicit scheme is used, while in the another part an implicit scheme is employed.
Step 1. Error bound in the energy norm. The error $e_h^n = \bar{u}_h^n - \bar{u}_h(t^n) \in X_h$ solves

$$\begin{aligned}&(D^2_{\Delta t} e_h^n, v_h)_{\mathcal{T}} + (\partial_s e_h^n, \partial_s v_h)_{\mathcal{T}^m} + (\partial_s \{e_h^n\}_{1/4}, \partial_s v_h)_{\mathcal{T}\setminus\mathcal{T}^m} \\ &= -(D^2_{\Delta t}\bar{u}_h(t^n) - \partial_t^2 \bar{u}_h(t^n), v_h)_{\mathcal{T}} - (\partial_s \left(\{\bar{u}_h(t^n)\}_{1/4} - \bar{u}_h(t^n)\right), \partial_s v_h)_{\mathcal{T}\setminus\mathcal{T}^m},\end{aligned} \tag{58}$$

with the initial condition $e_h^0 = 0$, and $e_h^1 = \bar{u}_h^1 - \bar{u}_h(t^1) \equiv -\bar{u}_h(t^1)$ to be quantified later. Let us denote by

$$\delta_h^n := D^2_{\Delta t}\bar{u}_h(t^n) - \partial_t^2 \bar{u}_h(t^n), \qquad \varepsilon_h^n := \partial_s \left(\{\bar{u}_h(t^n)\}_{1/4} - \bar{u}_h(t^n)\right).$$

Testing (58), written for $n = k$, with $v_h^k = D_{\Delta t} e_h^k$, we obtain

$$\frac{\overline{E}_e^{k+\frac{1}{2}} - \overline{E}_e^{k-\frac{1}{2}}}{\Delta t} = -(\delta_h^k, D_{\Delta t} e_h^k)_{\mathcal{T}} - (\varepsilon_h^k, D_{\Delta t}\partial_s e_h^k)_{\mathcal{T}\setminus\mathcal{T}^m}, \tag{59}$$

where $\overline{E}_e^{k+\frac{1}{2}}$ is the discrete energy norm of the error e_h^k:

$$\begin{aligned}\overline{E}_e^{k+\frac{1}{2}} = &\frac{1}{2}\left(\left\|D_{\Delta t} e_h^{k+\frac{1}{2}}\right\|^2_{\mathcal{T}^m} - \left(\frac{\Delta t}{2}\right)^2 \left\|\partial_s D_{\Delta t} e_h^{k+\frac{1}{2}}\right\|^2_{\mathcal{T}^m} + \left\|\partial_s e_h^{k+\frac{1}{2}}\right\|^2_{\mathcal{T}^m}\right) \\ &+ \frac{1}{2}\left(\left\|D_{\Delta t} e_h^{k+\frac{1}{2}}\right\|^2_{\mathcal{T}\setminus\mathcal{T}^m} + \left\|\partial_s e_h^{k+\frac{1}{2}}\right\|^2_{\mathcal{T}\setminus\mathcal{T}^m}\right).\end{aligned} \tag{60}$$

Summing (59) in $k = 1, \dots, n$, and next applying the discrete integration by parts to the sum involving $D_{\Delta t}\partial_s e_h^k$, we end up with the following identity:

$$\begin{aligned}\overline{E}_e^{n+\frac{1}{2}} = &\overline{E}_e^{\frac{1}{2}} - \Delta t \sum_{k=1}^{n} \left(\delta_h^k, D_{\Delta t} e_h^k\right)_{\mathcal{T}} \\ &- (\varepsilon_h^n, \partial_s e_h^{n+\frac{1}{2}})_{\mathcal{T}\setminus\mathcal{T}^m} + \Delta t \sum_{k=1}^{n-1} \left(\frac{\varepsilon_h^{k+1} - \varepsilon_h^k}{\Delta t}, \partial_s e_h^{k+\frac{1}{2}}\right)_{\mathcal{T}\setminus\mathcal{T}^m}.\end{aligned}$$

The second term in the rhs can be bounded like in the proof of Th. 11, cf. (55). For the two last terms we use the Cauchy-Schwartz inequality and (60):

$$\begin{aligned}\overline{E}_e^{n+\frac{1}{2}} \le &\overline{E}_e^{\frac{1}{2}} + C\left(\frac{\Delta t}{2}\|\delta_h^n\|\sqrt{\overline{E}_e^{n+\frac{1}{2}}} + \Delta t \sum_{k=0}^{n-1} \frac{\|\delta_h^k\| + \|\delta_h^{k+1}\|}{2}\sqrt{\overline{E}_e^{k+\frac{1}{2}}}\right. \\ &\left. + \|\varepsilon_h^n\|_{\mathcal{T}\setminus\mathcal{T}^m}\sqrt{\overline{E}_e^{n+\frac{1}{2}}} + \Delta t \sum_{k=1}^{n-1} \left\|\frac{\varepsilon_h^{k+1} - \varepsilon_h^k}{\Delta t}\right\|_{\mathcal{T}\setminus\mathcal{T}^m} \sqrt{\overline{E}_e^{k+\frac{1}{2}}}\right)\end{aligned}$$

The constant C depends on the CFL (50). Applying to the above the discrete Gronwall inequality, we obtain

$$\begin{aligned}\sqrt{\overline{E}_e^{n+\frac{1}{2}}} \leq \sqrt{\overline{E}_e^{\frac{1}{2}}} + C \Bigg(\Delta t \sum_{k=1}^{n} \|\delta_h^k\| \\ + \max_{0\leq k\leq n} \|\varepsilon_h^k\|_{\mathcal{T}\setminus\mathcal{T}^m} + \Delta t \sum_{k=1}^{n-1} \left\| \frac{\varepsilon_h^{k+1}-\varepsilon_h^k}{\Delta t} \right\|_{\mathcal{T}\setminus\mathcal{T}^m} \Bigg).\end{aligned} \tag{61}$$

Step 2.1. Bounding (61): the error stemming from approximating the initial conditions. This is very classical: indeed,

$$\overline{E}_e^{\frac{1}{2}} \leq \frac{1}{2}\left(\left\| D_{\Delta t} e_h^{\frac{1}{2}} \right\|_{\mathcal{T}}^2 + \left\| \partial_s e_h^{\frac{1}{2}} \right\|_{\mathcal{T}}^2 \right) = \frac{1}{2}\left(\Delta t^{-2} \|\bar{u}_h(t^1)\|^2 + \|\partial_s \bar{u}_h(t^1)\|^2 \right).$$

For the first term, using first the Taylor expansion, and then extending the bound of Corollary 1 to (35), cf. Lemma 2, we obtain

$$\|\bar{u}_h(t^1)\| \leq c(\Delta t)^2 \sup_{0\leq t\leq t^1} \|\partial_t^2 \bar{u}_h(t)\| \leq \int_0^{\Delta t} \|f'(t)\| dt \leq \Delta t \int_0^{\Delta t} \|f^{(2)}(t)\| dt.$$

The bound on the second term follows directly from Lemma 2:

$$\|\partial_s \bar{u}_h(t^1)\| \leq \int_0^{\Delta t} \|f(t)\| dt = \int_0^{\Delta t} \| \int_0^t \int_0^{\tau_2} f^{(2)}(\tau_1) d\tau_1 d\tau_2 \| dt \leq (\Delta t)^2 \int_0^{\Delta t} \|f^{(2)}(t)\| dt.$$

Combining the above bounds results in

$$\sqrt{\overline{E}_e^{\frac{1}{2}}} \leq C(\Delta t)^2 \int_0^t \|\partial_t^2 f\|_{\mathcal{T}^m} dt. \tag{62}$$

Bounding (61): the consistency error. To obtain a bound on the terms in the rhs in the above, we use the Taylor theorem:

$$\begin{aligned}\|\delta_h^k\| &\leq c(\Delta t)^2 \sup_{t\in(t^{k-1},t^{k+1})} \|\partial_t^4 \bar{u}_h(t)\|, \\ \|\varepsilon_h^k\|_{\mathcal{T}\setminus\mathcal{T}^m} &\leq c(\Delta t)^2 \sup_{t\in(t^{k-1},t^{k+1})} \|\partial_t^2 \partial_s \bar{u}_h(t)\|_{\mathcal{T}\setminus\mathcal{T}^m}, \\ \left\| \frac{\varepsilon_h^k - \varepsilon_h^{k-1}}{\Delta t} \right\|_{\mathcal{T}\setminus\mathcal{T}^m} &\leq c(\Delta t)^2 \sup_{t\in(t^{k-1},t^{k+1})} \|\partial_t^3 \partial_s \bar{u}_h(t)\|_{\mathcal{T}\setminus\mathcal{T}^m}\end{aligned}$$

Thus, plugging in the above and (62) into (61), results in (for some $C > 0$),

$$\sqrt{\overline{E}_e^{n+\frac{1}{2}}} \leq C(\Delta t)^2 \int_0^t \|\partial_t^2 f\|_{\mathcal{T}^m} dt + C(\Delta t)^2 \left(\sup_{t\in(0,t^{n+1})} \|\partial_t^2 \partial_s \bar{u}_h(t)\|_{\mathcal{T}\setminus\mathcal{T}^m} \right)$$
$$+ C(\Delta t)^2 (n\Delta t) \left(\sup_{t\in(0,t^{n+1})} \|\partial_t^3 \partial_s \bar{u}_h(t)\|_{\mathcal{T}\setminus\mathcal{T}^m} + \sup_{t\in(0,t^{n+1})} \|\partial_t^4 \bar{u}_h(t)\|_{\mathcal{T}\setminus\mathcal{T}^m} \right).$$

Finally, we

– employ the bound

$$\|\partial_t^2 \partial_s \bar{u}_h(t)\|_{\mathcal{T}\setminus\mathcal{T}^m} \leq \int_0^t \|\partial_\tau^3 \partial_s \bar{u}_h(\tau)\|_{\mathcal{T}\setminus\mathcal{T}^m} d\tau \leq t \sup_{\tau\in(0,t)} \|\partial_\tau^3 \partial_s \bar{u}_h(\tau)\|_{\mathcal{T}\setminus\mathcal{T}^m},$$

– apply the bound of Corollary 1, which can be extended to the semi-discretized system (35), to bound $\|\partial_t^3 \partial_s \bar{u}_h(t)\|$ and $\|\partial_t^4 \bar{u}_h\|$ (cf. Lemma 2).

This procedure yields the following bound, with $C > 0$ depending on C_{CFL}:

$$\sqrt{\overline{E}_e^{n+\frac{1}{2}}} \leq C(\Delta t)^2 \int_0^t \|\partial_t^2 f\|_{\mathcal{T}^m} dt + C(\Delta t)^2 t^{n+1} \|\partial_t^3 f\|_{L^1(0,t^{n+1};\mathrm{L}^2_\mu(\mathcal{T}^m))}.$$

The above, combined with (50), yields

$$\left\| \frac{e_h^{n+1} - e_h^n}{\Delta t} \right\|_{\mathcal{T}} + \left\| \partial_s e_h^{n+\frac{1}{2}} \right\|_{\mathcal{T}} \leq \tilde{C}(\Delta t)^2 t^{n+1} \left\| \partial_t^3 f \right\|_{L^1(0,t^{n+1};\mathrm{L}^2_\mu(\mathcal{T}))}. \tag{63}$$

Step 2. Estimating e_h^n. The bound for the error $\|e_h^n\|_{\mathcal{T}}$ from the statement of the theorem follows from a classical argument of telescopic sums. The estimate of $\|\partial_s e_h^n\|_{\mathcal{T}}$ is a corollary of

$$\|\partial_s \bar{u}_h(t^{n+1/2}) - \partial_s \bar{u}_h^{n+1/2}\|_{\mathcal{T}} \leq \|\partial_s e_h^{n+1/2}\|_{\mathcal{T}} \tag{64}$$
$$+ \left\| \partial_s \left(\frac{\bar{u}_h(t^{n+1}) + \bar{u}_h(t^n)}{2} - \bar{u}_h(t^{n+1/2}) \right) \right\|_{\mathcal{T}}.$$

The first summand is estimated using (63). The latter quantity can be bounded using the Taylor theorem and the Corollary 1 extended to (35):

$$\left\| \partial_s \frac{\bar{u}_h(t^{n+1}) + \bar{u}_h(t^n)}{2} - \partial_s \bar{u}_h(t^{n+1/2}) \right\|_{\mathcal{T}} \leq C(\Delta t)^2 \sup_{0\leq t\leq (n+1)\Delta t} |\partial_t^2 \bar{u}_h|^2_{\mathrm{H}^1_\mu(\mathcal{T})}$$
$$\leq C(\Delta t)^2 \int_0^{t^{n+1}} \|\partial_t^2 f\| dt \leq C(\Delta t)^2 t^{n+1} \int_0^{t^{n+1}} \|\partial_t^3 f\| dt. \tag{65}$$

Step 3. Estimating the error between the solutions of (49) and (33). Because of Lemmas 3, 7, the error between the solutions of (49) and (33) does not exceed the error between the solutions of (56) and (33), and hence the conclusion. □

3.3.4 Convergence of the time and space discretizations

The following is a corollary of Theorems 10 and 12.

Theorem 13 *Given $f \in W^{3,1}(0,\, T; \mathrm{L}^2_\mu(\mathcal{T}^m))$ with $f(.,0) = \ldots = \partial_t^2 f(.,0) = 0$, let u_m solve (16), and let u_h^n be the solution to (49), with the CFL condition (50) holding true. Then, for all $n \in \mathbb{N}$, s.t. $n\Delta t \leq T$,*

$$\|u_m(t^n) - u_h^n\|_{\mathcal{T}^m} + \|\partial_s u_m(t^{n-\frac{1}{2}}) - \partial_s u_h^{n-\frac{1}{2}}\|_{\mathcal{T}^m} \\ \leq C \max(1, t^n)^2 \left((\Delta t)^2 + h\right) \int_0^{t^n} \|\partial_t^3 f\| dt,$$

where $C > 0$ depends on the CFL.

3.4 Solving the fully discrete system (49). Complexity

In practice, to solve (49), we use the mass lumped FEM. This renders the respective system fully explicit. In fact, the only implicit terms are the boundary ones, which are essentially one-dimensional (and thus in total there are $p^m = O(1)$ of such terms). To see this, let us assume that $\ell > 0$ is s.t. u_ℓ^n (with an obvious abuse of notation: ℓ here is a spatial index, rather than m from $\mathcal{T}^m$) is a nodal value of u_h^n in $M_{m,j}$, and $u_{\ell-1}^n$ is the nodal value in the closest to $M_{m,j}$ node. Then mass-lumped (49) for u_ℓ^{n+1} reads

$$\frac{u_\ell^{n+1} - 2u_\ell^n + u_\ell^{n-1}}{(\Delta t)^2} + 2\frac{u_\ell^n - u_{\ell-1}^n}{h^2} \\ + \frac{2}{h}\frac{1}{4}\left(\sum_{k=0}^{n+1} b_{m,j;k}^{\Delta t} u_\ell^{n+1-k} + 2\sum_{k=0}^{n} b_{m,j;k}^{\Delta t} u_\ell^{n-k} + \sum_{k=0}^{n-1} b_{m,j;k}^{\Delta t} u_\ell^{n-1-k}\right) = 0.$$

It is easy to see that the above can be written in an explicit form. This nonetheless requires evaluating several discrete convolutions, each of $O(n)$ size, in order to compute the right-hand side. The total complexity of computing the solution to (56) is thus $O(N_t N_s) + O(N_t^2)$, where $O(N_t^2)$ comes from computation of the convolutions in the boundary terms.

4 Convolution quadrature: computing convolution weights

One of the major practical difficulties of the application of the CQ is linked to the computation of convolution weights $\boldsymbol{b}_{m,n}^{\Delta t}$, that is to say, $\lambda_n^{\Delta t}$, cf. (30), particularly in our case, as the symbol $\boldsymbol{\Lambda}(\omega)$ is not known in an explicit form.

4.1 Classical FFT-based algorithm for computing convolution weights

The convolution weights for $\mathcal{B}_m(\partial_t)$ can be expressed via the reference DtN convolution weights, see (30). The latter, in turn, can be evaluated by discretizing the Cauchy integral (26), first by choosing the contour γ as a circle of radius ρ, and next applying the N-point trapezoid quadrature ($N \geq N_t+1$):

$$\lambda_n^{\Delta t} \approx \frac{\rho^{-n}}{N} \sum_{k=0}^{N-1} \mathrm{e}^{-i\frac{2\pi kn}{N}} \mathbf{\Lambda}\left(\omega_k\right), \quad \omega_k = i\frac{\delta(\rho \mathrm{e}^{i\frac{2\pi k}{N}})}{\Delta t}, \qquad n = 0, \dots, N_t. \quad (66)$$

If the value of (26) does not depend on ρ, this is not the case for the above approximation. An optimal choice of ρ is ensured by minimizing the numerical error in the above expression, which is the sum of the quadrature error $O(\rho^N)$ and the error stemming from imprecise evaluation of $\mathbf{\Lambda}(\omega)$, estimated by $O(\rho^{-N_t}\varepsilon)$, cf. (66), where ε is the accuracy of evaluation of $\mathbf{\Lambda}(\omega)$. Crucially, this latter error can not be smaller than the machine epsilon. More details can be found in [34], [7] and [4]; see as well Section 4.3.1. In particular, the choice $N = N_t + 1$ and $\rho = \varepsilon^{\frac{1}{2N}}$ results in the error $O(\sqrt{\varepsilon})$.

Obviously, (66) can be easily computed via the FFT. Provided that the computational cost of evaluation of $\mathbf{\Lambda}(\omega_k)$ is bounded by $c_{\mathbf{\Lambda}}$, the above computations require $O(N_t \log N_t)$ time to perform the FFT, and $O(N_t c_{\mathbf{\Lambda}})$ to evaluate all $\mathbf{\Lambda}(\omega_k)$. Of course, these costs depend on ω_k, and, just like in the case of the exterior problem for the wave equation, cf. [4,5], increase with $\Delta t \to 0$. One of the main goals of this section is to quantify the efficiency of the CQ method for the approximation of the transparent BCs in fractal trees. This section is organized as follows:

- in Section 4.2 we present an algorithm to evaluate $\mathbf{\Lambda}(\omega)$, and very briefly discuss its stability, convergence and complexity. In the end, we will demonstrate how $\mathbf{\Lambda}(\omega)$ can be approximated efficiently when $\operatorname{Im}\omega$ is large enough.
- in Section 4.3 we will discuss the numerical aspects of (66): dependence of the error of evaluation of $\lambda_n^{\Delta t}$ depending on the error of evaluation of $\mathbf{\Lambda}(\omega)$, and, as a result, the choice of the parameters in (66); next, we will present a strategy to compute convolution weights, and then provide the respective asymptotic complexity bounds, as $\Delta t \to 0$.

Remark 11 When $\Delta t \to 0$, $|\mathbf{\Lambda}(\omega_k)| \sim |\omega_k|$, cf. Theorem 4. Since the frequencies $|\omega_k|$ grow at least as $O((\Delta t)^{-1})$ (cf. (66)), to preserve the $O(1)$ scaling as $\Delta t \to 0$, instead of computing the convolution weights for $\mathbf{\Lambda}(\omega)$, we compute the convolution weights for $\mathbf{\Lambda}^s(\omega) := (-i\omega)^{-1}\mathbf{\Lambda}(\omega)$. This can be incorporated into the coupled formulation (49) as follows. With (28),

$$\begin{aligned}\mathcal{B}_{m,j}(\partial_t^{\Delta t}) &= \mu_{m,j}\alpha_{m,j}^{-1} \sum_{k=0}^{p-1} \frac{\mu_k}{\alpha_k} \alpha_{m,j}\alpha_k \partial_t^{\Delta t} \Lambda^s\left(\alpha_{m,j}\alpha_k \partial_t^{\Delta t}\right) \\ &= \mu_{m,j}\partial_t^{\Delta t} \sum_{k=0}^{p-1} \mu_k \Lambda^s\left(\alpha_{m,j}\alpha_k \partial_t^{\Delta t}\right).\end{aligned}$$

Let us define the discrete operator

$$\mathcal{B}^s_{m,j}(\partial_t^{\Delta t}) := \mu_{m,j} \sum_{k=0}^{p-1} \mu_k \Lambda^s \left(\alpha_{m,j}\alpha_k \partial_t^{\Delta t}\right),$$

so that $\mathcal{B}_{m,j}(\partial_t^{\Delta t}) \equiv \partial_t^{\Delta t}\mathcal{B}^s_{m,j}(\partial_t^{\Delta t})$. Its discrete symbol reads

$$\boldsymbol{\mathcal{B}}^{s,\Delta t}_{m,j}(z) = \mu_{m,j} \sum_{k=0}^{p-1} \mu_k \boldsymbol{\Lambda}^s \left(i\alpha_{m,j}\alpha_k \frac{\delta(z)}{\Delta t}\right).$$

and the respective aggregate operator $\mathcal{B}^s_m(\partial_t^{\Delta t})$ is defined like in (11); see also Section 3.1.2. In the formulation (49) it suffices to replace $\{\mathcal{B}_m(\partial_t^{\Delta t})\boldsymbol{\gamma}_m u^n\}_{\frac{1}{4}}$ by $D_{\Delta t}\left(\mathcal{B}^s_m(\partial_t^{\Delta t})\boldsymbol{\gamma}_m u^n\right)$.

4.2 Evaluation of $\boldsymbol{\Lambda}(\omega)$

4.2.1 A method for computing $\boldsymbol{\Lambda}(\omega)$

The method for computation of $\boldsymbol{\Lambda}(\omega)$ presented in this section resembles the method of [29], which aims at approximation of $\boldsymbol{\Lambda}(\omega)$ in a domain of $\mathbb{C}^+ = \{\omega : \operatorname{Im}\omega > 0\}$. However, the approach of this article is better suited to the case when a highly accurate evaluation of $\boldsymbol{\Lambda}(\omega)$ at a set of points on a curve in a complex plane is needed, like in (66). It is based on the following ideas:

- to be able to evaluate $\boldsymbol{\Lambda}(\omega)$, it suffices to know the values of $\boldsymbol{\Lambda}(\alpha_i\omega)$, $i = 0, \dots, p-1$ (i.e., for p 'smaller' frequencies);
- for $|\omega| < r$, where r is a fixed value smaller than the first pole of $\boldsymbol{\Lambda}(\omega)$, $\boldsymbol{\Lambda}(\omega)$ can be accurately approximated by $2N_* + 2$ first terms of its Taylor expansion in zero. Provided $\{\lambda_{2n}\}_{n\in\mathbb{N}}$ even coefficients of the Taylor series for $\boldsymbol{\Lambda}(\omega)$ in $\omega = 0$ ($\boldsymbol{\Lambda}$ is even by Theorem 4), this approximation reads

$$\boldsymbol{\Lambda}(\omega) \approx \boldsymbol{\Lambda}^t_{r,N_*}(\omega) := \sum_{n=0}^{N_*} \lambda_{2n}\omega^{2n}. \tag{67}$$

  The coefficients λ_{2n} are computable, cf. [29, Appendix C]. The index t in $\boldsymbol{\Lambda}^t_{r,N_*}$ stands for 'truncated'.

To formulate the algorithm, let us fix $\omega \in \mathbb{C}^+$ for which we need to evaluate $\boldsymbol{\Lambda}(\omega)$, and introduce the following sets:

$$\mathcal{L}_n(\omega) := \{\boldsymbol{\Lambda}(\alpha_0^{k_0}\cdots\alpha_{p-1}^{k_{p-1}}\omega) : 0 \le k_i \le n,\ i = 0, \dots, p-1, \sum_{i=0}^{p-1} k_i = n\}.$$

These sets possess the following properties:

(a) the set $\mathcal{L}_0 = \{\boldsymbol{\Lambda}(\omega)\}$.

(b) given $\mathcal{L}_n(\omega)$, it is possible to compute all the elements in $\mathcal{L}_{n-1}(\omega)$ using the expression (14), rewritten below for the convenience of the reader:

$$\mathbf{\Lambda}(\omega) = -\omega \frac{\omega \tan\omega - \mathbf{F}_{\alpha,\mu}(\omega)}{\tan\omega \mathbf{F}_{\alpha,\mu}(\omega) + \omega}, \qquad \mathbf{F}_{\alpha,\mu}(\omega) = \sum_{i=0}^{p-1} \frac{\mu_i}{\alpha_i} \mathbf{\Lambda}(\alpha_i \omega) \tag{68}$$

This is immediate when $n = 1$, and not difficult to check for $n > 1$.

(c) in $\mathcal{L}_n$, there are $C_{n+p-1}^{p-1} = O(n^p)$ elements.

Given r as described before (67), let us assume that $|\omega| > r$ and fix L s.t.

$$|\boldsymbol{\alpha}|_\infty^L |\omega| < r, \quad \text{i.e. } L := L(\omega, r) = \left\lceil \left(\log |\boldsymbol{\alpha}|_\infty^{-1}\right)^{-1} \log \frac{|\omega|}{r} \right\rceil. \tag{69}$$

The above ensures that all the arguments of $\mathbf{\Lambda}(.)$ in $\mathcal{L}_L(\omega)$ satisfy:

$$\prod_{\ell=0}^{p-1} \alpha_\ell^{k_\ell} |\omega| \le (|\boldsymbol{\alpha}|_\infty)^{\sum_{\ell=0}^{p-1} k_\ell} |\omega| = |\boldsymbol{\alpha}|_\infty^L |\omega| < r.$$

Knowing all the elements in the set $\mathcal{L}_L(\omega)$, we can compute exactly the elements of $\mathcal{L}_{L-1}(\omega)$, then $\mathcal{L}_{L-2}(\omega)$, and so on, up to $\mathbf{\Lambda}(\omega)$. The method presented here is based on this idea, with the only modification that the elements in $\mathcal{L}_L(\omega)$ are approximated with the help of (67). The respective approximation of the sets $\mathcal{L}_n(\omega)$ will be denoted by $\mathcal{L}_n^*(\omega) = \mathcal{L}_n^*$.

By $\mathbf{\Lambda}_{k_0,\cdots,k_{p-1}}$ we will denote the approximation to $\mathbf{\Lambda}\left(\prod_{\ell=0}^{p-1} \alpha_\ell^{k_\ell} \omega\right)$.

procedure EvalLambda($\omega, N_*, r, \{\lambda_{2n}\}_{n=0}^{N_*}$)
  for $n = L, L-1, \ldots, 0$ **do**
    if $n = L$ **then**
      $\mathcal{L}_L^* \leftarrow \emptyset$
      for $k_i : 0 \le k_i \le L$, $i = 0, \ldots, p-1$, $\sum_{i=0}^{p-1} k_i = L$ **do**
        $\omega_{\boldsymbol{k}} \leftarrow \prod_{i=0}^{p-1} \alpha_i^{k_i} \omega$
        $\mathbf{\Lambda}_{k_0,\cdots,k_{p-1}} \leftarrow \sum_{n=0}^{N_*} \lambda_{2n} \omega_{\boldsymbol{k}}^{2n}$, see (67)
        $\mathcal{L}_L^* := \mathcal{L}_L^* \bigcup \{\mathbf{\Lambda}_{k_0,\cdots,k_{p-1}}\}$
      store $\mathcal{L}_L^*$
    else
      $\mathcal{L}_n^* \leftarrow \emptyset$
      for $k_i : 0 \le k_i \le n$, $i = 0, \ldots, p-1$, $\sum_{i=0}^{p-1} k_i = n$ **do**
        $\mathbf{F}_{\boldsymbol{k}}^* \leftarrow \sum_{\ell=0}^{p-1} \frac{\mu_\ell}{\alpha_\ell} \mathbf{\Lambda}_{k_0,k_1,\cdots,k_{\ell-1},k_\ell+1,k_{\ell+1},\cdots,k_{p-1}}$
  ▷ Remark that $\mathbf{\Lambda}_{k_0,k_1,\cdots,k_{\ell-1},k_\ell+1,k_{\ell+1},\cdots,k_{p-1}} \in \mathcal{L}_{n+1}^*$ for all $\ell = 0, \ldots, p-1$
  ▷ {$\mathbf{F}_{\boldsymbol{k}}$ plays a role of $\boldsymbol{F}_{\alpha,\mu}(\omega_{\boldsymbol{k}})$ in (68)}

$\omega_{\boldsymbol{k}} \leftarrow \prod_{i=0}^{p-1} \alpha_i^{k_i} \omega$

$\boldsymbol{\Lambda}_{k_0,\cdots,k_{p-1}} \leftarrow -\omega_{\boldsymbol{k}} \frac{\omega_{\boldsymbol{k}} \tan \omega_{\boldsymbol{k}} - \mathbf{F}^*_{\boldsymbol{k}}}{\tan \omega_{\boldsymbol{k}} \mathbf{F}^*_{\boldsymbol{k}} + \omega_{\boldsymbol{k}}}$

$\mathcal{L}^*_n := \mathcal{L}^*_n \bigcup \{\boldsymbol{\Lambda}_{k_0,\cdots,k_{p-1}}\}$

store $\mathcal{L}^*_n$

erase $\mathcal{L}^*_{n+1}$

return $\mathcal{L}^*_0$

Remark 12 A somewhat tricky part in the practical implementation of the above procedure is arranging and accessing the computed values in the sets $\mathcal{L}^*_n$; this nonetheless can be done efficiently, as described in the small section that follows.

Remark 13 In the above algorithm, the choice whether the DtN for the Dirichlet or Neumann problem is computed is encoded in the coefficients $\{\lambda_{2n}\}_{n=0}^{N_*}$.

Storing and accessing the values in $\mathcal{L}^*_n$; implementation of the method In our implementation of the method, we store and access the values of $\boldsymbol{\Lambda}$ in the sets $\mathcal{L}_n$ in the following manner.

Let L be fixed. We construct the tree which will store the values of $\boldsymbol{\Lambda}$ from $\mathcal{L}_n$ for all $n = 0, \ldots, p-1$. This leads to an extra minor memory overhead (which we will discuss later) compared to storing the sets $\mathcal{L}^n$ for each $n = L, \ldots, 0$ separately, but is somewhat easier to implement, and allows to generate a single tree for all the sets, as well as reformulate the above algorithm in terms of a simple recursive algorithm for computing $\boldsymbol{\Lambda}(\omega)$.

The main idea of this construction is that the value $\boldsymbol{\Lambda}(\prod_{k=0}^{p-1} \alpha_k^{n_k})$ is stored in the leaf of the tree, which can be located by the path $(n_0, 0) - (n_1, 1) - \ldots - (n_{p-1}, p-1)$, where (n_j, j) is the label of each of the vertices.

1. this tree has in total $p+1$ levels
2. each vertex is labelled by (k, ℓ), where ℓ is the level at which the vertex is located, and k corresponds to a power of α_ℓ (we'll explain later what it means). The root vertex is located at the level -1, and $n_\ell := 0$.
3. the root vertex has $L+1$ children, labelled as $(j, 0)$, with $j = 0, \ldots, L$.
4. the vertex $(j, 0)$ has $L+1-j$ children, labelled as $(L-j, 1)$, with $j = 0, \ldots, L$; In particular, the vertex $(L, 0)$ has 1 child, labelled as $(0, 1)$.
5. if the level $k < p$, and the vertex (j, k) has q children, its children are labelled as $(0, k+1), \cdots (q-1, k+1)$ and have correspondingly $q, q-1, \ldots, 1$ children.

Remark that the tree above can accomodate $\boldsymbol{\Lambda}(\prod_{k=0}^{p-1} \alpha_k^{n_k})$, for all $\sum_{k=0}^{p-1} n_k \leq L$.

An illustration of such a tree for $L = 2$ and $p = 3$ is given below.

This tree has the following properties.

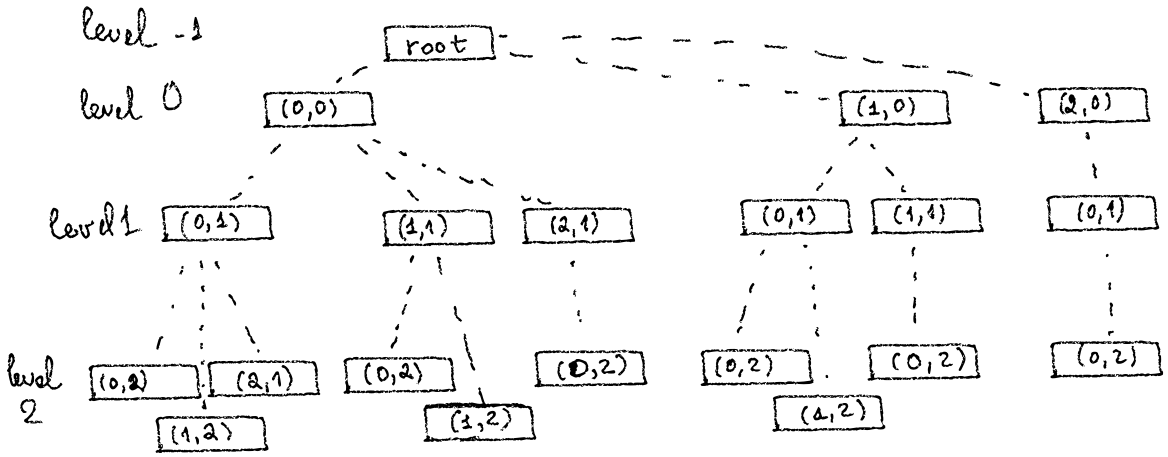

Fig. 3 The tree described in Section 4.2.1 for $L = 2$ and $p = 3$.

- in total it has $O(L^p)$ nodes. The number of nodes at each level $k = 0, \dots, p-1$ is bounded by L^k, and there are in total p levels. Then this is a geometric progression sum.
- the leaf vertices are uniquely identified by the sequences $(n_0, \dots, n_{p-1})$.
- accessing any vertex, provided the values $(n_0, \dots, n_{p-1})$, requires $O(p) = O(1)$ operations.

The recursive version of EvalLambda for computing $\mathbf{\Lambda}$ then proceeds as follows. Assume that each leaf vertex $(n_0, \dots, n_{p-1})$ has an extra label $IsLambdaSet$, which takes the value $true$, if $\mathbf{\Lambda}(\alpha^{n_0} \cdots \alpha^{n_{p-1}}\omega)$ had been computed, and $false$ otherwise.

We initialize it by the constructed tree with all leaf vertices having labels $IsLambdaSet = false$, and $(n_0, \dots, n_{p-1}) = (0, 0, \dots, 0)$.

We will assume that $Vertex(Tree, n_0, \dots, n_{p-1})$ returns a corresponding leaf vertex and $Vertex(Tree, n_0, \dots, n_{p-1}) \to \mathbf{\Lambda}$ the stored value in this vertex.

procedure EvalLambdaRecursive(Tree, $(n_0, \dots, n_{p-1}), \omega, N_*, r, \{\lambda_{2n}\}_{n=0}^{N_*}$)
  if Vertex(Tree, $n_0, \dots, n_{p-1}$)$\to$ IsLambdaSet **then**
    return Vertex(Tree, $n_0, \dots, n_{p-1}$)$\to \mathbf{\Lambda}$
  else
    for $k = 0, p-1$ **do**
      $\boldsymbol{n}_k \to (n_0, \dots, n_k + 1, \dots, n_{p-1})$
      if Vertex(Tree, $\boldsymbol{n}_k$)$\to$ IsLambdaSet **then**
        $\mathbf{\Lambda}_{\boldsymbol{n}_k} \leftarrow$ (Vertex(Tree, $\boldsymbol{n}_k$)$\to \mathbf{\Lambda}$)
      else
        if $\sum_{k=0}^{p-1} n_k + 1 = L$ **then**
          $\mathbf{\Lambda}_{\boldsymbol{n}_k} \leftarrow \sum_{n=0}^{N_*} \lambda_{2n} \omega_{\boldsymbol{n}_k}^{2n}$, see (67)
        else

$\mathbf{\Lambda}_{\boldsymbol{n}_k} \leftarrow$ EvalLambdaRecursive (Tree, $(\boldsymbol{n}_k), \omega, N_*, r, \{\lambda_{2n}\}_{n=0}^{N_*}$)
(Vertex(Tree, $\boldsymbol{n}_k$)$\rightarrow \mathbf{\Lambda}) \leftarrow \mathbf{\Lambda}_{\boldsymbol{n}_k}$
(Vertex(Tree, $\boldsymbol{n}_k$)$\rightarrow$ IsLambdaSet)$\leftarrow$ true
$\mathbf{F}^*_{\boldsymbol{n}} \leftarrow \sum_{k=0}^{p-1} \frac{\mu_k}{\alpha_k} \mathbf{\Lambda}_{\mathbf{n}_k}$
$\mathbf{\Lambda}_{\boldsymbol{n}} \leftarrow -\omega_{\boldsymbol{n}} \frac{\omega_{\boldsymbol{n}} \tan \omega_{\boldsymbol{n}} - \mathbf{F}^*_{\boldsymbol{n}}}{\tan \omega_{\boldsymbol{n}} \mathbf{F}^*_{\boldsymbol{n}} + \omega_{\boldsymbol{n}}}$
return $\mathbf{\Lambda}_{\boldsymbol{n}}$

4.2.2 Well-definiteness and convergence of the method

Well-definiteness. One could wonder whether using (68) may result in division by zero in the course of **EvalLambda**. The answer is given below.

Proposition 1 *There exists $r_H > 0$, s.t. for all $r < r_H$, $N_* \geq 0$, no division by zero occurs in the course of the procedure **EvalLambda** $(\omega, N_*, r, \{\lambda_{2n}\}_{n=0}^{N_*})$.*

The proof is based on the following auxiliary result. We remark that r_H in the result below is the same as in Proposition 1.

Lemma 8 *Let $\{\lambda_{2n}\}_{n=0}^{\infty}$ be even coefficients of the Laurent expansion of $\mathbf{\Lambda}(\omega)$ around $\omega = 0$. Then, there exists $r_H > 0$, s.t. for any $N_* > 0$,*

$$\operatorname{Im}\left(\omega^{-1} \sum_{k=0}^{N_*} \lambda_{2k} \omega^{2k}\right) < 0, \quad \text{for all } \omega \in \mathbb{C}^+ \cap \{z : |z| < r_H\}.$$

When $N_* = 0$, the inequality in the above is not necessarily strict.

Proof We will show that for all sufficiently small $\omega \in \mathbb{C}^+$,

$$\operatorname{sign} \operatorname{Im}\left(\omega^{-1} \sum_{k=0}^{N_*} \lambda_{2k} \omega^{2k}\right) = \operatorname{sign} \operatorname{Im}(\lambda_0 \omega^{-1} + \lambda_2 \omega) < 0, \qquad \text{for all } N_* \geq 1.$$

With Lemma 5.5, Corollary 5.6 in [29], we observe that

$$\lambda_0 \geq 0 \text{ and } \lambda_2 < 0. \tag{70}$$

Case $N_* \leq 1$. When $N_* = 1$, a direct calculation gives

$$\operatorname{Im}\left(\omega^{-1} \sum_{k=0}^{N_*} \lambda_{2k} \omega^{2k}\right) = \lambda_0 \operatorname{Im} \omega^{-1} + \lambda_2 \operatorname{Im} \omega < 0 \qquad \text{for all } \omega \in \mathbb{C}^+,$$

while when $N_* = 0$, the above holds with $<$ replaced by $\leq$.
Case $N_* \geq 2$. Let us now assume that $N_* \geq 2$. Given $\omega = |\omega| e^{i\varphi}$, $\varphi \in (0, \pi)$,

$$\begin{aligned} \operatorname{Im}\left(\omega^{-1} \sum_{k=0}^{N_*} \lambda_{2k} \omega^{2k}\right) &= \sum_{k=0}^{N_*} \lambda_{2k} |\omega|^{2k-1} \sin(2k-1)\varphi \\ &= -\lambda_0 |\omega|^{-1} \sin \varphi + \lambda_2 |\omega| \sin \varphi + \sum_{k=2}^{N_*} \lambda_{2k} |\omega|^{2k-1} \sin(2k-1)\varphi. \end{aligned}$$

Provided that the sum of the first two terms is strictly negative, cf. (70), it suffices to show that the latter sum can be controlled. For this we use the following expression:

$$\sin(2k-1)\varphi = \sum_{\ell=0}^{k-1}(-1)^\ell C_{2k-1}^\ell \sin^{2\ell+1}\varphi\cos^{2(k-\ell-1)}\varphi,$$

which allows to rewrite

$$\operatorname{Im}\left(\omega^{-1}\sum_{k=0}^{N_*}\lambda_{2k}\omega^{2k}\right) = \sin\varphi\,\left(-\lambda_0|\omega|^{-1}+\lambda_2|\omega|+Q(\omega,\varphi)\right), \tag{71}$$

$$Q(\omega,\varphi) = \sum_{k=2}^{N_*}\lambda_{2k}\,|\omega|^{2k-1}\sum_{\ell=0}^{k-1}(-1)^\ell C_{2k-1}^\ell \sin^{2\ell}\varphi\cos^{2(k-\ell-1)}\varphi.$$

A uniform in φ bound for $Q(\omega,\varphi)$ follows from the Cauchy estimate for $\lambda_{2\ell}$ [19, p.118]:

$$|\lambda_{2\ell}| \le M_\rho \rho^{-2\ell}, \qquad \text{for all } 0<\rho<\omega_0, \tag{72}$$

where ω_0 is the smallest positive pole of $\mathbf{\Lambda}(\omega)$, and $M_\rho = \max\limits_{z\in B_\rho(0)}|\mathbf{\Lambda}(\omega)|$. Fixing $\rho>0$, and applying the above estimate to bound $|\lambda_{2k}|$ in $Q(\omega,\varphi)$ results in

$$\begin{aligned}|Q(\omega,\varphi)| &\le M_\rho\sum_{k=2}^{N_*}\rho^{-2k}\,|\omega|^{2k-1}\sum_{\ell=0}^{k-1}C_{2k-1}^\ell\left|\sin^{2\ell}\varphi\cos^{2(k-\ell-1)}\varphi\right| \\ &\le M_\rho\sum_{k=2}^{N_*}\rho^{-2k}\,|\omega|^{2k-1}\sum_{\ell=0}^{2k-1}C_{2k-1}^\ell = 2M_\rho\sum_{k=2}^{N_*}\rho^{-2k}\,|2\omega|^{2k-1} \le C_\rho|\omega|^3,\end{aligned}$$

for some $C_\rho>0$, where the last bound holds for all sufficiently small $|\omega|$. By (71), for all $\omega=|\omega|\mathrm{e}^{i\varphi}\in\mathbb{C}^+$, s.t. $|\omega|$ is sufficiently small, it holds

$$\operatorname{sign}\operatorname{Im}\left(\omega^{-1}\sum_{k=0}^{N_*}\lambda_{2k}\omega^{2k}\right) = \operatorname{sign}\left(\sin\varphi\left(-\lambda_0|\omega|^{-1}+\lambda_2|\omega|\right)\right) \overset{(70)}{<} 0. \qquad \square$$

Proof (Proof of Proposition 1) To prove the statement of the proposition, we will use the same idea as in Lemma 5.15 in [29]. It suffices to show that

$$\operatorname{Im}\left(\omega^{-1}\mathbf{\Lambda}_{r,N_*}\left(\prod_{k=0}^{p-1}\alpha_k^{n_k}\omega\right)\right)<0, \qquad \text{s.t. } \sum_{k=0}^{p-1}n_k = L, \tag{73}$$

i.e. for all elements of $\mathcal{L}_L^*(\omega)$. Then, by Lemma 5.13 in [29], the same holds true for the elements of $\mathcal{L}_{L-1}^*$, as they are computed with the help of (68) (and thus by induction for $\mathcal{L}_n^*$, $n\le L-2$). Let us remark that it can be shown (by a trivial generalization of the result of Lemma 5.13), that it suffices to have the equality sign in (73).

Recall that the elements from $\mathcal{L}_L^*$ are computed with the help of (67). Provided $\sum_{k=0}^{p-1} n_k = L$, the quantity $\prod_{k=0}^{p-1} \alpha_k^{n_k}\omega \in \mathbb{C}^+$, and, moreover, belongs to $B(0,r)$, where r is from (69). Hence it suffices to show that exists $r_0 > 0$, s.t. for all $r < r_0$, $N_* \geq 0$,

$$\mathrm{Im}\left(\omega^{-1}\sum_{n=0}^{N_*}\lambda_{2n}\omega^{2n}\right) \leq 0, \qquad \omega \in \mathbb{C}^+ \cap B(0,r).$$

This had been shown in Lemma 8.

From the proof of the above result we obtain the corollary almost immediately (in the formulation of the corollary we use the notation from the procedure ***EvalLambda***).

Corollary 2 *With $r_H > 0$ like in Proposition 1, all the quantities $\mathbf{\Lambda_k}$ computed in the course of the algorithm* $\boldsymbol{EvalLambda}(\omega, r, N_*, \{\lambda_{2n}\}_{n=0}^{N_*})$*, with $r < r_H$, $N_* \geq 0$, $\omega \in \mathbb{C}^+$, satisfy*

$$\mathrm{Im}\,(\omega_{\boldsymbol{k}}\mathbf{\Lambda_k}) \leq 0.$$

Convergence. There are two parameters in the method that affect its accuracy: N_* and r. Let us denote by $\mathbf{\Lambda}_{r,N_*}(\omega)$ the solution computed with the help of the procedure **EvalLambda** $(\omega, N_*, r, \{\lambda_{2n}\}_{n=0}^{N_*})$, and let

$$E_{r,N_*}(\omega) := \left|\mathbf{\Lambda}_{r,N_*}(\omega) - \mathbf{\Lambda}(\omega)\right|.$$

We study separately two cases: the 'low-frequency' case $|\omega| \leq r$, i.e. $\mathbf{\Lambda}(\omega)$ is approximated by (67), and the 'high-frequency' case $|\omega| > r$.

Theorem 14 (Low-frequency case) *For all $\rho < \omega_0$, where ω_0 is the smallest positive pole of $\mathbf{\Lambda}(\omega)$, and all $r < \rho$, $N_* \geq 0$, for all $\omega \in \mathbb{C}^+$, s.t. $|\omega| \leq r$,*

$$E_{r,N_*}(\omega) < C_\rho\left(1 - \frac{r^2}{\rho^2}\right)^{-1}\left(\frac{r}{\rho}\right)^{2N_*+2}, \qquad C_\rho > 0.$$

Proof The estimate is a trivial consequence of the Cauchy estimates for the coefficients of $\mathbf{\Lambda}(\omega)$. Recall that the coefficients $\{\lambda_{2n}\}_{n\geq 0}$ of the Taylor expansion of $\mathbf{\Lambda}(\omega)$ in $\omega = 0$ satisfy the Cauchy estimate (72).

Thus, for all $|\omega| < \rho$ and $N_* \geq 0$,

$$\begin{aligned} |E_{r,N_*}(\omega)| &= \left|\sum_{n=N_*+1}^{\infty}\lambda_{2n}\omega^{2n}\right| \leq \sum_{n=N_*+1}^{\infty}|\lambda_{2n}||\omega^{2n}| \\ &\leq M_\rho\left(\frac{|\omega|}{\rho}\right)^{2N_*+2}(1-|\omega|^{-2}\rho^{-2})^{-1}. \end{aligned} \tag{74}$$

The estimate in the statement of Theorem follows by taking $|\omega| = r$.

To formulate the high-frequency counterpart of the above, let us introduce

$$N_0 = \min\left\{\ell \geq 0 : \sum_{i=0}^{p-1} \mu_i \alpha_i^{2\ell+1} < 1\right\}, \tag{75}$$

$$\mathbb{C}^+_{a,r_b} := \{z \in \mathbb{C} : \operatorname{Im} z > a,\ |z| > r_b\}. \tag{76}$$

Theorem 15 (High-frequency case) *Let $\rho > 0$ be fixed, and be like in Theorem 14. There exists r_0, which depends on ρ, $\boldsymbol{\mu}$, $\boldsymbol{\alpha}$ only, s.t. for all $r < r_0$, $N_* \geq N_0$, and all $\omega \in \mathbb{C}^+_{a,r}$, where $a \in (0,1]$, it holds*

$$E_{r,N^*} \leq C_{\rho,\boldsymbol{\mu},\boldsymbol{\alpha}} \left(a^{-2}A\right)^{\gamma_\omega} B^{\gamma_\omega^2} \left(\frac{r}{\rho}\right)^{2N_*+2} r^{-\nu},$$

$$\gamma_\omega = \frac{\log|\omega|}{\log|\boldsymbol{\alpha}|_\infty^{-1}}, \quad \nu = \frac{\log(a^{-2}A)}{\log|\boldsymbol{\alpha}|_\infty^{-1}}.$$

The constants $C_{\rho,\boldsymbol{\mu},\boldsymbol{\alpha}}$, A, $B > 1$ depend only on ρ, $\boldsymbol{\alpha}$, $\boldsymbol{\mu}$ and the problem (Dirichlet or Neumann) in question.

Remark 14 Necessarily, $\tilde{r}_0 < r_0$, where r_0 is the same as in Proposition 1.

Theorems 14, 15 show that in order to ensure that $E(r, N_*) < \varepsilon$, we may fix $r > 0$ sufficiently small, and choose N_* so that, for some $C_j \geq 0$, $j = 1, \dots, 4$,

$$N_* \geq C_1 \log \varepsilon^{-1} + C_2 + \max(C_3 \log^2|\omega| + C_4 \log|\omega| \log a^{-1}, 0). \tag{77}$$

Let us now prove Theorem 15. The proof is quite technical and requires several additional lemmas.

Because the elements of $\mathcal{L}^*_{n-1}$ are computed using the set $\mathcal{L}^*_n$ and (14) (and the errors of approximation of elements computed from $\mathcal{L}_L$ are essentially given by 74), it suffices to understand how the error of approximating $\boldsymbol{\Lambda}(\alpha_i z)$ in (68) affects the computation of $\boldsymbol{\Lambda}(z)$.

Let z be fixed, and $\boldsymbol{\Lambda}_i^\varepsilon$ be an approximation to $\boldsymbol{\Lambda}(\alpha_i z)$, $i = 0, \dots, p-1$, and

$$\boldsymbol{\Lambda}^\varepsilon(z) := -z\frac{z\tan z - \boldsymbol{F}^\varepsilon_{\alpha,\mu}}{\tan z \boldsymbol{F}^\varepsilon_{\alpha,\mu} + z}, \qquad \boldsymbol{F}^\varepsilon_{\alpha,\mu} := \sum_{i=0}^{p-1} \frac{\mu_i}{\alpha_i} \boldsymbol{\Lambda}_i^\varepsilon. \tag{78}$$

Then, by replacing $\boldsymbol{\Lambda}^\varepsilon(z)$ from the above expression and $\boldsymbol{\Lambda}(z)$ from (68), we obtain

$$\begin{aligned}\boldsymbol{\Lambda}^\varepsilon(z) - \boldsymbol{\Lambda}(z) &= -z^2\left(\tan^2 z + 1\right)\frac{\boldsymbol{F}_{\alpha,\mu}(z) - \boldsymbol{F}^\varepsilon_{\alpha,\mu}}{(\boldsymbol{F}^\varepsilon_{\alpha,\mu}\tan z + z)(\boldsymbol{F}_{\alpha,\mu}\tan z + z)} \qquad (79)\\ &= T(z)\left(\boldsymbol{F}_{\alpha,\mu}(z) - \boldsymbol{F}^\varepsilon_{\alpha,\mu}\right),\\ T(z) &= \left(1 + \frac{1}{\tan^2 z}\right)\frac{1}{(\boldsymbol{F}^\varepsilon_{\alpha,\mu} z^{-1} + \cot z)(\boldsymbol{F}_{\alpha,\mu} z^{-1} + \cot z)}. \qquad (80)\end{aligned}$$

It remains to provide an adequate estimate on $T(z)$. It is given in Proposition below.

Proposition 2 *Let $z \in \mathbb{C}^+$ be fixed, and let $\mathbf{\Lambda}_i^\varepsilon \in \mathbb{C}$, $i = 0, \dots, p-1$, be s.t.* $\operatorname{Im}\left(\alpha_i^{-1} z^{-1} \mathbf{\Lambda}_i^\varepsilon\right) \le 0$ *for all $i = 0, \dots, p-1$. Let $T(z)$ be defined like in (80). Then there exists $C > 0$, independent of $\mathbf{\Lambda}_i^\varepsilon$, $\boldsymbol{\mu}$, $\boldsymbol{\alpha}$, z, s.t.*

$$|T(z)| \le C \max(1, (\operatorname{Im} z)^{-2}).$$

Proof First of all,

$$\left|\boldsymbol{F}^\varepsilon_{\alpha,\mu} z^{-1} + \cot z\right| \ge \left|\operatorname{Im}(\boldsymbol{F}^\varepsilon_{\alpha,\mu} z^{-1}) + \operatorname{Im}\cot z\right| \ge \left|\operatorname{Im}\cot z\right|,$$

because $\operatorname{Im}\cot z < 0$ (see (108), and $\operatorname{Im}(\boldsymbol{F}^\varepsilon_{\alpha,\mu} z^{-1}) < 0$, by the condition of Lemma. Using the same argument as in (129), we arrive at

$$\left|\boldsymbol{F}^\varepsilon_{\alpha,\mu} z^{-1} + \cot z\right| \ge |\operatorname{Im}\cot z| = \frac{1 - |\mathrm{e}^{iz}|^2}{|1 - \mathrm{e}^{iz}|^2}, \qquad \text{where } \mathrm{e}^{iz} = \mathrm{e}^{2iz}. \tag{81}$$

For the same reason (cf. Theorem 4(a)), the same lower bound holds for $\left|\boldsymbol{F}_{\boldsymbol{\alpha},\boldsymbol{\mu}} z^{-1} + \cot z\right|$. Thus,

$$\left|\frac{1}{(\boldsymbol{F}^\varepsilon_{\alpha,\mu} z^{-1} + \cot z)(\boldsymbol{F}_{\boldsymbol{\alpha},\boldsymbol{\mu}} z^{-1} + \cot z)}\right| \le \frac{|1 - \mathrm{e}^{iz}|^4}{(1 - |\mathrm{e}^{iz}|^2)^2}. \tag{82}$$

Next let us consider

$$1 + \frac{1}{\tan^2 z} = \frac{1}{\sin^2 z} = -\frac{4\mathrm{e}^{2iz}}{\left(\mathrm{e}^{2iz} - 1\right)^2} = -\frac{4\mathrm{e}^{iz}}{(\mathrm{e}^{iz} - 1)^2}.$$

Hence, combining the above with (82), we deduce

$$|T(z)| \le \frac{4|\mathrm{e}^{iz}|}{(1 - |\mathrm{e}^{iz}|^2)^2} |1 - \mathrm{e}^{iz}|^2 \overset{|\mathrm{e}^{iz}| \le 1}{\le} \frac{16}{\left(1 - \mathrm{e}^{-2\operatorname{Im} z}\right)^2} \le C \max(1, (\operatorname{Im} z)^{-2}),$$

where the last bound follows the same arguments as in the end of proof of Lemma 12 in Appendix B.

The problem with using the above result in (79) lies in the fact that the respective bound clearly deteriorates when $\operatorname{Im} z \to 0$, and that is why the above result is not sufficient to demonstrate the convergence of the method EvalLambda : the obtained bound is too pessimistic when $|z|$ is small. However, we can show that in the vicinity of $z = 0$, the dependence of the bound on $T(z)$ on $\operatorname{Im} z$ can be waived; this idea will be important for understanding the convergence of the method. To see this, we will rewrite the quantity $T(z)$ from (80) as follows:

$$T(z) = (1 + \tan^2 z) D^{-1}(z) \left(D^\varepsilon(z)\right)^{-1}, \tag{83}$$

$$D(z) := z^{-1} \tan z \sum_{i=0}^{p-1} \mu_i \alpha_i^{-1} \mathbf{\Lambda}(\alpha_i z) + 1, \tag{84}$$

$$D^\varepsilon(z) := z^{-1} \tan z \sum_{i=0}^{p-1} \mu_i \alpha_i^{-1} \mathbf{\Lambda}_i^\varepsilon + 1. \tag{85}$$

This is very easy to see when $\mathbf{\Lambda}_i^\varepsilon \equiv \mathbf{\Lambda}(\alpha_i z)$, and $\mathbf{\Lambda}(0) = 0$ (cf. Theorem 3): for small $|z|$, $D(z) = 1 + O(z^2)$, $D^\varepsilon(z) = 1 + O(z^2)$, and $(1 + \tan^2 z) = 1 + O(z^2)$, which shows that $T(z)$ is uniformly bounded in the vicinity of 0. This remains true if $\mathbf{\Lambda}_i^\varepsilon$ is sufficiently close to $\mathbf{\Lambda}(\alpha_i z)$.

The following proposition shows that the quantity $T(z)$ is bounded from above, when z is sufficiently small and $\mathbf{\Lambda}_i^\varepsilon$ are quantities from $\mathcal{L}_n^*$, with n sufficiently large, computed in the course of the procedure $\mathbf{EvalLambda}(\omega, N_*, r, \{\lambda_{2k}\}_{k=0}^{N_*})$.

Proposition 3 *Let N_0 be defined in (75), and $N_* \geq N_0$. Let ρ be like in Theorem 14.*

There exists $r_b > 0$, which depends on ρ, $\boldsymbol{\mu}$, $\boldsymbol{\alpha}$ only, s.t. the following holds true. Let the elements in $\mathcal{L}_n^*(\omega)$, $n \geq 0$, be evaluated in the course of $\boldsymbol{EvalLambda}(\omega, N_*, r, \{\lambda_{2k}\}_{k=0}^{N_*})$, with $r < r_b$.

Let n be s.t. $|\omega||\boldsymbol{\alpha}|_\infty^n < r_b$ and $n > L$. We denote by $\boldsymbol{n} := (n_0, \dots, n_{p-1})$, $\sum_{k=0}^{p-1} n_k = n$, $\boldsymbol{n}_k := (n_0, n_1, \dots, n_k + 1, \dots n_{p-2}, n_{p-1})$, and $\omega_{\boldsymbol{n}} = \omega \prod_{k=0}^{p-1} \alpha_k^{n_k}$. Then the quantities $T(\omega_{\boldsymbol{n}})$, defined in (83), with

$$\mathbf{\Lambda}_i^\varepsilon = \mathbf{\Lambda}_{\boldsymbol{n}_i},$$

are uniformly bounded: $|T(\omega_{\boldsymbol{n}})|\,| \leq \left(\sum_{i=0}^{p-1} \mu_i \alpha_i^{2N_0+1} \right)^{-1}$.

The proof of the above statement requires several auxiliary lemmas:

- we will first bound from below $|D(z)|$ for $|z|$ in the vicinity of $z = 0$
- next we bound $|D^\varepsilon(z)|$, provided that $|\mathbf{\Lambda}_i^\varepsilon - \mathbf{\Lambda}(\alpha_i z)| < C_\rho \left|\alpha_i z \rho^{-1}\right|^{2N_*+2}$, $N_* \geq 0$
- finally we show that when N_* is sufficiently large, the above approximation property holds for all values from $\mathcal{L}_n^*$.

Lemma 9 *Let $D(z)$ be defined in (84). There exists $w_0 > 0$ and a constant c, $c^* > 0$, s.t. for all $|z| < w_0$,*

$$|D(z)| > 1 - c|z|^2 > c^* > 0. \tag{86}$$

The quantities w_0, c, c^* depend on the problem in question (Neumann/Dirichlet), $\boldsymbol{\mu}$ and $\boldsymbol{\alpha}$.

Proof By to Theorem 3, $\mathbf{\Lambda}(0) = 0$ or $\mathbf{\Lambda}(0) = 1 - \left\langle \frac{\boldsymbol{\mu}}{\boldsymbol{\alpha}} \right\rangle^{-1}$. We consider accordingly the two cases:

1. let $\mathbf{\Lambda}(0) = 0$. In this case, with (74), we deduce that there exists $\tilde{\omega}_0$, s.t. for all $|z| < \tilde{\omega}_0$,

$$\left| \sum_{i=0}^{p-1} \mu_i \alpha_i^{-1} \mathbf{\Lambda}(\alpha_i z) \right| \leq M_{\tilde{\omega}_0} \tilde{\omega}_0^{-2} |z|^2 \leq C(\tilde{\omega}_0) |z|^2.$$

Also, there exists C_t and $\omega_t > 0$, s.t.

$$\left|\frac{\tan z}{z}\right| < C_t, \qquad \text{for all } |z| < \omega_t. \tag{87}$$

Hence, for all $|z| < \min(\tilde{\omega}_0, \omega_t)$

$$\left|z^{-1}\tan z \sum_{i=0}^{p-1} \mu_i \alpha_i^{-1} \mathbf{\Lambda}(\alpha_i z) + 1\right| > 1 - C(\tilde{\omega}_0) C_t |z|^2.$$

2. let $\mathbf{\Lambda}(0) = 1 - \left\langle \frac{\boldsymbol{\mu}}{\boldsymbol{\alpha}} \right\rangle^{-1}$. Recall, cf. Theorem 3, that this is possible only if $\left\langle \frac{\boldsymbol{\mu}}{\boldsymbol{\alpha}} \right\rangle > 1$.
Then $D(z)$ can be rewritten as follows

$$\begin{aligned} D(z) &= 1 + z^{-1}\tan z\, \mathbf{\Lambda}(0)\left\langle \frac{\boldsymbol{\mu}}{\boldsymbol{\alpha}} \right\rangle + z^{-1}\tan z \sum_{i=0}^{p-1} \frac{\mu_i}{\alpha_i}(\mathbf{\Lambda}(\alpha_i z) - \mathbf{\Lambda}(0)) \\ &= 1 + \mathbf{\Lambda}(0)\left\langle \frac{\boldsymbol{\mu}}{\boldsymbol{\alpha}} \right\rangle + (z^{-1}\tan z - 1)\mathbf{\Lambda}(0)\left\langle \frac{\boldsymbol{\mu}}{\boldsymbol{\alpha}} \right\rangle + z^{-1}\tan z \sum_{i=0}^{p-1} \frac{\mu_i}{\alpha_i}(\mathbf{\Lambda}(\alpha_i z) - \mathbf{\Lambda}(0)) \\ &= \left\langle \frac{\boldsymbol{\mu}}{\boldsymbol{\alpha}} \right\rangle + (z^{-1}\tan z - 1)\mathbf{\Lambda}(0)\left\langle \frac{\boldsymbol{\mu}}{\boldsymbol{\alpha}} \right\rangle + z^{-1}\tan z \sum_{i=0}^{p-1} \frac{\mu_i}{\alpha_i}(\mathbf{\Lambda}(\alpha_i z) - \mathbf{\Lambda}(0)). \end{aligned} \tag{88}$$

With (74), for all $|z| < \tilde{\omega}_0$,

$$\left|\sum_{i=0}^{p-1} \frac{\mu_i}{\alpha_i}(\mathbf{\Lambda}(\alpha_i z) - \mathbf{\Lambda}(0))\right| < C(\tilde{\omega}_0)|z|^2. \tag{89}$$

Moreover, there exists $\omega_{t,2} > 0$, s.t.

$$\left|\frac{\tan z}{z} - 1\right| < C_{t,2}|z|^2, \qquad \text{for all } |z| < \omega_{t,2}.$$

Then, using the above bound for the second term in (88), (87) and (89) for the third term, we deduce that there exists $C_1 > 0$, s.t. for all $|z| <$ sufficiently small, it holds

$$|D(z)| > \left\langle \frac{\boldsymbol{\mu}}{\boldsymbol{\alpha}} \right\rangle - C_1|z|^2.$$

The desired result follows by recalling that $\left\langle \frac{\boldsymbol{\mu}}{\boldsymbol{\alpha}} \right\rangle > 1$.

The above result can be extended to the case when $\mathbf{\Lambda}(\alpha_i\omega)$ is replaced by its first-order approximation $\mathbf{\Lambda}_i^{\varepsilon}$.

Lemma 10 *Let $D^\varepsilon(z)$ be defined in (85), and let, additionally, $C_\rho, \rho > 0$ and $k \geq 0$, be s.t. $|z| < \rho$ and*

$$|\mathbf{\Lambda}_i^\varepsilon - \mathbf{\Lambda}(\alpha_i z)| \leq C_\rho \left| \frac{\alpha_i z}{\rho} \right|^{2k+2}, \qquad i = 0, \dots, p-1. \tag{90}$$

Then there exists $c_\varepsilon = c(\rho, \langle \boldsymbol{\mu}\boldsymbol{\alpha} \rangle)$, w_0^ε, s.t.

$$|D^\varepsilon(z)| > 1 - c_\varepsilon(\rho)|z|^2, \qquad \text{for all } |z| < w_0^\varepsilon.$$

Proof With $D(z)$ defined like in Lemma 9, with (90),

$$\begin{aligned} |D^\varepsilon(z) - D(z)| &\leq \left| z^{-1} \tan z \sum_{i=0}^{p-1} \frac{\mu_i}{\alpha_i} C_\rho \left| \frac{\alpha_i z}{\rho} \right|^{2k+2} \right| \\ &\leq C_t C(\rho) \rho^{-2} |z|^2 \sum_{i=0}^{p-1} \mu_i \alpha_i^{2k+1}, \qquad \forall |z| < \min(\omega_t, \rho), \end{aligned} \tag{91}$$

where in the last expression we used (87) to bound $z^{-1} \tan z$, and the fact that $|z\rho^{-1}| < 1$. Now it remains to notice that because $\alpha_i < 1 \; \forall i$,

$$\sum_{i=0}^{p-1} \mu_i \alpha_i^{2k+1} \leq \langle \boldsymbol{\mu}\boldsymbol{\alpha} \rangle, \qquad \forall k \geq 0,$$

and hence

$$|D^\varepsilon(z) - D(z)| \leq \tilde{C}(\rho) |z|^2 \langle \boldsymbol{\mu}\boldsymbol{\alpha} \rangle, \qquad \forall |z| < \min(\omega_t, \rho). \tag{92}$$

Obviously,

$$|D^\varepsilon(z)| \geq |D(z)| - |D^\varepsilon(z) - D(z)|,$$

and the conclusion follows from (86) and the above estimates.

The above two results suffice to show that the order of convergence is not destroyed when computing the elements from the set $\mathcal{L}_n^*$ from the elements of $\mathcal{L}_{n+1}^*$.

Lemma 11 *Let N_0 be defined in (75), and $N \geq N_0$. Let ρ be like in Theorem 14. There exists $r_0 : 0 < r_0 < \rho$, which depends on ρ, $\boldsymbol{\mu}$, $\boldsymbol{\alpha}$ only, s.t. the following holds true for all $|z| < r_b$. If, with some $C_\rho > 0$,*

$$|\mathbf{\Lambda}_i^\varepsilon - \mathbf{\Lambda}(\alpha_i z)| \leq C_\rho \left| \frac{\alpha_i z}{\rho} \right|^{2N+2}, \qquad i = 0, \dots, p-1, \tag{93}$$

then $\mathbf{\Lambda}^\varepsilon(z)$ defined in (78), satisfies

$$|\mathbf{\Lambda}^\varepsilon(z) - \mathbf{\Lambda}(z)| \leq C_\rho \left| \frac{z}{\rho} \right|^{2N+2}, \qquad i = 0, \dots, p-1. \tag{94}$$

Moreover, $T(z)$ defined as in (83) satisfies $|T(z)| \leq \left(\sum_{i=0}^{p-1} \mu_i \alpha_i^{2N_0+1} \right)^{-1}$.

Proof By (79), and using (93),

$$|\mathbf{\Lambda}^{\varepsilon}(z) - \mathbf{\Lambda}(z)| \leq C_{\rho}|T(z)| \sum_{i=0}^{p-1} \mu_i \alpha_i^{2N+1} \left|\frac{z}{\rho}\right|^{2N+2}. \tag{95}$$

Next, by definition of $T(z)$,

$$T(z) = (1 + \tan^2 z) D^{-1}(z) D_{\varepsilon}^{-1}(z).$$

By (87), Lemmas 9 and 10, there exists w_0 sufficiently small, s.t. for all $|z| < w_0$, it holds

$$|T(z)| \leq (1 + C_t^2|z|^2)(1 - c_1|z|^2)^{-1}(1 - c_{1,\varepsilon}|z|^2)^{-1}, \qquad c_1,\, c_{1,\varepsilon}, C_t > 0.$$

Notice that w_0 depends only on ρ, $\boldsymbol{\mu}$, $\boldsymbol{\alpha}$. Replacing $T(z)$ in (95) by the above bound yields

$$|\mathbf{\Lambda}^{\varepsilon}(z) - \mathbf{\Lambda}(z)| \leq C_{\rho} \left|\frac{z}{\rho}\right|^{2N+2} (1 + C_t^2|z|^2)(1 - c_1|z|^2)^{-1}(1 - c_{1,\varepsilon}|z|^2)^{-1} \sum_{i=0}^{p-1} \mu_i \alpha_i^{2N+1}$$

Because $N \geq N_0$, and $\alpha_i < 1\ \forall i$, the above can be rewritten as

$$|\mathbf{\Lambda}^{\varepsilon}(z) - \mathbf{\Lambda}(z)| \leq C_{\rho} \left|\frac{z}{\rho}\right|^{2N+2} (1 + C_t^2|z|^2)(1 - c_1|z|^2)^{-1}(1 - c_{1,\varepsilon}|z|^2)^{-1} \sum_{i=0}^{p-1} \mu_i \alpha_i^{2N_0+1}.$$

Because the function

$$B(|z|) := \sum_{i=0}^{p-1} \mu_i \alpha_i^{2N_0+1} (1 + C_t^2|z|^2)(1 - c_1|z|^2)^{-1}(1 - c_{1,\varepsilon}|z|^2)^{-1}$$

is monotonically increasing in $|z|$, changes its value from $\sum_{i=0}^{p-1} \mu_i \alpha_i^{2N_0+1} < 1$ to ∞, as $|z|$ varies from 0 to $\min(c_{1,\varepsilon}^{-1}, c_1^{-1})$, there exists

$$r_b = r_b \left(c_{1,\varepsilon}, c_1^{-1}, C_t, \sum_{i=0}^{p-1} \mu_i \alpha_i^{2N_0+1} \right),$$

s.t. for all $|z| < z_{min}$,

$$(1 + C_t^2|z|^2)(1 - c_1|z|^2)^{-1}(1 - c_{1,\varepsilon}|z|^2)^{-1} \sum_{i=0}^{p-1} \mu_i \alpha_i^{2N_0+1} \leq 1.$$

Therefore, if $|z| < r_b$,

$$|T(z)| \left(\sum_{i=0}^{p-1} \mu_i \alpha_i^{2N_0+1} \right) | \leq 1,$$

and, in particular,

$$|\mathbf{\Lambda}^{\varepsilon}(z) - \mathbf{\Lambda}(z)| \leq C_\rho \left|\frac{z}{\rho}\right|^{2N+2},$$

and hence the conclusion of the lemma. Notice that this value r_b depends only on ρ, $\boldsymbol{\mu}$, $\boldsymbol{\alpha}$.

We now have all the necessary ingredients to write down the proof of Proposition 3.

Proof (Proof of Proposition 3)

Let us choose r_0 properly. Let $N = N_* \geq N_0$, and let r_b be like in Lemma 11. Let r_H be like in Lemma 8.

We prove the result by induction,showing that the approximation property (94) holds. We first show it for $n = L-1$, then for $n = L-2$, and the rest follows similarly.

- $n = L-1$. Because $\mathbf{\Lambda}_{\boldsymbol{n}_k} \in \mathcal{L}^*_L$ for all k, by (74), as $\alpha_k|\omega_{\boldsymbol{n}}| < r_b < \rho_0 < \rho$, where ρ_0 is fixed (e.g. $\rho_0 = \gamma\rho$), we have

$$|\mathbf{\Lambda}_{\boldsymbol{n}_k} - \mathbf{\Lambda}(\omega_{\boldsymbol{n}}\alpha_k)| < M_\rho \left(1 - \frac{\rho_0^2}{\rho^2}\right)^{-1} \left|\frac{\alpha_k\omega_{\boldsymbol{n}}}{\rho}\right|^{2N_*+2} < C_\rho \left|\frac{\alpha_k\omega_{\boldsymbol{n}}}{\rho}\right|^{2N_*+2}. \tag{96}$$

  By Lemma 11, because $|\omega_{\boldsymbol{n}}| < r_b$,

$$|\mathbf{\Lambda}_{\boldsymbol{n}} - \mathbf{\Lambda}(\omega_{\boldsymbol{n}})| < C_\rho \left|\frac{\omega_{\boldsymbol{n}}}{\rho}\right|^{2N+2}. \tag{97}$$

  Moreover, by the same lemma, $|T(\omega_{\boldsymbol{n}})| \leq \left(\sum_{i=0}^{p-1} \mu_i \alpha_i^{2N_0+1}\right)^{-1}$.
- $n = L-2$. Thanks to the previous statement, shown in (97), for all elements of $\mathcal{L}^*_{L-1}$ the following approximation property holds :

$$|\mathbf{\Lambda}_{\boldsymbol{n}_k} - \mathbf{\Lambda}(\alpha_k\omega_{\boldsymbol{n}})| < C_\rho \left|\alpha_k\frac{\omega_{\boldsymbol{n}}}{\rho}\right|^{2N+2}.$$

  By Lemma 11, because $|\omega_{\boldsymbol{n}}| < r_b$, we deduce the same property as (67). Using the same lemma, $|T(\omega_{\boldsymbol{n}})| \leq \left(\sum_{i=0}^{p-1} \mu_i \alpha_i^{2N_0+1}\right)^{-1}$.

The proof for $n > L-2$ follows the same lines. For application of Lemma 11, it is crucial that $|\omega_{\boldsymbol{n}}| < r_b$, and thus the above result may hold only when $|\omega_{\boldsymbol{n}}| \leq |\boldsymbol{\alpha}|^n_\infty|\omega| < r_b$.

We are now able to prove the result of Theorem 15.

Proof (Proof of Theorem 15) Let r_H be like in Corollary 2, and r_b like in Proposition 2. We take $r_0 :=$, and assume that r is sufficiently small, $r < r_b$. To estimate the error propagation in $\mathcal{L}_n^*$, we use the expression (79), where we will use the bound of Proposition 2 for n sufficiently small (i.e. the arguments of $\mathbf{\Lambda}$ in $\mathcal{L}_n$ are large enough), and Proposition 3 otherwise (when the arguments of $\mathbf{\Lambda}$ in $\mathcal{L}_n$ are smaller in their modulus than r_b). Let us remark that one could use the bound (90) for this latter case, but one would not get a desired convergence result in r (i.e. the convergence will be regulated by N_* only).

Provided $n > 0$, let us denote by $\boldsymbol{n} = (n_0, \dots, n_{p-1})$, $\omega_{\boldsymbol{n}} = \prod_{k=0}^{p-1} \alpha_k^{n_k} \omega$ and $\mathbf{\Lambda}_{\boldsymbol{n}} \in \mathcal{L}_n^*$ the approximation to $\mathbf{\Lambda}(\omega_{\boldsymbol{n}})$ computed in the course of the algorithm. Let

$$E_n := \max_{\boldsymbol{n}} |\mathbf{\Lambda}_{\boldsymbol{n}} - \mathbf{\Lambda}(\omega_{\boldsymbol{n}})| .$$

Let us estimate the error committed when passing from one level to another, in terms of the error E_L. Thanks to (79),

$$E_n \le \max_{\boldsymbol{n}} |T(\omega_{\boldsymbol{n}})| \left\langle \frac{\boldsymbol{\mu}}{\boldsymbol{\alpha}} \right\rangle E_{n+1}.$$

Denoting by

$$T_n := \max_{\boldsymbol{n}} |T(\omega_{\boldsymbol{n}})|,$$

we arrive at the following simple bound:

$$E_{r,N_*} \equiv E_0 \le \left\langle \frac{\boldsymbol{\mu}}{\boldsymbol{\alpha}} \right\rangle^L \left(\prod_{\ell=0}^{L-1} T_\ell \right) E_L. \tag{98}$$

Now let us estimate the product of T_ℓ. We split it into two parts. First of all, if n is s.t. $|\omega_{\boldsymbol{n}}| < r_0$, we can apply Proposition 3:

$$|T_n| \le \left(\sum_{i=0}^{p-1} \mu_i \alpha_i^{2N_0+1} \right)^{-1} := \eta, \qquad n \ge n_*. \tag{99}$$

Remark that $\eta > 1$.

The smallest n for which this bound still holds true is given by

$$n_* = \lfloor \log \left(\frac{|\omega|}{r_0} \right) (\log \boldsymbol{\alpha}_\infty^{-1})^{-1} \rfloor + 1.$$

For $n < n_*$, we use the bound valid for all $\omega_{\boldsymbol{n}}$, provided by Proposition 2. Remark that because we chose $r < r_H$, where r_H is like in Corollary 2, the positivity condition $\mathrm{Im}(\omega_{\boldsymbol{n}} \mathbf{\Lambda}_{\boldsymbol{n}}) \le 0$ holds true. Therefore, the result of Proposition 2 applies, and gives, as $\mathrm{Im}\, \omega > a$ and $\mathrm{Im}\, \omega_{\boldsymbol{n}} > a(\min_i \alpha_i)^n$,

$$T_n \le \max \left(1, \left((\min_i \alpha_i)^n a \right)^{-2} \right) \le \left(\min_i \alpha_i \right)^{-2n} a^{-2}, \text{ since } a \le 1.$$

Denoting by $a_{min} := \min_i \alpha_i$, we obtain the following bound:

$$T_n \leq a_{min}^{-2n} a^{-2}, \qquad n < n_*. \tag{100}$$

Combining (99) and (100) into (98) gives

$$E_{r,N_*} \leq \left\langle \frac{\boldsymbol{\mu}}{\boldsymbol{\alpha}} \right\rangle^L \eta^{L-n_*+1} a_{min}^{-2\sum_{k=0}^{n_*-1} k} a^{-2n_*+2} E_L \tag{101}$$

$$\leq \left\langle \frac{\boldsymbol{\mu}}{\boldsymbol{\alpha}} \right\rangle^L \eta^{L-n_*+1} a^{-2n_*+2} a_{min}^{-n_*^2} E_L \tag{102}$$

$$\leq \left\langle \frac{\boldsymbol{\mu}}{\boldsymbol{\alpha}} \right\rangle^L \eta^{L} a^{-2L} a_{min}^{-n_*^2} E_L, \tag{103}$$

which holds true because $\eta > 1$, $a^{-1} < 1$ and $n_* + 1 < L$.

It remains to make the above bound explicit in r, N_* and ω. Denoting $A := \left\langle \frac{\boldsymbol{\mu}}{\boldsymbol{\alpha}} \right\rangle \eta$, we get, with (69),

$$\left(Aa^{-2}\right)^L = \left(Aa^{-2}\right)^{\gamma_\omega} r^{-\nu},$$

where γ_ω, ν are defined in the statement of the theorem.

Remark now that

$$n_* \leq \gamma_\omega + 1 - \log|r_0| \left(\log \boldsymbol{\alpha}_\infty^{-1}\right)^{-1}, \text{ hence} \tag{104}$$

$$n_*^2 \leq 2\gamma_\omega + 2(1 - \log|r_0| \left(\log \boldsymbol{\alpha}_\infty^{-1}\right)^{-1})^2. \tag{105}$$

Therefore, denoting by $B := a_{min}^{-2}$ and by $C = a_{min}^{2(1-\log|r_0|\left(\log \boldsymbol{\alpha}_\infty^{-1}\right)^{-1})^2}$, we obtain

$$a_{min}^{-n_*^2} \leq B^{\gamma_\omega^2} C.$$

Finally, it remains to insert the above bounds into (103), and replace E_L by the bound from Theorem 14 (because the elements in $\mathcal{L}_L^*$ are approximated like ω from Theorem 14). This gives

$$E_{r,N_*} \leq CC_\rho B^{\gamma_\omega^2} \left(Aa^{-2}\right)^{\gamma_\omega} r^{-\nu} \left(1 - \frac{r^2}{\rho^2}\right)^{-1} \left(\frac{r}{\rho}\right)^{2N_*+2}.$$

Next, because $r_0 < \rho$, we replace in the above

$$\left(1 - \frac{r^2}{\rho^2}\right)^{-1} < \left(1 - \frac{r_0^2}{\rho^2}\right)^{-1},$$

and obtain the desired bound in the statement of the theorem.

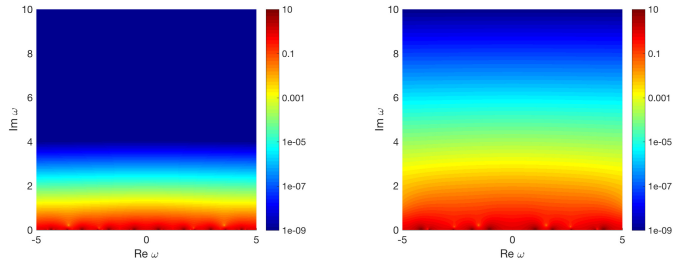

Fig. 4 Left: $|\mathbf{\Lambda}(\omega)\omega^{-1}+i|$ for the Neumann problem, $\boldsymbol{\alpha}=\{0.6,0.8\}$, $\boldsymbol{\mu}=\{0.8,0.2\}$. Right: $|\mathbf{\Lambda}(\omega)\omega^{-1}+i|$ for the Neumann problem, $\boldsymbol{\alpha}=\{0.2,0.7\}$, $\boldsymbol{\mu}=\{0.3,0.3\}$. Remark that the color scale is logarithmic. The respective plots for $\mathbf{\Lambda}(\omega)$ for the Dirichlet problems with the same parameters are similar to the above plots.

4.2.3 Asymptotic computational complexity of the method of Section 4.2.1

In this section we estimate the computational complexity of the procedure **EvalLambda**, in terms of ω and the desired accuracy ε. We fix $r>0$ sufficiently small (cf. Theorem 15), and consider the case when $\omega\in\mathbb{C}^+_{a,r}$, cf. (76), with $0<a\le 1$ fixed. First of all, the evaluation of each value in $\mathcal{L}_n$, $n\le L-1$, requires $O(p)=O(1)$ operations, while to compute each of the values in $\mathcal{L}_L$ we need $O(N_*)$ operations. Thus the total computational complexity costs scale as $O\left(\#\bigcup_{n=0}^{L-1}\mathcal{L}_n\right)+O(N_*\#\mathcal{L}_L)$. With the property (c) from Section 4.2.1,

$$\#\bigcup_{n=0}^{L-1}\mathcal{L}_n=\sum_{n=0}^{L-1}C_{n+p-1}^{p-1}=O(L^{p+1}),\qquad \#\mathcal{L}_L=O(L^p).$$

With L given in (69), the cost of evaluating $\mathbf{\Lambda}(\omega)$ as $|\omega|\to\infty$, and ω is s.t. $\operatorname{Im}\omega>a$, where $a\le 1$, scales as

$$\begin{aligned} c_{\mathbf{\Lambda}} &= O\left((\log|\omega|)^{p+1}+N_*(\log|\omega|)^p\right)\\ &\overset{(77)}{=} O\left(\log^{p+2}|\omega|+\log^{p+1}|\omega|\log a^{-1}\right)+O\left(\log^{p+1}|\omega|\log\varepsilon^{-1}\right). \end{aligned} \tag{106}$$

4.2.4 Approximating $\mathbf{\Lambda}(\omega)$ for ω with large imaginary parts

The complexity of the method of Section 4.2.1 scales as $O(\log^{p+2}|\omega|)$ for $|\omega|\to\infty$. Nonetheless, when $\operatorname{Im}\omega$ is sufficiently large, $\mathbf{\Lambda}(\omega)$ can be approximated with high accuracy by $-i\omega$ (see Figure 4.2.4 for the numerical illustration).

Theorem 16 *There exists $C>0$, s.t for all $\omega\in\mathbb{C}^+$,*

$$|\mathbf{\Lambda}(\omega)+i\omega|\le C|\omega|\mathrm{e}^{-2\operatorname{Im}\omega}\max(1,(\operatorname{Im}\omega)^{-3}). \tag{107}$$

Remark 15 When $\omega\in\mathbb{C}^-=\{z\in\mathbb{C}:\operatorname{Im}z<0\}$, it is possible to show that

$$|\mathbf{\Lambda}(\omega)-i\omega|\le C|\omega|\mathrm{e}^{-2|\operatorname{Im}\omega|}\max(1,|\operatorname{Im}\omega|^{-3}).$$

The proof of the above theorem relies on the following auxiliary result.

Lemma 12 *There exist $c, C > 0$, s.t. all $\omega \in \mathbb{C}^+$,*

$$-\operatorname{Im}(\tan\omega)^{-1} \geq c\min(1, \operatorname{Im}\omega), \tag{108}$$

$$\left|1 - i\,(\tan\omega)^{-1}\right| \leq C\max(1,\ (\operatorname{Im}\omega)^{-1})\mathrm{e}^{-2\operatorname{Im}\omega}. \tag{109}$$

Proof See Appendix B.

Proof (Proof of Theorem 16) Expressing $\mathbf{\Lambda}(\omega)$ via (68), we get

$$\mathbf{\Lambda}(\omega) + i\omega = -\omega\frac{\omega\tan\omega - \mathbf{F}_{\alpha,\mu}(\omega) - i\omega - i\mathbf{F}_{\alpha,\mu}(\omega)\tan\omega}{\omega + \mathbf{F}_{\alpha,\mu}(\omega)\tan\omega} = -\omega\frac{\mathcal{N}(\omega)}{\mathcal{D}(\omega)}, \tag{110}$$

$$\mathcal{N}(\omega) = \frac{(\tan\omega - i)}{\tan\omega}(1 - i\omega^{-1}\mathbf{F}_{\alpha,\mu}(\omega)) = \left(1 - i(\tan\omega)^{-1}\right)(1 - i\omega^{-1}\mathbf{F}_{\alpha,\mu}(\omega)),$$

$$\mathcal{D}(\omega) = (\tan\omega)^{-1} + \omega^{-1}\mathbf{F}_{\alpha,\mu}(\omega), \qquad \mathbf{F}_{\alpha,\mu} = \sum_{i=0}^{p-1}\frac{\mu_i}{\alpha_i}\mathbf{\Lambda}(\alpha_i\omega).$$

Let us first bound the numerator:

$$|\mathcal{N}(\omega)| = \left|1 - i(\tan\omega)^{-1}\right|\left(1 + \sum_{i=0}^{p-1}\mu_i\left|\frac{\mathbf{\Lambda}(\alpha_i\omega)}{\alpha_i\omega}\right|\right).$$

To bound the first term in the product in the right-hand side above we use (109), and to bound the second one, we make use of Theorem 4(b). This gives

$$|\mathcal{N}(\omega)| \leq C_{\mathcal{N}}\max(1, (\operatorname{Im}\omega)^{-2})\mathrm{e}^{-2\operatorname{Im}\omega}, \tag{111}$$

where the constant $C_{\mathcal{N}} > 0$ depends on $\boldsymbol{\mu}$ and $\boldsymbol{\alpha}$.
It remains to deal with the denominator. For this we use the bound:

$$|\mathcal{D}(\omega)| \geq |\operatorname{Im} D(\omega)| \geq \left|\operatorname{Im}(\tan\omega)^{-1} + \sum_{i=0}^{p-1}\mu_i\operatorname{Im}\left((\alpha_i\omega)^{-1}\mathbf{\Lambda}(\alpha_i\omega)\right)\right|.$$

It remains to notice that $\operatorname{Im}(\tan\omega)^{-1}$ and $\operatorname{Im}\left((\alpha_i\omega)^{-1}\mathbf{\Lambda}(\alpha_i\omega)\right)$ are all negative for $\operatorname{Im}\omega > 0$, cf. (108) and Theorem 4(a). Therefore,

$$|\mathcal{D}(\omega)| \geq \left|\operatorname{Im}(\tan\omega)^{-1}\right| \overset{(108)}{\geq} c\min(1, \operatorname{Im}\omega). \tag{112}$$

Combining the bounds (111) and (112) in (110),we obtain the desired statement.

4.3 Computing convolution weights: error, algorithm, complexity

Evaluation of convolution weights based on (66) requires computing $\mathbf{\Lambda}(\omega_k)$ for a range of $\omega_k \in \mathbb{C}^+$. In this section we comment on the choice of the parameters ρ and N in (66), see Section 4.3.1, discuss how $\mathbf{\Lambda}(\omega)$ is computed within (66) in Section 4.3.2 and present some complexity studies in Section 4.3.3.

4.3.1 Accuracy of evaluation of convolution weights and choice of ρ, N

Let us relate the accuracy ε of evaluation of $\mathbf{\Lambda}$ and the parameters ρ and N in (66) to the numerical error of evaluation of N_t values of $\lambda_n^{\Delta t}$. Because we compute convolution weights for the scaled value of $\mathbf{\Lambda}(\omega)$, namely $\mathbf{\Lambda}^s(\omega) = (-i\omega)^{-1}\mathbf{\Lambda}(\omega)$, see Remark 11, we will perform the error analysis for these re-scaled quantities $\lambda_{s,n}^{\Delta t}$, defined as, cf. (25),

$$\mathbf{\Lambda}^s_{\Delta t}(z) = \sum_{n=0}^{\infty} \lambda_{s,n}^{\Delta t} z^n, \qquad \mathbf{\Lambda}^s_{\Delta t}(z) = \left(\frac{\delta(z)}{\Delta t}\right)^{-1} \mathbf{\Lambda}\left(i\frac{\delta(z)}{\Delta t}\right). \tag{113}$$

The convolution weights $\lambda_{s,n}^{\Delta t}$ are computed the help of (66):

$$\begin{aligned} \lambda_{s,n}^{\Delta t} &\approx \lambda_{s,n}^{\Delta t,\varepsilon} := \frac{\rho^{-n}}{N} \sum_{k=0}^{N-1} \mathrm{e}^{-i\frac{2\pi k n}{N}} \mathbf{\Lambda}^{s,\varepsilon}\left(\omega_k\right), \\ \omega_k &= i\frac{\delta(\rho \mathrm{e}^{i\frac{2\pi k}{N}})}{\Delta t}, \qquad n = 0, \ldots, N_t, \end{aligned} \tag{114}$$

where each $\mathbf{\Lambda}^{s,\varepsilon}\left(\omega_k\right)$ is an approximation with an error ε to $\mathbf{\Lambda}^s\left(\omega_k\right)$.

Before analyzing the error induced by the approximation (114), let us show that the exact $\lambda_{s,n}^{\Delta t}$ are bounded. To prove the result that follows, we will use the following observation (see (133) in Appendix D):

$$\mathrm{Im}\left(\frac{\delta(\rho \mathrm{e}^{i\varphi})}{\Delta t}\right) > \frac{1-\rho}{\Delta t}, \qquad \varphi \in [0, 2\pi). \tag{115}$$

Proposition 4 *The convolution weights satisfy, with some $C > 0$,*

$$\left|\lambda_{s,n}^{\Delta t}\right| \le C \max(1, n\Delta t), \qquad n \ge 0. \tag{116}$$

Proof The idea of the proof is from Lemma 5.3, Section 5.1 in [7]. Application of the Cauchy estimate to (26), evaluated for $\ell = n$, with γ being a circle of radius $r_n := \frac{n}{n+1}$ centered in the origin, and $\mathbf{\Lambda}$ replaced by $\mathbf{\Lambda}^s$, yields

$$\begin{aligned} |\lambda_{s,n}^{\Delta t}| &\le r_n^{-n} \sup_{z \in \partial B_{r_n}(0)} \left| \left(\frac{\delta(z)}{\Delta t}\right)^{-1} \mathbf{\Lambda}^s\left(i\frac{\delta(z)}{\Delta t}\right) \right| \\ &\le \left(\frac{n}{n+1}\right)^{-n} \sup_{z \in \partial B_{r_n}(0)} \max\left(1, \left(\mathrm{Im}\left(\frac{\delta(z)}{\Delta t}\right)\right)^{-1}\right), \end{aligned}$$

where the last bound follows from Theorem 4 (b). With (115),

$$|\lambda_{s,n}^{\Delta t}| \le \left(\frac{n}{n+1}\right)^{-n} \max(1, (n+1)\Delta t) \le C \max(1, n\Delta t). \square$$

The error of the approximation (114) is given below.

Proposition 5 *Let $N \geq N_t + 1$, and $\lambda_{s,n}^{\Delta t,\varepsilon}$, $n = 0, \dots, N_t$ be given by (114), where $\max_k |\mathbf{\Lambda}^{s,\varepsilon}(\omega_k) - \mathbf{\Lambda}^s(\omega_k)| < \varepsilon$, for some $\varepsilon > 0$, and $\rho = \varepsilon^{\frac{1}{N+N_t}}$. Then*

$$\max_{n=0,\dots,N_t} |\lambda_{s,n}^{\Delta t,\varepsilon} - \lambda_{s,n}^{\Delta t}| < C_\delta \varepsilon^{\frac{N}{N+N_t}}(1+T), \qquad T = N_t \Delta t.$$

Proof As the proof is rather classical in CQ theory, and some of its elements appear in various works (cf. e.g. [7,34,4]), we postpone it to Appendix C.

Therefore, to ensure that the convolution weights are evaluated with an accuracy $O(\sqrt{\varepsilon})$ for a given ε, it suffices to choose

$$N = N_t + 1, \qquad \rho = \varepsilon^{\frac{1}{2N_t}}, \tag{117}$$

and evaluate $\mathbf{\Lambda}^{s,\varepsilon}(\omega_k)$ in (114) with an accuracy ε for all k.

4.3.2 Evaluating convolution weights: algorithmic details

To compute $\mathbf{\Lambda}^{s,\varepsilon}(\omega)$ in (114), for a given precision ε, we use the following strategy, based on the results of Sections 4.2, 4.3.1 (here $\gamma_\varepsilon > 0$ to be fixed later):

- if $\operatorname{Im}\omega_k < \gamma_\varepsilon$, evaluate $\mathbf{\Lambda}(\omega_k)$ using the procedure **EvalLambda**, with r fixed and N_* chosen as in (77) with $|\omega| = \max_k\{|\omega_k| : \operatorname{Im}\omega_k < \gamma_\varepsilon\}$;
- if $\operatorname{Im}\omega_k \geq \gamma_\varepsilon$, approximate $\mathbf{\Lambda}(\omega_k)$ by $-i\omega_k$, by Theorem 16.

Choosing $\gamma_\varepsilon = \frac{1}{2}\log\varepsilon^{-1} + C$, with some $C > 0$, ensures that $\mathbf{\Lambda}^s(\omega) = (-i\omega)^{-1}\mathbf{\Lambda}(\omega)$ is approximated with an accuracy ε, cf. Remark 11, and Theorem 16. The above strategy is illustrated in Figure 5 (left).

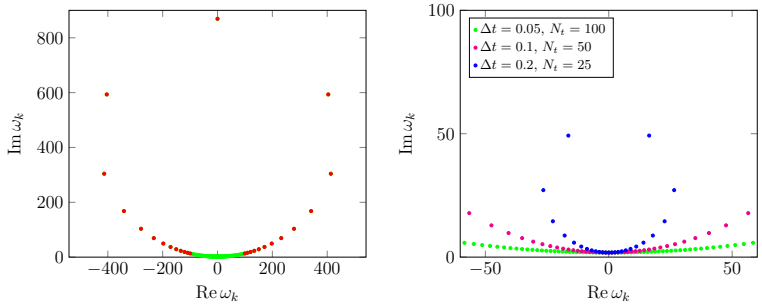

Fig. 5 Left: $N_t = 100$ frequencies ω_k defined in (66), with $\Delta t = 0.05$ and $\rho = \varepsilon^{\frac{1}{2N_t}}$, $\varepsilon = 10^{-8}$. In red we mark ω_k s.t. $\operatorname{Im}\omega_k > \gamma$ (we choose $\gamma = 12$), s.t. $\mathbf{\Lambda}(\omega_k)$ is approximated by $-i\omega_k$. Right: N_t frequencies ω_k defined in (66) with given Δt, chosen so that $N_t\Delta t = 5$. Remark that in all cases $\operatorname{Im}\omega_k > \text{const}$.

4.3.3 Complexity estimates

Let us estimate the complexity of the evaluation of (114) in terms of N, Δt, ε. Let us assume that $T = N_t \Delta t$ fixed, and consider the regime $N_t \to \infty$; we also assume that ε is sufficiently small.As discussed in the end of Section 4.1, this necessitates a bound on the cost of computing $\mathbf{\Lambda}(\omega_k)$ in (114). This bound, cf. (106), depends on ω_k; thus, we must study how ω_k behaves with N, Δt, ε. The following proposition is a minor refinement of some of the results from [4].

Lemma 13 *Let ω_k, $k = 0, \dots, N_t$, be given by (114), with N, ρ defined in (117), and $\varepsilon < \delta < 1$. Then, with some $c_\delta, C_\delta > 0$, (a) $\operatorname{Im} \omega_k > c \min\left(1, \frac{\log \delta^{-1}}{T}\right)$ and (b) $|\omega_k| < \frac{C}{T} N_t \max\left(1, N_t \left(\log \delta^{-1}\right)^{-1}\right)$.*

Proof See Appendix D.

An illustration to the statement (a) is provided in Figure 5 (right).

By Lemma 13, $\omega_k \in C_{a_\delta, a_\delta}$, with $a_\delta = c \min\left(1, \frac{\log \delta^{-1}}{T}\right)$, and thus the results of Section 4.2.3 about the evaluation of $\mathbf{\Lambda}$ apply. The complexity of evaluation of each of $\mathbf{\Lambda}(\omega_k)$ is $O(1)$ when $\operatorname{Im} \omega_k \geq \gamma_\varepsilon$, and scales as (106) when $\operatorname{Im} \omega_k < \gamma$. Replacing $|\omega_k|$ by $O(N_t^2)$, according to Lemma 13, the worst-case complexity is given by

$$c_{\mathbf{\Lambda}} = O(\log^{p+2} N_t + \log^{p+1} N_t \log \varepsilon^{-1}).$$

Because (114) requires computing at most $O(N_t)$ values of $\mathbf{\Lambda}(\omega_k)$, and then performing the FFT, see the discussion in Section 4.1, the total complexity of computing N convolution weights with an accuracy $O\left(\sqrt{\varepsilon}\right)$ scales as

$$O(N_t \log^{p+2} N_t + N_t \log^{p+1} N_t \log \varepsilon^{-1}).$$

Remark that this complexity scales, in general, better, than $O(N_t^2)$ complexity of the solution of the problem, cf. Section 3.4.

5 Numerical results

In all the numerical results of this section we use the mass-lumped finite element for the space discretization, and a regular spatial grid. This, in particular, implies that the CFL number is $C_{CFL} = \frac{\Delta t}{h}$, cf. (50) and Remark 9. In most of the experiments we fixed r, N_* in the procedure of Section 4.2.1 for computation of $\mathbf{\Lambda}(\omega)$ to a (numerically determined) fixed value that allows to approximate $\mathbf{\Lambda}$ in the convolution weight computation with high accuracy. As for the evaluation of the convolution weights, we choose $\varepsilon = 10^{-12}$ in (117).

5.1 Validity of the method

In this section we would like to verify the validity of the transparent boundary conditions constructed in the present article, by comparing a solution computed on the truncated tree to an (ideally) solution computed on the tree $\mathcal{T}$. However, because the tree $\mathcal{T}$ is infinite, it is in general impossible to compute such a reference solution. Thus, one of the options would be to truncate the tree up to $\mathcal{N}$ generations, where $\mathcal{N} \gg 1$, and perform the computation on this truncated tree, as it was done e.g. in [29]. Because this is costly, we adapt an alternative approach: given $\mathcal{N}$ generations, we compute the solution to the problem (16) on $\mathcal{T}^m$ with $m = \mathcal{N} - 1$, where we use the transparent boundary conditions approximated with the help of the convolution quadrature. This is the reference solution. We compare this solution with the CQ approximation to (16), where m is fixed, $m < \mathcal{N} - 1$.

Let us remark that no analysis had been made in this article about the convergence of the method with respect to the number of the truncated generations $m + 1$ (a related issue was addressed in [28]).

We solve the Neumann problem on the binary tree $\mathcal{T}$, s.t. the length of the root edge equals to $\ell_{0,0} = 2$, with $\boldsymbol{\alpha} = (0.3, 0.5)$ and $\boldsymbol{\mu} = (1, 0.25)$. The source term is supported on the root branch of the tree and defined as

$$f(t,s) = 10^6(s-1.5)\mathrm{e}^{-\sigma(s-1.5)^2-\sigma(t-0.1)^2}, \qquad \sigma = 5\cdot 10^3. \tag{118}$$

The reference solution $u_{\mathcal{N}-1}$ is computed on the truncated tree $\mathcal{T}^{\mathcal{N}-1}$ with $\mathcal{N} = 5$ generations; $\Delta t = 9.9\cdot 10^{-5}$, $h = 10^{-4}$. The dependence of the solutions $u_m(s_0, t)$ on t is depicted in Figure 5.1; here $s_0 = 1$ is the middle of the root branch. The complex behaviour of the solution is attributed to the multiple reflection phenomena on the tree $\mathcal{T}$: in general, waves are reflected from each of the vertices of the tree. In particular, the second peak of the solution $u_m(s_0, t)$ is due to the wave reflected of the vertex $M_{0,0}$. The first reflections from the infinite boundary of the tree reach $s_0 = 1$ at $t \approx 3.3$.

We compare it to the solution u_m computed on the truncated tree with $(m+1)$ generations, where $m = 1, 2, 3$, and the same discretization parameters. For this we compute the relative errors by evaluating norms on the first two generations (since 2 is the minimal value for the number of the truncated generations in our experiments):

$$e_m^n = \frac{\|u_{\mathcal{N}-1}^n - u_m^n\|_{\mathrm{L}^2_\mu(\mathcal{T}^{k-1})}}{\max\limits_{n=0,\dots,N_t}\|u_{\mathcal{N}-1}^n\|_{\mathrm{L}^2_\mu(\mathcal{T}^{k-1})}}, \qquad k = 2, \qquad e_m := \max_{n=0,\dots,N_t} e_m^n. \tag{119}$$

Let us remark that these norms are computed with the help of the mass-lumped matrices. They are correspondingly

$$e_1 \approx 7.1\cdot 10^{-4}, \qquad e_2 \approx 3.7\cdot 10^{-4} \qquad e_3 \approx 1.6\cdot 10^{-4}.$$

The errors e_m^n as functions of $t^n = n\Delta t$ are shown in Figure 5.1, bottom. Numerical experiments indicate that they grow linearly in time; this is not

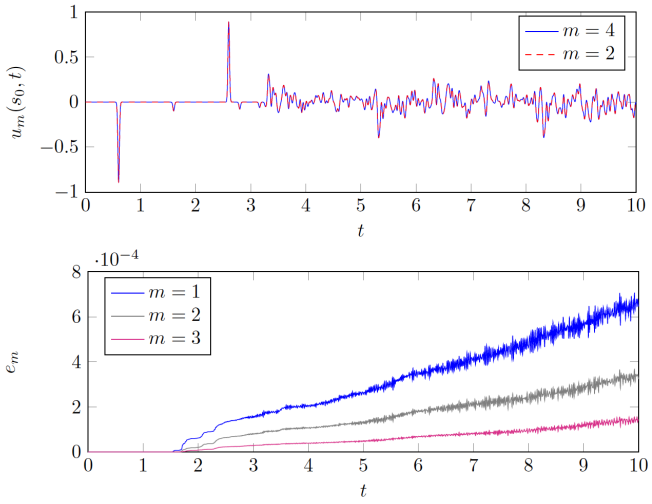

Fig. 6 Top: dependence on t of the solution to the problem (16) $u_m(s_0,t)$ in the point s_0 (which is the middle of the root branch). We study the Neumann problem on the tree with $\ell_{0,0} = 2.0$, $\boldsymbol{\alpha} = (0.3, 0.5)$ and $\boldsymbol{\mu} = (1, 0.25)$, the right hand side (118). Bottom: relative errors e_m^n (cf. (119)) as functions of $t^n = n\Delta t$

surprising, in view of the results of Theorem 13. Figure 5.1 shows that the errors almost vanish for smaller times (even where the solution is non-zero). This can be explained by the fact that the wave reaches the outer boundary of $\mathcal{T}^m$ (where we use the approximated transparent boundary conditions) and reflects into the tree $\mathcal{T}^1$ (where we measured errors) at $t \approx 1.2$ for $m = 1$, $t \approx 1.6$ for $m = 2$ and $t \approx 1.7$ for $m = 3$.

5.2 Convergence rates and stability

5.2.1 Convergence.

We perform the convergence experiments on the tree with $\boldsymbol{\alpha} = (0.2, 0.4)$ and $\boldsymbol{\mu} = (1, 0.25)$, and the length of the root edge $\ell_{0,0} = 2$. Because no closed form solution is, in general, available, we compare the numerical solution computed on a coarse grid $(h,\ \Delta t)$ to the numerical ('reference') solution computed on the finest grid $(h_f,\ \Delta t_f) = (10^{-4}, 0.99 \cdot 10^{-4})$. The solutions are computed on the tree $\mathcal{T}^2$ (i.e. on 3 generations, cf. (2)), on the time interval $(0, 10)$ and with the right hand side supported on the root edge $\Sigma_{0,0}$:

$$f(t,s) = 10^4 \mathrm{e}^{-100(t-0.75)^2 - 100(s-1)^2}(s-1), \qquad s \in \Sigma_{0,0}.$$

We consider the Neumann problem. We fix the CFL (50), i.e. the ratio $\frac{\Delta t}{h} = \frac{\Delta t_f}{h_f}$, and perform the experiments on the sequence of grids $(h_k,\ \Delta t_k)$, $1 \le k \le$

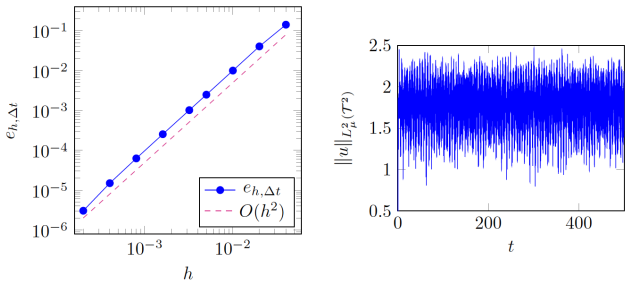

Fig. 7 Left: convergence rates for the experiment of Section 5.2.1. Right: dependence on time of the L^2-norm of the solution computed on the tree $\mathcal{T}^2$.

9, with $\min_k h_k = 2 \cdot 10^{-4}$. The reference solution computed at the time t^k is denoted by $u_{ref}(t^k)$, and the solution on the grid $(h, \Delta t)$ by u_h^k. The evolution of the relative error $e_{h,\Delta t}$, defined below, is shown in Figure 7.

$$\begin{aligned} e_{h,\Delta t} &= \max_n e^n_{h,\Delta t}, \qquad \text{where } e^n_{h,\Delta t} = \frac{\|u_h^n - u_{ref}(n\Delta t)\|_{\mathrm{L}^2_\mu(\mathcal{T}^m)}}{\|u_{ref}\|_{L^\infty(0,T;L^2_\mu(\mathcal{T}^m))}}, \\ \|u_{ref}\|_{L^\infty(0,T;L^2_\mu(\mathcal{T}^m))} &= \max_{k=0,\dots,N_t} \|u_{ref}(t^k)\|_{\mathrm{L}^2_\mu(\mathcal{T}^m)}, \qquad N_t = \left\lceil \frac{T}{\Delta t_f} \right\rceil. \end{aligned} \tag{120}$$

5.2.2 Long-time stability.

To study the stability of the numerical method, we compute the solution to the problem described in Section 5.2.1 on the time interval $(0, T)$ with $T = 500$, with the discretization $(h, \Delta t) = (5 \cdot 10^{-4}, 4.99 \cdot 10^{-4})$. The diameter of the computational domain equals 2.8. Figure 7 depicts $\mathrm{L}^2_\mu(\mathcal{T}^m)$-norm of the solution, which clearly stays bounded on the whole time interval.

5.3 Performance of the method on different trees.

To explain the experiments that follow, let us provide more information about $\mathbf{\Lambda}(\omega)$. Recall that $\mathbf{\Lambda}(\omega)$ is an even meromorphic in $\mathbb{C}$ function (cf. Theorem 4) with real poles. The number of poles of $\mathbf{\Lambda}$ on an interval $(0, \lambda)$ grows asymptotically as $\lambda^{\frac{d}{2}}$, where $d \geq 1$ and depends on $\boldsymbol{\alpha}$ (see [28]). In particular, when $\langle \boldsymbol{\alpha} \rangle := \sum_{i=0}^{p-1} \alpha_i < 1$, one has $d = 1$, while when $\langle \boldsymbol{\alpha} \rangle > 1$, it holds that $d \leq d_s$, where $d_s > 1$ is a unique number s.t. $\sum_{i=0}^{p-1} \alpha_i^{d_s} = 1$. Although these estimates are asymptotic, the difference between these cases is observed already for small λ. In particular, in Figure 8 we depict numerically computed poles of $\mathbf{\Lambda}(\omega)$ for two sets of parameters: $\boldsymbol{\alpha} = (0.4, 0.4)$, $\boldsymbol{\mu} = (0.5, 1)$ (case $d = 1$) and $\boldsymbol{\alpha} = (0.8, 0.4)$, $\boldsymbol{\mu} = (0.5, 1)$ (case $d \leq d_s \approx 1.4$).

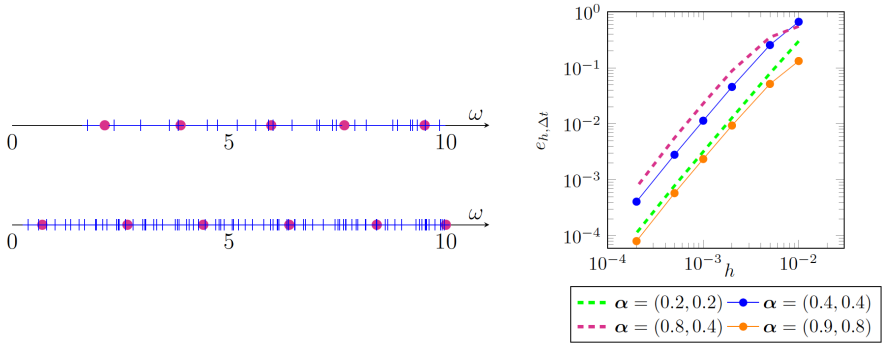

Fig. 8 Left: On top we show the poles of $\boldsymbol{\Lambda}(\omega)$ on the interval $(0, 10)$ for the Dirichlet problem. Bottom: poles of $\boldsymbol{\Lambda}(\omega)$ on the interval $(0, 10)$ for the Neumann problem. On both plots with blue vertical dashes we mark the poles corresponding to $\boldsymbol{\alpha} = (0.8, 0.4)$, $\boldsymbol{\mu} = (0.5, 1)$, while with magenta circles the poles corresponding to $\boldsymbol{\alpha} = (0.4, 0.4)$, $\boldsymbol{\mu} = (0.5, 1)$. **Right:** Errors $e_{h,\Delta t}$, cf. (120), for different discretizations for the experiments of Section 5.3. In all the experiments $\boldsymbol{\mu} = (0.5, 1.0)$.

Our goal is to find out whether the density of poles influences the behaviour of the convolution quadrature. For this we compute the solutions to the Dirichlet and Neumann problems on the reference tree $\mathcal{T}$ (length of its root edge equals $\ell_{0,0} = 1$), constructed with different sets of the parameters, on the time interval $(0, 20)$. As a source we take

$$f(t, s) = 10^6 \mathrm{e}^{-\sigma(s-0.5)^2 - \sigma(t-0.25)^2}(s - 0.5), \quad \sigma = 10^3,$$

supported on the root edge. We repeat the experiment of Section 5.2.1, by computing the solutions for different discretizations, the only difference being that we compare the solutions computed on the truncated tree $\mathcal{T}^1$ to the reference solution computed on a fine discretization on the tree $\mathcal{T}^2$. The time interval is chosen so that the reflections from the 'infinite' boundary of the tree are able to reach the computational domain.

We do not observe any clear correlation between the density of poles and the error behaviour, cf. Figure 8, right. We present the results for the Dirichlet problem only, since in the Neumann case they are very similar. Let us remark that in the experiment $\boldsymbol{\alpha} = (0.9, 0.8)$ the Dirichlet and Neumann problems coincide, see Theorem 2.

However, as expected, in these experiments we observe a difference in terms of the computational times (in particular, since the complexity of evaluating $\boldsymbol{\Lambda}(\omega)$, see Section 4.2.3, depends on $|\boldsymbol{\alpha}|_\infty$, this is the case for the convolution weights as well). In the largest computations on the tree $\mathcal{T}^2$, discretized with $h = 10^{-4}$, $\Delta t = 0.99 \cdot 10^{-4}$, we computed $\sim 2 \cdot 10^5$ convolution weights. On a laptop, this requires about 5 seconds for the problem with $\boldsymbol{\alpha} = (0.2, 0.2)$, 12 seconds for $\boldsymbol{\alpha} = (0.4, 0.4)$, 167 seconds for $\boldsymbol{\alpha} = (0.8, 0.4)$ and almost 12 minutes for $\boldsymbol{\alpha} = (0.9, 0.8)$. These numbers can be improved by optimizing the parameters in the computations.

6 Conclusions

In this work we approximated the transparent boundary conditions for wave propagation in fractal trees with the help of the convolution quadrature method. Besides stability and convergence analysis, we have additionally considered practical aspects of the algorithm, in particular, computation of the convolution weights. Obtained results, both theoretical and numerical, indicate stability and efficiency of the method.

Nonetheless, some numerical analysis questions remain open (e.g. stability of the problem under perturbation of convolution weights); such analysis may affect some estimates of Section 4.3.3 by imposing constraints on the choice of parameters (in particular, the parameter ρ in (66)), cf. e.g. the respective analysis for time-domain boundary integral equations in [7]. We nonetheless believe that the results obtained in this work provide a technical background for continuing the research in this direction.

One of the drawbacks of the CQ method is its complexity, which scales as $O(N_t^2)$ where N_t is the number ot time steps; this is prohibitive when computations on long times are required. This can be overcome using an algorithm similar to the one proposed in [4], see also [22] and [5]. Additionally, alternative ideas for approximating the transparent boundary conditions, based on the meromorphic expansion of the symbol of the DtN, are currently under investigation.

Acknowledgments

We are deeply grateful to Adrien Semin (TU Darmstadt, Germany) for providing his code Netwaves.

A Proof of Theorem 4

It remains to prove the upper bound on $\mathbf{\Lambda}_{\mathfrak{a}}(\omega)$. Without loss of generality, we will show it for $\mathbf{\Lambda}_{\mathfrak{n}}(\omega)$. First, $\mathbf{\Lambda}_{\mathfrak{n}}(\omega)$ can be defined via the solution of the frequency-domain problem:

$$\mathbf{\Lambda}_{\mathfrak{n}}(\omega) = -\partial_s \lambda(M^*), \qquad \omega \in \mathbb{C}^+, \tag{121}$$

where $\lambda \in \mathrm{H}^1_\mu(\mathcal{T})$ solves the boundary-value problem:

$$\omega^2 \int_{\mathcal{T}} \mu(s)\, \lambda\, \overline{v} - \int_{\mathcal{T}} \mu(s)\, \partial_s \lambda\, \partial_s \overline{v} = 0, \qquad \text{for all } v \in V_{\mathfrak{n}}, \qquad \lambda(M^*) = 1. \tag{122}$$

We proceed as follows, defining $\|v\|_\omega := \int_{\mathcal{T}} \mu \left(|\partial_s v|^2 + |\omega v|^2\right)$,

- first bound $|\mathbf{\Lambda}_{\mathfrak{n}}(\omega)|^2$ by the energy of the solution (notice $\lambda(M^*) = 1$):

$$|\mathbf{\Lambda}_{\mathfrak{n}}(\omega)|^2 \le |\omega|^2 + C_0(1 + \operatorname{Im}\omega)\|\lambda\|^2_\omega, \qquad C_0 > 0. \tag{123}$$

- next show that the energy of the solution is bounded by $\frac{1}{2}|\mathbf{\Lambda}_{\mathfrak{n}}(\omega)|^2$, with C_0 as above:

$$C_0(1 + \operatorname{Im}\omega)\|\lambda\|^2_\omega \le \frac{1}{2}|\mathbf{\Lambda}_{\mathfrak{n}}(\omega)|^2 + C_1 \max(1, (\operatorname{Im}\omega)^{-2})|\omega|^2, \quad C_1 > 0. \tag{124}$$

– combine (123) and (124) to obtain the desired bound:

$$|\mathbf{\Lambda}_{\mathfrak{n}}(\omega)|^2 \le C \max(1, (\operatorname{Im}\omega)^{-2})|\omega|^2.$$

Proof of the bound (123). Let $v_0(s) = \chi(s)\partial_s\lambda$, where $\chi \in C^1(\mathcal{T};\mathbb{R})$, $\operatorname{supp}\chi(s) \subseteq \Sigma_{0,0}$, $\chi(M^*) = 1$ and $\chi(M_{0,0}) = 0$. The weak form (122) implies that

$$\partial_s^2\lambda + \omega^2\lambda = 0 \text{ on } \Sigma_{0,0}.$$

Testing the above with $v_0(s)$, we obtain the following identity on the edge $\Sigma_{0,0}$, parametrized by $s \in [0,1]$ (recall that we work with the reference tree, and thus the length of $\Sigma_{0,0}$ is 1):

$$I_1 + I_2 = 0, \qquad \text{where } I_1 = \int_0^1 \partial_s^2\lambda\,\chi(s)\,\overline{\partial_s\lambda}ds, \quad I_2 = \omega^2\int_0^1 \lambda\,\chi(s)\,\overline{\partial_s\lambda}ds. \tag{125}$$

Let $\omega = \omega_r + i\omega_i$, $\omega_r \in \mathbb{R}$ and $\omega_i > 0$. Let us consider the real part of the above:

$$\operatorname{Re} I_1 = \frac{1}{2}\int_0^1 \frac{d}{ds}|\partial_s\lambda|^2\chi(s)ds = -\frac{1}{2}\,|\mathbf{\Lambda}_{\mathfrak{n}}(\omega)|^2 + \frac{1}{2}\int_0^1 \chi'(s)|\partial_s\lambda|^2ds, \tag{126}$$

where in the last identity we used $\chi(0) = 1$ and $\chi(1) = 0$. Similarly,

$$\begin{aligned}\operatorname{Re} I_2 &= \frac{1}{2}\operatorname{Re}\omega^2\int_0^1 \chi(s)\frac{d}{ds}|\lambda|^2ds - \operatorname{Im}\omega^2\int_0^1 \chi(s)\operatorname{Im}(\lambda\overline{\partial_s\lambda})ds\\ &= -\frac{1}{2}(\omega_r^2 - \omega_i^2) + \frac{1}{2}(\omega_r^2 - \omega_i^2)\int_0^1 \chi'(s)|\lambda|^2ds - 2\omega_i\omega_r\int_0^1 \chi(s)\operatorname{Im}(\lambda\overline{\partial_s\lambda})ds.\end{aligned}$$

where we used $\chi(0) = 1$, $\chi(1) = 0$ and $\lambda(0) = 1$. Applying to the last integral the Young inequality we obtain the following bound, with $c_1, c_2 > 0$,

$$|\operatorname{Re} I_2| \le \frac{1}{2}|\omega|^2 + c_1|\omega|^2\int_0^1 |\lambda|^2ds + c_2\omega_i\left(|\omega_r|^2\int_0^1 |\lambda|^2ds + \int_0^1 |\partial_s\lambda|^2ds\right). \tag{127}$$

Combining (125), (126), we deduce that

$$|\mathbf{\Lambda}_{\mathfrak{n}}(\omega)|^2 \le 2|\operatorname{Re} I_2| + c_3\int_0^1 |\partial_s\lambda|^2ds, \quad c_3 > 0,$$

and inserting into the above (127) we prove (123).

Proof of the bound (124). Testing the Helmholtz equation corresponding to (122) with $\omega\lambda(s)$ and integrating by parts we obtain the following identity (recall that $\lambda(M^*) = 1$):

$$\overline{\omega}\mathbf{\Lambda}(\omega) = \overline{\omega}\int_{\mathcal{T}} \mu|\partial_s\lambda|^2 - |\omega|^2\omega\int_{\mathcal{T}} \mu|\lambda|^2.$$

Taking the imaginary part of the above results in

$$\operatorname{Im}(\overline{\omega}\mathbf{\Lambda}(\omega)) = -\omega_i\left(\int_{\mathcal{T}} \mu|\partial_s\lambda|^2 + |\omega|^2\int_{\mathcal{T}} \mu|\lambda|^2\right) = -\omega_i\|\lambda\|_\omega^2.$$

Multiplying both sides of the above by $-C_0(1+\omega_i)\omega_i^{-1}$, with C_0 is as in (123), we obtain

$$-C_0(\omega_i^{-1}+1)\,\mathrm{Im}\,(\overline{\omega}\mathbf{\Lambda}(\omega)) = C_0(1+\omega_i)\|\lambda\|_\omega^2. \tag{128}$$

It suffices to notice that the lhs in the above equality is bounded

$$\left|-C_0(\omega_i^{-1}+1)\,\mathrm{Im}\,(\overline{\omega}\mathbf{\Lambda}(\omega))\right| \le C_0(\omega_i^{-1}+1)|\omega||\mathbf{\Lambda}(\omega)| \le \frac{1}{2}|\mathbf{\Lambda}(\omega)|^2 + \frac{C_0^2}{2}(\omega_i^{-1}+1)^2|\omega|^2,$$

where we used the Young inequality. In the above we bound further $C_0(\omega_i^{-1}+1) \le 2\max(1,\omega_i^{-1})$. Inserting the bound into (128) gives

$$C_0(1+\omega_i)\|\lambda\|_\omega^2 \le \frac{1}{2}|\mathbf{\Lambda}(\omega)|^2 + 2C_0^2\max(1,\omega_i^{-2})|\omega|^2,$$

i.e. (124). Combining (123) and (124) proves the statement of the theorem.

B Proof of Lemma 12

We first show (108). By definition, $\tan\omega = i\frac{1-z}{1+z}$, with $z = \mathrm{e}^{2i\omega}$, $\omega = \omega_r + i\omega_i$. Then,

$$\begin{aligned} -\,\mathrm{Im}\,(\tan\omega)^{-1} &= \mathrm{Re}\,\frac{1+z}{1-z} = \mathrm{Re}\,\frac{(1+z)(1-\overline{z})}{|1-z|^2} = \frac{1-|z|^2}{1+|z|^2-2\,\mathrm{Re}\,z} \ge \frac{1-|z|^2}{(1+|z|)^2} \qquad (129)\\ &= \frac{1-|z|}{1+|z|} = \frac{1-\mathrm{e}^{-2\omega_i}}{1+\mathrm{e}^{-2\omega_i}} \ge \begin{cases} \frac{\mathrm{e}^{2\omega_i}-1}{\mathrm{e}^{2\omega_i}+1} \ge \frac{2\omega_i}{\mathrm{e}^2+1}, & \text{if } 0<\omega_i\le 1,\\ \frac{1-\mathrm{e}^{-2}}{1+\mathrm{e}^{-2}}, & \text{if } \omega_i > 1, \end{cases} \end{aligned}$$

hence the bound (108). Let us show (109). After straightforward computations,

$$\left|1 - i\,(\tan\omega)^{-1}\right| = \frac{2|z|}{|1-z|} \le \frac{2|z|}{|1-|z||} = \frac{2\mathrm{e}^{-2\omega_i}}{1-\mathrm{e}^{-\omega_i}} \le C\max(1,\omega_i^{-1})\mathrm{e}^{-2\omega_i},$$

where the last bound follows by noticing that, for $\omega_i > 0$,

$$1-\mathrm{e}^{-\omega_i} \ge \begin{cases} 1-\mathrm{e}^{-1}, & \text{if } \omega_i \ge 1,\\ \mathrm{e}^{-1}\omega_i, & \text{if } \omega_i < 1 \end{cases} \qquad \ge c\min(1,\omega_i), \qquad c>0. \tag{130}$$

C Proof of Proposition 5

To prove Proposition 5, we need the following auxiliary result.

Lemma 14 *Let $0<\rho<1$, $N \ge N_t+1$, $\varepsilon>0$ and $\lambda_{s,n}^{\Delta t,\varepsilon}$, $n=0,\dots,N_t$ be given by (114), where $\max_k |\mathbf{\Lambda}^{s,\varepsilon}(\omega_k) - \mathbf{\Lambda}^s(\omega_k)| < \varepsilon$. Then*

$$\max_{n=0,\dots,N_t} |\lambda_{s,n}^{\Delta t,\varepsilon} - \lambda_{s,n}^{\Delta t}| < \rho^{-N_t}\varepsilon + \rho^N C_N(\rho),$$
$$C_N(\rho) = (1-\rho^N)^{-1}\left(1 + N_t\Delta t + \Delta t(1-\rho^N)^{-1}\right).$$

Proof (Proof of Lemma 14) For all $n=0,\dots,N_t$,

$$\begin{aligned} |\lambda_{s,n}^{\Delta t,\varepsilon} - \lambda_{s,n}^{\Delta t}| &\le \left|\frac{\rho^{-n}}{2\pi i N}\sum_{k=0}^{N-1}\mathrm{e}^{-i\frac{2\pi kn}{N}}\left(\mathbf{\Lambda}^{s,\varepsilon}(\omega_k) - \mathbf{\Lambda}^s(\omega_k)\right)\right|\\ &\quad + \left|\frac{\rho^{-n}}{2\pi i N}\sum_{k=0}^{N-1}\mathrm{e}^{-i\frac{2\pi kn}{N}}\mathbf{\Lambda}^s(\omega_k) - \lambda_{s,n}^{\Delta t}\right| = S_1 + S_2. \end{aligned} \tag{131}$$

An upper bound for S_1 follows from the triangle inequality: $S_1 \le \rho^{-N_t}\varepsilon$.
As for S_2, it suffices to replace $\mathbf{\Lambda}^s(\omega_k)$ in the above sum by $\sum_{\ell=0}^{\infty} \lambda_{s,\ell}^{\Delta t}\rho^\ell \mathrm{e}^{i\frac{2\pi\ell k}{N}}$, cf. (113), and then use the aliasing argument. In particular,

$$\frac{\rho^{-n}}{2\pi i N}\sum_{k=0}^{N-1}\mathrm{e}^{-i\frac{2\pi kn}{N}}\mathbf{\Lambda}^s(\omega_k) = \frac{\rho^{-n}}{2\pi i N}\sum_{k=0}^{N-1}\sum_{\ell=0}^{\infty}\lambda_{s,\ell}^{\Delta t}\rho^\ell \mathrm{e}^{i\frac{2\pi k(\ell-n)}{N}}.$$

It remains to remark that

$$N^{-1}\sum_{k=0}^{N-1}\mathrm{e}^{i\frac{2\pi k(\ell-n)}{N}} = \begin{cases} 1, & (\ell-n) \bmod N = 0,\\ 0, & \text{otherwise.}\end{cases}$$

Therefore,

$$\frac{\rho^{-n}}{2\pi i N}\sum_{k=0}^{N-1}\mathrm{e}^{-i\frac{2\pi kn}{N}}\mathbf{\Lambda}^s(\omega_k) = \lambda_{s,n}^{\Delta t} + \frac{\rho^{-n}}{2\pi i N}\sum_{k=1}^{\infty}\lambda_{s,kN+n}^{\Delta t}\rho^{kN+n}, \quad \text{and}$$

$$S_2 \le \frac{\rho^{-n}}{2\pi N}\sum_{k=1}^{\infty}\left|\lambda_{s,n+kN}^{\Delta t}\right|\rho^{n+kN} \overset{(116)}{\le} C\sum_{k=1}^{\infty}\max(1,(n+kN)\Delta t)\rho^{kN}.$$

The above sum is then estimated as follows:

$$\begin{aligned} S_2 &\le \sum_{k=1}^{\infty}\rho^{kN} + \sum_{k=1}^{\infty}\rho^{kN}(n+kN)\Delta t\\ &\le \rho^N(1-\rho^N)^{-1}(1+n\Delta t) + \Delta t\rho^N(1-\rho^N)^{-2}.\end{aligned}$$

The result follows by bounding in the above $n\Delta t$ by $N_t\Delta t$ and combining bounds for S_1 and S_2 into (131). □

The bound of Lemma 14 allows us to quantify the choice of ρ, N in (114).

Proof (Proof of Proposition 5) The desired bound follows by applying the result of Lemma 14. In particular, $C_N(\rho)$ can be estimated by remarking that, because $N \ge N_t + 1$,

$$1-\rho^N = 1-\varepsilon^{\frac{N}{N+N_t}} \ge 1-\varepsilon^{\frac{N_t+1}{2N_t+1}} > 1-\varepsilon^{\frac{1}{2}} > 1-\sqrt{\delta}. \qquad \square$$

D Proof of Lemma 13

Let us show (a), which basically follows from Section 5.2.1 in [4]. It is not difficult to verify that the frequencies ω_k defined in (66), namely,

$$\omega_k = i\frac{\delta(\rho\mathrm{e}^{i\frac{2\pi k}{N}})}{\Delta t}$$

lie on the circle centered at $c_{\rho,\Delta t}$ of radius $R_{\rho,\Delta t}$:

$$c_\rho = \frac{2i}{\Delta t}\frac{1+\rho^2}{1-\rho^2}, \qquad R_\rho = \frac{2}{\Delta t}\frac{2\rho}{1-\rho^2}, \tag{132}$$

i.e. $\omega_k = c_\rho + R_\rho \mathrm{e}^{i\psi_k}$, for some $\psi_k \in [0, 2\pi)$. Hence

$$\operatorname{Im}\omega_k \ge \inf_{0\le\varphi<2\pi}\operatorname{Im}\left(i\frac{\delta(\rho\mathrm{e}^{i\varphi})}{\Delta t}\right) = \frac{2}{\Delta t}\frac{1+\rho^2-2\rho}{1-\rho^2} = \frac{2}{\Delta t}\frac{1-\rho}{1+\rho}, \tag{133}$$

and because $\rho < 1$, $\operatorname{Im}\omega_k > \frac{1-\rho}{\Delta t}$. For ρ defined in (117),

$$1-\rho = 1-\varepsilon^{\frac{1}{2N_t}} = 1-\exp\left(-\frac{\log\varepsilon^{-1}}{2N_t}\right) > \min\left(1, \frac{\log\varepsilon^{-1}}{N_t}\right), \tag{134}$$

where the last bound follows from (130). Therefore, as $\Delta t < 1$,

$$\operatorname{Im}\omega_k > c\min\left(1, \frac{\log\delta^{-1}}{N_t\Delta t}\right).$$

To show (b), we use the same property (132), which results in

$$|\omega_k| \le \frac{2}{\Delta t}\left(\frac{1+\rho^2}{1-\rho^2} + \frac{2\rho}{1-\rho^2}\right) \le \frac{2(1+\rho)}{\Delta t(1-\rho)} < \frac{4}{\Delta t(1-\rho)}.$$

Using (134), we deduce

$$|\omega_k| < \frac{C}{\Delta t}\max\left(1, N_t\left(\log\varepsilon^{-1}\right)^{-1}\right) \le \frac{C}{\Delta t}\max\left(1, N_t\left(\log\delta^{-1}\right)^{-1}\right).$$

E Gronwall inequalities

Lemma 15 (Continuous Gronwall inequality) *Let $E(t) \ge 0$, $E(0) = 0$. Let $\frac{d}{dt}E(t) \le f(t)\sqrt{E(t)}$. Then $\sqrt{E(T)} \le \|f\|_{L^1(0,T)}$ for all $T \ge 0$.*

Proof Integrating from 0 to t the inequality in the statement of the theorem gives

$$\int_0^t E'(\tau)d\tau \le \int_0^t f(\tau)\sqrt{E(\tau)}d\tau \implies E(t) \le \sup_{0\le\tau\le t} E(\tau)\|f\|_{L^1(0,t)}$$
$$\implies \sup_{0\le t\le T} E(t) \le \sup_{0\le t\le T}\left(\sup_{0\le\tau\le t} E(\tau)\|f\|_{L^1(0,t)}\right) \le \sqrt{\sup_{0\le t\le T} E(t)}\|f\|_{L^1(0,T)},$$

and hence the result.

Lemma 16 (Discrete Gronwall inequality) *Let $E^m \ge 0$, for all $m \in \mathbb{N}$, and let, with $A \ge 0$,*

$$E^n \le A + \gamma^n\sqrt{E^n} + \sum_{\ell=0}^{n}\delta^\ell\sqrt{E^\ell}, \qquad n \ge 0.$$

Then $\sqrt{E^n} \le \sqrt{A} + \max_{\ell=0,\dots,n}|\gamma^\ell| + \sum_{\ell=0}^{n}|\delta^\ell|$.

Proof Taking $\max_{0\le n\le N}$ from both sides of the inequality in the statement of the lemma:

$$\max_{0\le n\le N} E^n \le A + \sup_{0\le n\le N}\sqrt{E^n}\left(\max_{0\le n\le N}|\gamma^n| + \sum_{\ell=0}^{N}|\delta^\ell|\right).$$

Next, if $\max_{0\le n\le N}\sqrt{E^n} < \sqrt{A}$, then obviously the desired bound holds true. Otherwise, it suffices to replace

$$\max_{0\le n\le N} E^n \le \sqrt{A}\max_{0\le n\le N}\sqrt{E^n} + \sup_{0\le n\le N}\sqrt{E^n}\left(\max_{0\le n\le N}|\gamma^n| + \sum_{\ell=0}^{N}|\delta^\ell|\right),$$

which results in the desired statement.

F Proof of Theorem 6

We proceed like in the proof of Theorem 4. We will show the result for $\mathfrak{a} = \mathfrak{n}$, the proof for the Dirichlet problem being almost verbatim the same.
Step 1. Let $\chi(s)$ be like in the proof of Theorem 4. Testing the wave equation (13) in its strong form by $\partial_s u \chi(s)$ results in (where we parametrized $\Sigma_{0,0}$ by $s \in [0,1]$):

$$\int_0^1 \partial_t^2 u\, \chi(s)\, \partial_s u - \int_0^1 \partial_s^2 u\, \partial_s u\, \chi(s) = 0.$$

Let us rewrite the first term in the above:

$$\begin{aligned} I_1 := \int_0^1 \partial_t^2 u\, \chi(s)\, \partial_s u &= \frac{d}{dt}\left(\int_0^1 \partial_t u\, \chi\, \partial_s u\right) - \int_0^1 \partial_t u\, \partial_t \partial_s u\, \chi(s) \\ &= \frac{d}{dt}\left(\int_0^1 \partial_t u\, \chi\, \partial_s u\right) - \frac{1}{2}\int_0^1 \left(\partial_s(|\partial_t u|^2 \chi(s)) - \chi'(s)|\partial_t u|^2\right) \\ &= \frac{d}{dt}\left(\int_0^1 \partial_t u\, \chi\, \partial_s u\right) + \frac{1}{2}|\partial_t g|^2 + \frac{1}{2}\int_0^1 \chi'(s)|\partial_t u|^2. \end{aligned}$$

The second term

$$I_2 := -\int_0^1 \partial_s^2 u\, \partial_s u\, \chi(s) = -\frac{1}{2}\int_0^1 \partial_s(|\partial_s u|^2 \chi(s)) - \chi'(s)|\partial_s u|^2 = -\frac{1}{2}|\Lambda_{\mathfrak{n}}(\partial_t) g|^2 + \frac{1}{2}\int_0^1 \chi'(s)|\partial_s u|^2.$$

Since $I_1 + I_2 = 0$, we obtain, with $E = \frac{1}{2}\int_{\mathcal{T}} \left(|\partial_t u|^2 + |\partial_s u|^2\right)$,

$$\frac{1}{2}|\Lambda_{\mathfrak{n}}(\partial_t) g|^2 \le \frac{1}{2}|\partial_t g|^2 + \frac{d}{dt}\left(\int_0^1 \partial_t u\, \chi\, \partial_s u\right) + CE(t).$$

Integrating the above from 0 to T we get, together with vanishing initial conditions :

$$\begin{aligned} \|\Lambda_{\mathfrak{n}}(\partial_t) g\|_{L^2(0,T)} &\le \|\partial_t g\|^2_{L^2(0,T)} + C\int_0^T E(t)dt + \int_0^1 \partial_t u(s,T)\chi(s)\partial_s u(s,T) ds \\ &\le \frac{1}{2}\|\partial_t g\|^2_{L^2(0,T)} + C\int_0^T E(t)dt + CE(T), \end{aligned} \tag{135}$$

where we used the Young inequality to bound the latter term.
Step 2. Testing the wave equation (13) in the strong form by $\partial_t u$ and integrating by parts gives

$$\frac{d}{dt}E(t) = (\Lambda_{\mathfrak{n}}(\partial_t) g)\partial_t g.$$

Integrating from 0 to t the above we get

$$E(t) \le \int_0^t |\Lambda_{\mathfrak{n}}(\partial_t) g||\partial_t g| dt \le \frac{\eta}{2}\|\Lambda_{\mathfrak{n}}(\partial_t) g\|^2_{L^2(0,t)} + \frac{1}{2\eta}\|\partial_t g\|^2_{L^2(0,t)}, \qquad \eta > 0, \tag{136}$$

where the last expression follows by the Young inequality.

In particular, the above implies, with $\eta = \eta_1$ to be fixed later

$$\int_0^T E(t)dt \leq T\frac{1}{2\eta_1}\|\partial_t g\|^2_{L^2(0,T)} + \frac{T\eta_1}{2}\|\Lambda_{\mathfrak{n}}(\partial_t)g\|^2_{L^2(0,T)}. \tag{137}$$

Therefore, replacing in (135):

- $E(T)$ by its bound (136) with $\eta = \frac{1}{2C}$
- $\int_0^T E(t)dt$ by its bound (137) with $\eta_1 = \frac{1}{2TC}$,

we obtain the following bound for $\|\Lambda_{\mathfrak{n}}(\partial_t)g\|_{L^2(0,T)}$:

$$\|\Lambda_{\mathfrak{n}}(\partial_t)g\|^2_{L^2(0,T)} \leq C_* \max(1,T)\|\partial_t g\|^2_{L^2(0,T)},$$

and hence the continuity. Let us finally remark that we fixed $g(0) = 0$ for the compatibility conditions, as $u(0) = 0$.

References

1. The Audible Human Project of Acoustics and Vibrations Laboratory of University of Illinois at Chicago (2007-2014). URL http://acoustics.mie.uic.edu/ahp/htdocs/default.php
2. Arioli, M., Benzi, M.: A finite element method for quantum graphs. IMA J. Numer. Anal. **38**(3), 1119–1163 (2018)
3. Arnold, A., Ehrhardt, M., Sofronov, I.: Discrete transparent boundary conditions for the Schrödinger equation: fast calculation, approximation, and stability. Commun. Math. Sci. **1**(3), 501–556 (2003)
4. Banjai, L.: Multistep and multistage convolution quadrature for the wave equation: algorithms and experiments. SIAM J. Sci. Comput. **32**(5), 2964–2994 (2010)
5. Banjai, L., Kachanovska, M.: Fast convolution quadrature for the wave equation in three dimensions. J. Comput. Phys. **279**, 103–126 (2014)
6. Banjai, L., Lubich, C., Sayas, F.J.: Stable numerical coupling of exterior and interior problems for the wave equation. Numer. Math. **129**(4), 611–646 (2015)
7. Banjai, L., Sauter, S.: Rapid solution of the wave equation in unbounded domains. SIAM J. Numer. Anal. **47**(1), 227–249 (2008/09)
8. Berkolaiko, G., Kuchment, P.: Introduction to quantum graphs, Mathematical Surveys and Monographs, vol. 186. American Mathematical Society, Providence, RI (2013)
9. Besse, C., Ehrhardt, M., Lacroix-Violet, I.: Discrete artificial boundary conditions for the linearized Korteweg–de Vries equation. Numer. Methods Partial Differential Equations **32**(5), 1455–1484 (2016)
10. Besse, C., Mésognon-Gireau, B., Noble, P.: Artificial boundary conditions for the linearized Benjamin-Bona-Mahony equation. Numer. Math. **139**(2), 281–314 (2018)
11. Besse, C., Noble, P., Sanchez, D.: Discrete transparent boundary conditions for the mixed KDV-BBM equation. J. Comput. Phys. **345**, 484–509 (2017)
12. Cazeaux, P., Grandmont, C., Maday, Y.: Homogenization of a model for the propagation of sound in the lungs. Multiscale Model. Simul. **13**(1), 43–71 (2015)
13. Cazeaux, P., Hesthaven, J.S.: Multiscale modelling of sound propagation through the lung parenchyma. ESAIM Math. Model. Numer. Anal. **48**(1), 27–52 (2014)
14. Chabassier, J., Imperiale, S.: Introduction and study of fourth order theta schemes for linear wave equations. J. Comput. Appl. Math. **245**, 194–212 (2013)
15. Dai, Z., Peng, Y., Mansy, H.A., Sandler, R.H., Royston, T.J.: Experimental and computational studies of sound transmission in a branching airway network embedded in a compliant viscoelastic medium. Journal of Sound and Vibration **339**, 215 – 229 (2015)

16. Domínguez, V., Sayas, F.J.: Some properties of layer potentials and boundary integral operators for the wave equation. J. Integral Equations Appl. **25**(2), 253–294 (2013)
17. Ern, A., Guermond, J.L.: Theory and practice of finite elements, vol. 159. Springer Science & Business Media (2013)
18. Eruslu, H., Sayas, F.J.: Brushing up a theorem by Lehel Banjai on the convergence of Trapezoidal Rule Convolution Quadrature. arXiv e-prints arXiv:1903.09031 (2019)
19. Gamelin, T.W.: Complex analysis. Undergraduate Texts in Mathematics. Springer-Verlag, New York (2001)
20. Grandmont, C., Maury, B., Meunier, N.: A viscoelastic model with non-local damping application to the human lungs. M2AN Math. Model. Numer. Anal. **40**(1), 201–224 (2006)
21. Gruhne, V.: Numerische Behandlung zeitabhngiger akustischer Streuung im Außen- und Freiraum. Ph.D. thesis (2013)
22. Hairer, E., Lubich, C., Schlichte, M.: Fast numerical solution of nonlinear Volterra convolution equations. SIAM J. Sci. Statist. Comput. **6**(3), 532–541 (1985)
23. Hassell, M.E., Sayas, F.J.: A fully discrete BEM-FEM scheme for transient acoustic waves. Comput. Methods Appl. Mech. Engrg. **309**, 106–130 (2016)
24. Henry, B.: The Audible Human Project: Geometric and acoustic modeling in the airways, lungs and torso. Ph.D. thesis (2018)
25. Henry, B., Royston, T.J.: A multiscale analytical model of bronchial airway acoustics. The Journal of the Acoustical Society of America **4**(142) (2017)
26. Johnson, C., Nédélec, J.C.: On the coupling of boundary integral and finite element methods. Math. Comp. **35**(152), 1063–1079 (1980)
27. Joly, P.: Variational methods for time-dependent wave propagation problems. In: Topics in computational wave propagation, pp. 201–264. Springer (2003)
28. Joly, P., Kachanovska, M.: Transparent boundary conditions for wave propagation in fractal trees: Approximation by local operators In preparation.
29. Joly, P., Kachanovska, M., Semin, A.: Wave propagation in fractal trees. Mathematical and numerical issues. Netw. Heterog. Media **14**(2), 205–264 (2019)
30. Joly, P., Semin, A.: Construction and analysis of improved Kirchoff conditions for acoustic wave propagation in a junction of thin slots. In: Paris-Sud Working Group on Modelling and Scientific Computing 2007–2008, ESAIM Proc., vol. 25, pp. 44–67. EDP Sci., Les Ulis (2008)
31. Kazakova, M., Noble, P.: Discrete transparent boundary conditions for the linearized Green-Naghdi system of equations (2017). URL https://hal.archives-ouvertes.fr/hal-01613071. Working paper or preprint
32. Kovács, B., Lubich, C.: Stable and convergent fully discrete interior-exterior coupling of Maxwell's equations. Numer. Math. **137**(1), 91–117 (2017)
33. Lubich, C.: Convolution quadrature and discretized operational calculus. I. Numer. Math. **52**(2), 129–145 (1988)
34. Lubich, C.: Convolution quadrature and discretized operational calculus. II. Numer. Math. **52**(4), 413–425 (1988)
35. Maury, B.: The Respiratory System in Equations. Springer-Verlag (2013)
36. Maury, B., Salort, D., Vannier, C.: Trace theorems for trees, application to the human lungs. Network and Heteregeneous Media **4**(3), 469 – 500 (2009)
37. Melenk, J.M., Rieder, A.: Runge-Kutta convolution quadrature and FEM-BEM coupling for the time-dependent linear Schrödinger equation. J. Integral Equations Appl. **29**(1), 189–250 (2017)
38. Nelson, T.R., West, B.J., Goldberger, A.L.: The fractal lung: Universal and species-related scaling patterns. Experientia **46**(3), 251–254 (1990)
39. Pazy, A.: Semigroups of linear operators and applications to partial differential equations, Applied Mathematical Sciences, vol. 44. Springer-Verlag, New York (1983)
40. Royston, T.J., Zhang, X., Mansy, H.A., Sandler, R.H.: Modeling sound transmission through the pulmonary system and chest with application to diagnosis of a collapsed lung. The Journal of the Acoustical Society of America **111**(4), 1931–1946 (2002)
41. Schädle, A.: Non-reflecting boundary conditions for the two-dimensional Schrödinger equation. Wave Motion **35**(2), 181–188 (2002)
42. Semin, A.: Propagation d'ondes dans des jonctions de fentes minces. Ph.D. thesis (2010)
43. Weibel, E.R.: Morphometry of the Human Lung. Springer-Verlag (1963)